UNIVERSITÀ
DEGLI STUDI
FIRENZE

DOTTORATO DI RICERCA IN
Scienze della Terra

CICLO XXVI

Satellite interferometric applications for mapping and monitoring hydro-geological instability phenomena

Settore Scientifico Disciplinare GEO/05

Dottorando
Dott. Geol. Silvia Bianchini

Tutore
Prof. Sandro Moretti

Coordinatore
Prof. Lorenzo Rook

Anni 2011/2013

Abstract

Landslides represent a major natural hazard, threatening human lives, properties, structures and environment in most of the mountainous and hilly regions on Earth. Landslides are responsible for at least 17% of all fatalities from natural hazard worldwide.

Interferometric radar approach represents a powerful tool to detect movements on the Earth's surface. Thus, mapping and monitoring slope instability can greatly benefit from remote sensing and satellite data analysis due to the cost-effectiveness, great accuracy (up to 1 mm), high spatial resolution, non-invasiveness, good temporal coverage and measurement sampling. In particular advanced multi-temporal interferometric techniques, i.e. *Persistent Scatterer Interferometry* (PSI) have been successfully used in the last years for investigating natural hazards and, in particular, landslide processes.

This PhD research aims at exploiting PSI techniques for ground displacement detection and mapping at regional and local scale, and for quantitatively and qualitatively analysis of slow-moving landslide phenomena. The work is mainly based on the combined use of ground motion rates provided by PS radar data with conventional geomorphologic tools such as optical data, geo-thematic and *in situ* information, and further ground-truth data.

In particular, the research takes advantage of the potentials of PSI techniques for the spatial and temporal characterization of landslide ground displacements, in order to identify the most unstable areas and to spatially/temporally monitor them. The spatial detection of landslides is performed through the mapping and evaluation of phenomena, combined with the improving procedures for landslide activity and intensity assessment, exploiting more accurate PSI-based methodological tools. The temporal characterization of landslides is carried out through an advanced analysis of PS displacement time series and the integration of PS temporal information with other monitoring data. Finally, PSI-based methods are enhanced by proposing, for instance, new approaches for evaluating PSI suitability of a given study area and the reliability of PSI data for representing landslide-induced movements.

Riassunto

Le frane rappresentano uno dei maggiori pericoli naturali, minacciando le vite umane, i beni, le strutture e l'ambiente nelle regioni montuose e collinari della Terra. Le frane sono responsabili per almeno il 17 % di tutti i decessi per rischi naturali a scala globale.

L'approccio radar interferometrico rappresenta un potente strumento per rilevare i movimenti sulla superficie terrestre. Pertanto, la mappatura e il monitoraggio dell'instabilità dei versanti possono trarre grandi vantaggi dal telerilevamento e dall'analisi di dati satellitari, grazie al buon rapporto costo-efficacia, la grande precisione (fino ad 1 mm), l'alta risoluzione spaziale, la non invasività, buona copertura temporale e campionamento delle misure. In particolare, le tecniche interferometriche multi- temporali avanzate, i.e. la tecnica *Persistent Scatterer Interferometry* (PSI), sono state utilizzate con successo negli ultimi anni per investigare i rischi naturali e, in particolare, i fenomeni franosi.

Questa tesi di Dottorato mira a sfruttare le tecniche PSI per l'identificazione e la mappatura di spostamenti del terreno a scala regionale e locale, e per l'analisi quantitativa e qualitativa dei fenomeni franosi lenti. Il lavoro si basa sull'uso combinato dei valori di velocità fornite da dati radar PS con strumenti geomorfologici convenzionali quali dati ottici, informazioni geo-tematiche e *in situ*, dati relativi a verità a terra.

In particolare, la ricerca analizza e usa le potenzialità delle tecniche PSI per la caratterizzazione spaziale e temporale di movimenti franosi, al fine di individuare le aree più instabili e di monitorarle spazialmente e temporalmente. La individuazione spaziale delle frane viene eseguita attraverso la mappatura e valutazione dei fenomeni, combinata con procedure per migliorare la valutazione della loro attività e intensità, sfruttando le più accurate metodologie basate sull'approccio PSI. La caratterizzazione temporale delle frane è effettuata attraverso l'analisi avanzata delle serie temporali di spostamento dei PS e l'integrazione delle informazioni temporali PS con altri dati di monitoraggio. Infine, i metodi *PSI-based* vengono migliorati e implementati proponendo, per esempio, approcci innovativi per la valutazione dell'idoneità della tecnica PSI per studiare una determinata area di studio, e dell'affidabilità dei dati PSI per la rappresentazione di movimenti indotti da fenomeni franosi.

Acknowledgements

I would like to thank Prof. Nicola Casagli of the Earth Sciences Department - University of Firenze (DST- UNIFI), for giving me the opportunity to accomplish this PhD.

I thank prof. Sandro Moretti, my PhD supervisor at the Earth Sciences Department of Firenze, for his availability, constructive suggestions and revisions.

I thank Dr. Gerardo Herrera of the Instituto Geológico y Minero de España (IGME, Madrid) for his hospitality and welcome in Madrid, for his expertise, his invaluable help and research advices, which helped to make my Spanish stay a beautiful and unforgettable experience.

A big thank you to Dr. Gaia Righini, my first "tutor" and reference person within the "Geoapplicati" group at the University of Firenze, for her kindness and her guidance during my first period at the Arcetri headquarters of the DST- UNIFI.

I am also grateful to Dr. Francesca Cigna, for her great support and professional help, and for all her advices and encouragement, sharing the office room and my first "missions" for research projects and conferences, and making the first year of my PhD so productive and enjoyable.

Finally, thanks to my friends, to the people who love me and make me feel good. In particular, a deep and lovely thank you to my parents, to my sister and to Ivan, who have always supported me during this PhD experience and who have always believed in me.

Ringraziamenti

Vorrei ringraziare il Prof. Nicola Casagli del Dipartimento di Scienze della Terra di Firenze - Università degli Studi di Firenze (DST-UNIFI), per avermi dato la possibilità di svolgere questo Dottorato di Ricerca.

Ringrazio il prof. Sandro Moretti, mio supervisore di Dottorato al Dipartimento di Scienze della Terra di Firenze, per la disponibilità, i suggerimenti e le revisioni.

Ringrazio il Dr. Gerardo Herrera dell'Instituto Geológico y Minero de España (IGME, Madrid) per la sua ospitalità e accoglienza all'IGME a Madrid, per la sua competenza e per il suo preziosissimo aiuto, che hanno contribuito a rendere il mio soggiorno spagnolo una esperienza bellissima e indimenticabile.

Un caro ringraziamento alla Dott.ssa Gaia Righini, mia prima "tutor" e riferimento presso il Gruppo di Geoapplicati dell'Università di Firenze, per la sua gentilezza e il suo supporto durante il mio primo periodo di lavoro alla sede di Arcetri del DST-UNIFI.

Ringrazio la Dott.ssa Francesca Cigna, per il suo grandissimo sostegno e aiuto professionale, e per tutti i suoi consigli e incoraggiamenti, condividendo la stanza d'ufficio e le mie prime "missioni" per progetti e conferenze, e rendendo il primo anno del mio Dottorato così produttivo e piacevole.

Infine, grazie agli amici, alle persone che mi vogliono bene e che mi fanno stare bene. In particolare un grazie di cuore ai miei genitori, a mia sorella, a Ivan, che mi hanno sempre sostenuto durante questo percorso e che hanno sempre creduto in me.

Table of contents/Indice

Introduction

Hydrogeological phenomena such as landslides and subsidence are one of the most widespread geological hazards, occurring worldwide more frequently than any other natural disasters, including earthquakes, floods and volcanic eruptions (IGOS, 2004).

Ground instability ranges from devastating landslides, involving the chaotic mass movement of large quantities of rock or soil along steep, unstable slopes, to the progressive downward surface movements, commonly referred as subsidence, produced by ground water withdrawal, mineral extraction, underground storage and engineering works, and to the collapse of buried natural or man-made cavities and settlement of loose sediments.

Hydrogeological ground instability is observable through surface displacements, being one of the main processes by which geo-morphological settings evolve; hence, the related hazards result in a complex, changing landscape that must be mapped and understood in detail in order to assess its future behavior and evolution. Moreover, these phenomena, especially in case of catastrophic events such as landslides, can pose great threats to human lives, causing fatalities and injuries, and can produce huge direct and indirect socio-economical losses, in terms of damages and environmental degradation. In particular, the impact of such natural disasters in urbanized areas is stronger because of the higher value of the element at risk exposure.

The potential hazard of ground instability phenomena can be reduced or even prevented especially in highly settled and susceptible areas by performing a proper identification and mapping of such ground movements, in order to support an appropriate land use planning and to facilitate the risk mitigation design. Prevention and prediction of hydrogeological processes and failures need to be carried out for improving risk management activities and focusing resources according to distribution and intensity of landslide hazard.

Basic landslide inventory maps are lacking or not up to date in many regions and several aspects of ground instabilities need to be better studied and understood, including the causative factors, the triggering mechanisms and the different temporal and spatial scales and distributions involved.

Remote sensing and Earth Observation (EO) data and can play a major role for studying geohazard-related events at different stages, such as detection, mapping, monitoring, forecast, modeling, and hazard zonation.

In recent years, InSAR (Interferometric Synthetic Aperture Radar) techniques, both space-borne and terrestrial, have shown their capabilities in providing precise measurements of ground displacement on earth surface.

In particular, in case of slow movements, i.e. up to few cm per year, affecting urban areas, the multi-temporal interferometric InSAR techniques, such as the Persistent Scatterers Interferometry (PSI), are able to retrieve the spatial distribution of displacements and their evolution along the monitored period at a relatively low cost over wide areas.

Thanks to the availability of historical archive datasets of SAR images acquired by ERS1/2 and ENVISAT satellites (ESA - European Spatial Agency), spanning from 1992 to 2010, and images by RADARSAT 1/2 (CSA - Canadian Spatial Agency) sensors, as well as satellite data from current X-band high resolution satellite systems, i.e. COSMO-SkyMed (ASI - Italian Space Agency) and TerraSAR-X (DLR - German Aerospace Center), PSI techniques can be applied to provide back analysis and monitoring of ground displacements with high precision up to about 1 mm/yr (depending on the number of available images, the phase stability of each PS and its distance from the reference point) on a single measure.

As demonstrated by several works and applications in last decades, the PSI analysis, properly integrated with additional geo-thematic and/or ground-truth data, allowed detecting, characterizing and monitoring areas affected by slow-moving ground movements.

The radar-interpretation approach and further implementation of PSI data are a fundamental requirement for the use of InSAR data, as a consequence of some intrinsic characteristics, such as, for instance, their ability to detect only the satellite LOS (Line Of Sight) component of ground deformation and the point-wise spatial distribution of measures.

In this PhD programme, remote sensing technique, and in particular PSI analysis, are exploited for studying and characterize hydrogeological hazard such as landslides.

PSI data are firstly analyzed for spatial detection and mapping of slow-moving landslides, in order to create and/or update landslide inventory maps and to identify priority areas where detailed analysis and additional *in situ* investigations can be focused.

Then, PSI is exploited with regard to time series, for an advanced temporal characterization of landslide phenomena, in order to study evolution patterns or potential reactivations.

Finally, PSI data are implemented to achieve a qualitative and quantitative interpretation and reliable characterization of phenomena and related landslide-prone and -affected areas. The analysis aims at better understanding the distribution, activity and evolution of the investigated hydrogeological events and at assessing related damages and elements at risk, in order to assign a confidence degree and to potentially provide a preliminary tool for further hazard and risk analysis.

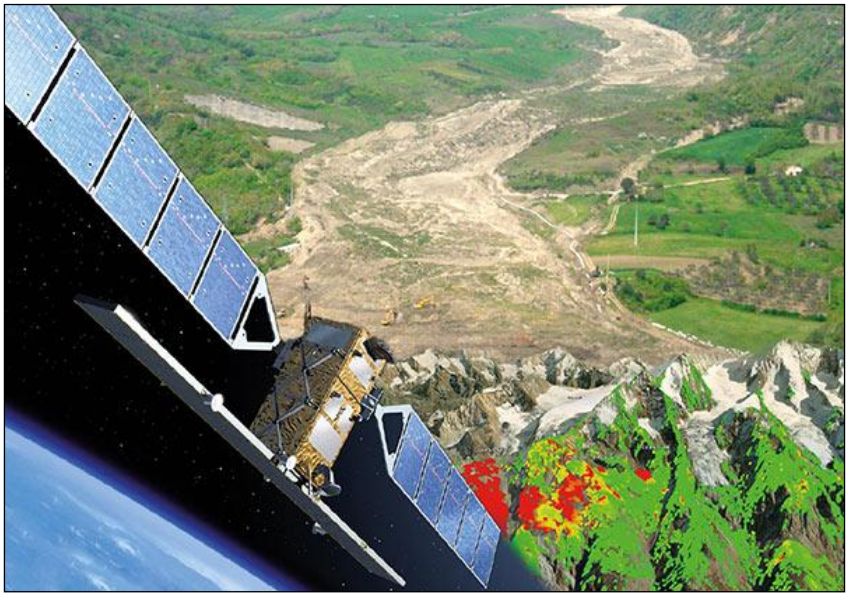

Fig. 1 - Space-borne observation of landslide phenomena (From http://www.doris-project.eu).

Chapter 1

Study scope and contents: objectives and structure of the research

1.1 Outline

Landslides represent a serious hazard worldwide and play an important role in the landscape evolution, as well as in the human strategies for environmental planning.

The global concern of landslide hazard and risk have increased the enhancement of valuable and efficient landslide analysis and assessment procedures.

Therefore, the need to better understand landslides and the capacity of improving investigation tools have led to effective research and development of activities for landslide studies, including the significant use of *remote sensing* techniques.

This PhD thesis work deals with satellite Earth Observation (EO) tools that contribute to geohazards analysis and characterization in landslide-prone and landslide-affected areas.

The research is set within the framework of the prediction and prevention of ground mass movements and landslide events, consistent with the activities of the Competence Centre of the Italian Department of Civil Protection at the Earth Sciences Department of the University of Firenze, Italy.

Most of data and performed activities described in this research thesis were obtained and carried out in the context of several research European projects.

The activities carried out within the research aim at the application of advanced multi-temporal interferometric techniques like Persistent Scatterer Interferometry (PSI) as operating tools for supporting the study, characterization, interpretation and monitoring of landslide phenomena.

1.2 Objectives of the research

The scope of this PhD work is to exploit, implement and test remote sensing data, processed by means of PSI (Persistent Scatterer Interferometry) technique, for landslide analysis with particular focuses on:

- Spatial detection and mapping of slow-moving landslides for creating and/or updating landslide inventory maps.
- Temporal investigation of landslide phenomena throughout the advanced analysis of displacement time series of radar data.
- Implementation of remote sensing tools for improving landslide investigation and for increasing the reliability and confidence degree of available data and delivered products.

Some test sites affected by ground motion have been selected in Italy and in Spain. In these sample areas, the suitability of SAR data is assessed and the landslide scenario critically studied.

Landslide investigation is carried out at different scales, from regional to basin and local scale, in various geomorphological settings.

Most of the test areas were chosen within European research projects (i.e. SAFER, Terrafirma, DORIS projects), and exploited for supporting local authorities within environmental planning and risk assessment initiatives led by the Italian National Department of Civil Protection.

Thus, some activities were carried out aimed at collecting, using and validating EO data in order to provide reliable services and useful information to the end-users and recipients, for hazard and risk prevention

purposes. Other activities were contextually carried out, aimed at providing new methodologies for SAR data analysis and validation in landslide studies.

1.3 Thesis roadmap

This thesis represents the main outcome of the three years-long PhD activity at the Earth Sciences Department of the University of Firenze (Centre of Competence of the Italian Civil Protection) and at the Geohazards InSAR laboratory and Modeling group (InSARlab) within the Geological Survey of Spain in Madrid (Instituto Geológico y Minero de España, IGME).

The present PhD thesis is organized as in Fig. 2 and it includes a total of ten chapters, outlined as follows.

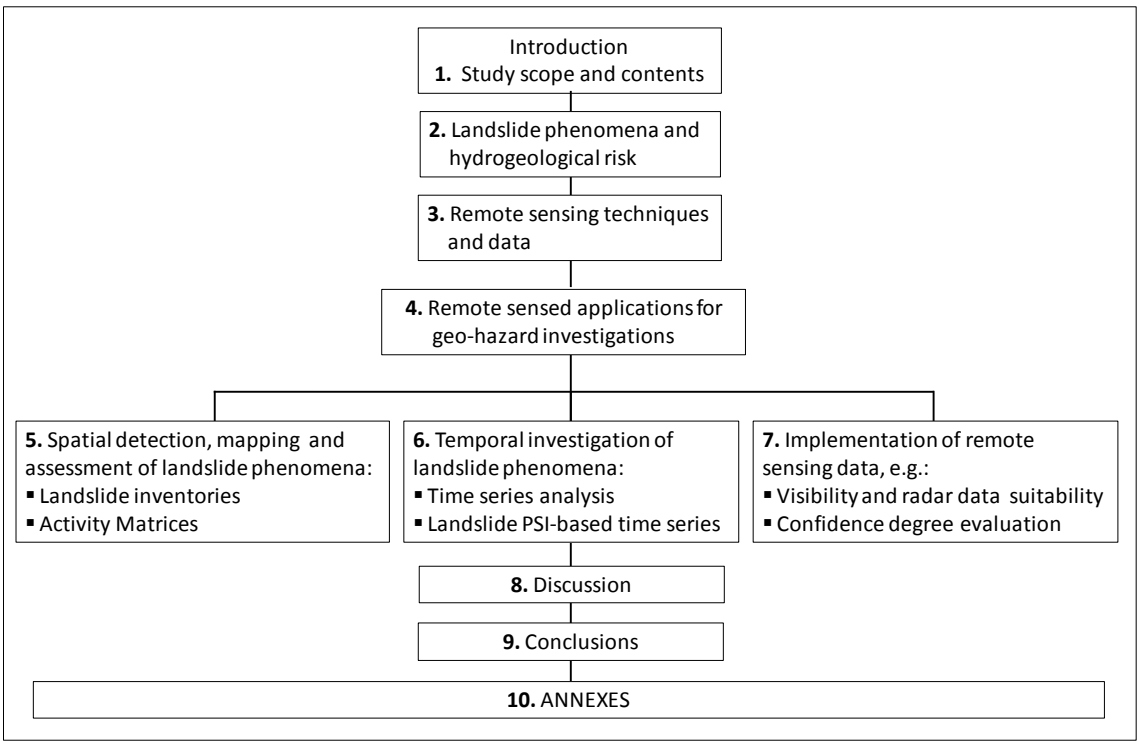

Fig. 2 - Flowchart of the PhD thesis roadmap.

Chapter 1 introduces contents, objectives and outline of this PhD thesis.

Chapter 2 presents a very short review regarding landslide phenomena and the most important concepts of landslide hazard and risk assessment.

Chapter 3 describes the basic principles of space-borne radar *remote sensing* and renders a review of radar interferometry techniques, both classical and advanced approaches.

Chapter 4 deals with a review of remote sensed data applications for geo-hazard investigations; the chapters also provides a state of art of the sensors used up to date and of the applicability of SAR techniques to landslide phenomena. The main geo-hazard scientific and end-users community background is also briefly presented, with particular attention to the Italian case.

Chapter 5 describes the contribution of PSI techniques for the spatial characterization of landslide phenomena at regional, local and basin scale. The Landslide Inventory Mapping (LIM) procedures for detection and mapping, and the matrix-based approach for defining the landslide state of activity are described. Some case studies demonstrate the applicability of these methodologies, respectively at regional, basin and local scale: Calabria Region (Italy), the Reno basin (Emilia-Romagna Region, Italy), Verbicaro site (Calabria region, Italy). Outcomes of the performed works for each test site are shown in the related Annex at the end of the thesis.

Chapter 6 explains about the temporal characterization of landslide phenomena, mainly by means of PSI time series analysis. Two case studies are related to this topic: Gimigliano area (Calabria region, Italy), and Lungro/Acquaformosa area (Calabria Region, Italy). Large temporal archives of ERS and ENVISAT C-Band SAR data are exploited within DORIS European research project in several test sites. The work carried out for each case study is included in the corresponding Annex at the end of the thesis.

Chapter 7 deals with the implementation of post-processing PS data elaborations and with the analysis of PSI applicability and suitability for landslide investigations, as well as with an innovative procedure developed to evaluate the confidence degree of the product-maps. In this chapter, the use of PS data combined with further additional data for different objectives, e.g. the impact and damage assessment, is also tackled and discussed. Three case studies are shown: the Tramuntana Range (Majorca island, Spain), Piemonte Region (North Italy) and the San Fratello site (Sicily Region, Italy). The whole efforts and results on these test sites are shown in the related Annexes at the end of the thesis work.

Chapter 8 deals with discussion issues regarding applicability, limitations and uncertainties of PSI data and techniques, as well as advantages, potentials and future potential improvements.

Chapter 9 summarizes the main findings of this thesis. Obviously, most of the conclusions included in this chapter are included in each single Annex.

Finally, after the references of this work, listed in alphabetical order, the *Chapter 10* includes all the Annexes, which are the core of this thesis.

Chapter 2

Landslide phenomena and hydrogeological risk

Landslides are one of the most hazardous and most frequent phenomena worldwide. They can cause negative and catastrophic impacts, including human losses, property damages, casualties and permanent landscape changes. Landslides are defined as movements of soil and/or rock down a slope, developing when the destabilizing forces exceeded the resisting ones (Varnes, 1978; Hutchinson, 1988; WP/WLI, 1990, 1993; Cruden, 1991; Cruden and Varnes, 1996). The occurrence of these natural phenomena can be prevented by understanding their hazard, and by properly mapping and analyzing potential unstable areas, in order to lead to successful mitigation strategies and reduce the risk.

2.1 Landslides

A landslide is defined by Cruden (1991) as a "movement of a mass of rock, debris or earth down a slope", induced by the gravity. Fig. 3 shows a graphic illustration of a landslide, with the commonly accepted terminology describing its features.

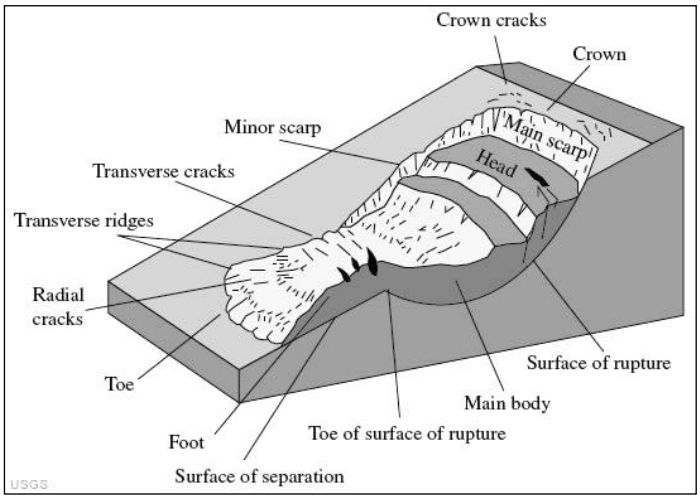

Fig. 3 - An idealized slump-earth flow, showing commonly used nomenclature for labeling the parts of a landslide (From http://geology.com/usgs/landslides).

Landslides represent one of the natural hazards that occur most frequently and globally distributed (they are even more frequent and widely distributed than earthquakes and volcanic activity) (IGOS, 2004). Although most of landslides usually occur in hilly and mountainous areas after extreme rainfall events, landslides can occur in many geographical, geological and climatic environments. Landslide phenomena are one of the main geomorphological processes by which landscape evolves, and include a wide range of surface deformations and displacements.

Even though the influence of gravity and the reduction of the shear strength of the material are the primary driving forces for a mass movement to take place, the occurrence of landslides depends on complex interactions among a large number of partially interrelated factors, such as geologic setting, geomorphic features, soil properties, land cover characteristics, hydrological and human impacts.

The main factors that influence landslides are discussed in Varnes (1984) and Hutchinson (1988) and encompass geology (lithology, structure, degree of weathering), geomorphology (e.g. slope gradient and aspect), soil (thickness, permeability, porosity), land use and hydrologic conditions.

Theoretically, the landslide process can occur as the result of the disturbance of the slope equilibrium, when the stress produced by the force of the gravity exceeds the resistance of the material. The disturbance of equilibrium of the slope is caused by the increasing of the shear stress and/or the decreasing of the shear strength. Selby (1991) classified these two major categories of factors contributing to landslides, i.e. (i) factors contributing to raise the shear stress, such as the removal of lateral support (stream water, increasing gradient) or overloading (rain, soil saturation) and (ii) the factors contributing to reduce shear strength, such as changes in composition and texture of the soil material or physical-chemical reactions due to weathering.

Moreover, we can distinguish on one hand the landslide predisposing (or preparatory) variables, which are the ones that make the original slope susceptible to failure and that include soil and rock geo-mechanical properties, slope aspect and elevation, land cover, lithology and drainage patterns. On the other hand, the triggering (or dynamic) factors are those initiating landslide movements, and might be either natural or human-induced, acting alone or in combination (Dai and Lee, 2002). Natural triggers include intense or prolonged rainfall, earthquakes, volcanic eruptions, rapid snowmelt and permafrost thawing, and slope undercutting by rivers or sea-waves. Other factors capable of acting as triggers for landslide failures are human activities, such as slope excavation and loading, land use changes (e.g. deforestation or cultivation), rapid reservoir drawdown, blasting vibrations, and water leakage from utilities.

Landslides can involve different moving processes like flowing, sliding, toppling or falling movements (Glade and Crozier, 2005), and many landslides exhibit a combination of two or more types of movements (Varnes, 1978; Crozier, 1986; Hutchinson, 1988; Cruden and Varnes, 1996; Dikau et al., 1996).

A complete classification of landslides is not easy to be determined. By the way, many systems have been proposed and the most commonly adopted ones are those of Varnes (1978) and Hutchinson (1988).

The well-known and widely accepted landslide classification was proposed by Varnes (1978) and subsequently improved by Cruden and Varnes (1996). It primarily focuses on the combination of movement and material types. In particular, this landslide classification system has two terms: the first term describes the material type (rock, earth, soil, mud or debris) in the landslide before it is displaced and the second term describes the type of movement, which means how the landslide movement is distributed through the displaced mass. The five kinematically distinct types of movements are described in the sequence: fall, topple, slide, spread and flow. Combining the two terms gives classifications such as rock fall, rock topple, debris slide, debris flow, earth slide, earth spread etc. (Tab. 1).

<table>
<tr><th colspan="2" rowspan="3">TYPE OF MOVEMENT</th><th colspan="3">TYPE OF MATERIAL</th></tr>
<tr><th rowspan="2">BEDROCK</th><th colspan="2">ENGINEERING SOILS</th></tr>
<tr><th>Predominantly coarse</th><th>Predominantly fine</th></tr>
<tr><td colspan="2">FALLS</td><td>Rock fall</td><td>Debris fall</td><td>Earth fall</td></tr>
<tr><td colspan="2">TOPPLES</td><td>Rock topple</td><td>Debris topple</td><td>Earth topple</td></tr>
<tr><td rowspan="2">SLIDES</td><td>ROTATIONAL</td><td rowspan="2">Rock slide</td><td rowspan="2">Debris slide</td><td rowspan="2">Earth slide</td></tr>
<tr><td>TRANSLATIONAL</td></tr>
<tr><td colspan="2">LATERAL SPREADS</td><td>Rock spread</td><td>Debris spread</td><td>Earth spread</td></tr>
<tr><td colspan="2">FLOWS</td><td>Rock flow
(deep creep)</td><td>Debris flow</td><td>Earth flow
(soil creep)</td></tr>
<tr><td colspan="2">COMPLEX</td><td colspan="3">Combination of two or more principal types of movement</td></tr>
</table>

Tab. 1 - Landslide classification with respect to the type of movement and the material (Varnes, 1978).

The report "A Suggested Method for Reporting a Landslide" produced in 1990 by the International Geotechnical Societies' UNESCO Working Party on World Landslide Inventory (WP/WLI, 1990) uses Varnes

(1978) classification and states that it is the most widely used system. The World Road Association (PIARC) report called "Landslides: Techniques for Evaluating Hazard" (Escario et al., 1997) also presents a classification based on Cruden and Varnes (1996).

The other commonly recognized classification, proposed by Hutchinson (1988), refers to morphological and geotechnical parameters of landslides in relation to geology and hydrogeology.

Moreover, Carson and Kirby (1972) have classified landslides on the basis of the movement velocity and of the water content of earth material (drier to wetter), as shown in the field-view of Figure 4.

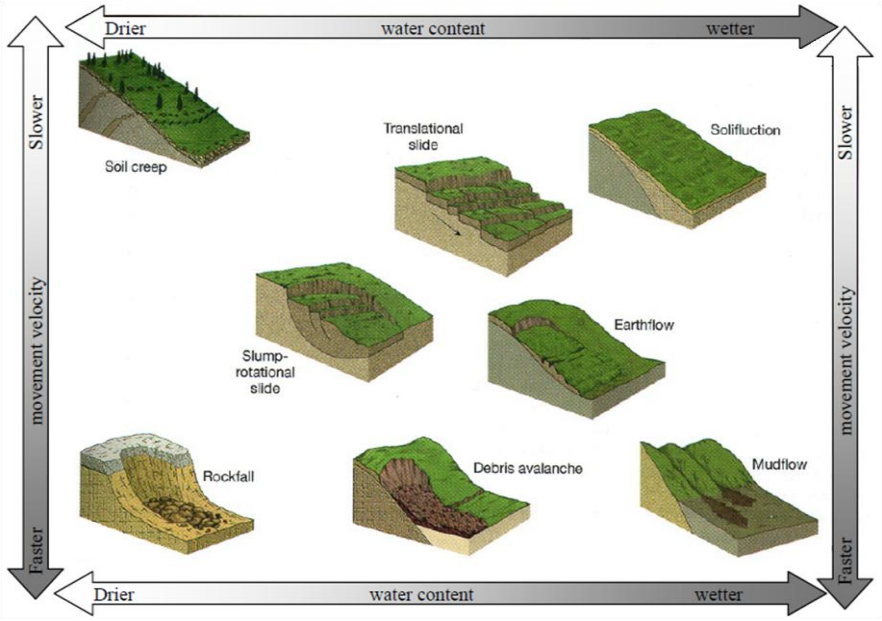

Fig. 4 – Field-view of landslide type according to Carson and Kirby (1972).

More recently, also Hungr et al. (2001) have proposed a landslide classification based on a new separation of landslide materials, with a more detailed consideration of material type, water content, pore pressure, recurrent path and velocity.

Landslides are usually classified also in terms of velocity and damages, according to the classification proposed by Cruden and Varnes (1996), as shown in Table 2.

Velocity Class	Description	Velocity (mm/sec)	Typical Velocity	Probable Destructive Significance
7	Extremely Rapid	5×10^{3}	5 m/sec	Catastrophe of major violence; buildings destroyed by impact of displaced material; many deaths; escape unlikely
6	Very Rapid	5×10^{1}	3 m/min	Some lives lost; velocity too great to permit all persons to escape
5	Rapid	5×10^{-1}	1.8 m/hr	Escape evacuation possible; structures; possessions, and equipment destroyed
4	Moderate	5×10^{-3}	13 m/month	Some temporary and insensitive structures can be temporarily maintained
3	Slow	5×10^{-5}	1.6 m/year	Remedial construction can be undertaken during movement; insensitive structures can be maintained with frequent maintenance work if total movement is not large during a particular acceleration phase
2	Very Slow	5×10^{-7}	15 mm/year	Some permanent structures undamaged by movement
	Extremely **SLOW**			Imperceptible without instruments; construction **POSSIBLE WITH PRECAUTIONS**

Tab. 2 - Landslide velocity classification by Cruden and Varnes (1996).

Landslides vary enormously both in their distribution in space and time, and in their size. The range of landslide phenomena is extremely large, making mass movements one of the most diversified and complex natural hazards. Landslides have been recognized in all continents, in the seas and in the oceans (Guzzetti, 2006). On Earth, the area of a landslide extends up nine orders of magnitude, since it can spans from a small soil slide involving a few square meters to large submarine landslides covering several hundreds of square kilometres of land and sea floor. The volume of mass movements spans sixteen orders of magnitude, from a single cobble falling from a rock cliff to huge submarine slides. Landslide velocity extends at least over fourteen orders of magnitude, from creeping failures moving at some millimeters per year (or even less) to rock avalanches travelling at hundreds of kilometres per hour. The lifetime of a single mass movement ranges from a few seconds in the case of individual rock falls, to several hundreds and possibly thousands of years in the case of large dormant landslides (Guzzetti, 2006).

Mass movements can occur singularly or in groups. Multiple landslides occur almost simultaneously when slopes are shaken by an earthquake or over a period of hours or days when for instance failures are triggered by intense or prolonged rainfall. Rapid snow melting can trigger slope failures several days after the onset of the triggering meteorological event. An individual landslide-triggering event (e.g., intense or prolonged rainfall or an earthquake) can involve a single slope or a group of slopes extending for a few hectares, or it can affect thousands of square kilometres spanning major physiographic regions. Total landslide area produced by an individual triggering event ranges from a few tens of square meters to hundreds of square kilometres.

2.2 Hydrogeological hazard and risk

Globally, landslides are responsible for significant loss of life and injury to people and their livestock, as well as loss and damage to lifelines, structure and infrastructure, agricultural lands, road network, housing and public or private buildings (USGS, 2001; JRC, 2003; Blöchl and Braun, 2005). The assessment of the vulnerability of communities prone to landslide-related disasters is a topic that is growing in importance. Few studies discuss this issue and limited research has been carried out on the relationship between types of landslide and their potential impact and risk on manufactures and properties (Papathoma-Köhle et al., 2007).

Landslide risk evaluation aims at determining the “expected degree of loss due to a landslide (specific risk) and the expected number of live lost, people injured, damage to property and disruption of economic activity (total risk)” (Varnes et al., 1984). Outlining the basic concepts of landslide hazard, risk and vulnerability, the definition of the “risk” around its various elements is here reported, through the following well-known equation:

$$R = H * E * V$$

where the Risk (R) refers to the expected number of lives lost, persons injured and damage to property and to economic activity due to a particular event. Thus, simplifying, the risk can be defined as the estimated degree of loss due to a particular landslide phenomenon. The hazard (H) is defined as the probability of occurrence of a potentially damaging event within a specified time and given area. The Elements at risk (E) include population, buildings and engineering structures, infrastructure areas and lines, public service utilities and economic activities. The Vulnerability (V) is related to the (potential) results from event occurrence expressed with qualitative, semi-quantitative or quantitative methods in terms of loss, disadvantage or gain, damage, injury or loss of life. In particular, Varnes et al. (1984) define the landslide hazard as the “probability of occurrence within a specific period of time and within a given area of potentially damaging phenomenon”.

Landslides represent a main hazard in mountainous and hilly regions as well as along steep riverbanks and coastlines, and their impacts depend largely on the area and volume involved, the movement velocity and intensity, number and distribution of the elements at risk, their vulnerability and their exposure value.

Landslides are not currently amenable to risk assessment since there is no basis to absolutely determine the probability of landslides occurring within a given time period. Moreover, the extraordinary breadth of the spectrum of mass movement phenomena makes it difficult to define a single methodology to ascertain landslide hazards and to evaluate the associated risk (Guzzetti, 2006).

Literature on landslide hazard, risk and vulnerability highlight that there is not a common approach used for the assessment of vulnerability for communities prone to landslide (and related disasters) that can be used as a tool for effective emergency and disaster management.

In the field of landslide research, most studies have focused on the landslide hazard part of the "Risk equation" and have resulted in the generation of landslide hazard zoning and maps (Guzzetti et al., 1999). Few works have concentrated on the risk and vulnerability elements (Gomes, 2003; Glade and Crozier, 2005). A number of studies have tried to examine both risk and community vulnerability and a very limited number have examined vulnerability specifically (Hollenstein, 2005).

Vulnerability to landslide hazards is a function of location, type of human activity and frequency of landslide events. Thus, the effects of landslides can be very significant and vary according to geographic location. For example, landslides in Europe cause significant economic losses, whereas, in Asia and Latin America, they cause great loss of life. It is also highly possible that climate change in combination with wide-scale development on steep slopes has increased the impact of landslide events and the disasters they may cause globally (Helmer and Hilhorst, 2006).

In Europe, large magnitude landslides have a low probability of generating "catastrophic" events (as defined by a significant loss of human life), but they do have considerable social, economic and ecologic consequences (Scavia and Castelli, 2003; Blöchl and Braun, 2005). The concentration of property on steep slopes, high standard of living and high population density make society vulnerable to landslide events, even those of small magnitude (Blöchl and Braun, 2005). Landslides may have very significant impacts on buildings and are very expensive in terms of the costs of rehabilitation, securing the structures and ongoing maintenance (Papathoma-Köhle et al., 2007).

Interestingly, the impact of landslide processes is often underestimated and overlooked because they frequently occur in combination with other events such as floods, earthquakes and volcanic eruptions (USGS, 2001; JRC, 2003; Blöchl and Braun, 2005).

The global impact of slope failures on population, structures, infrastructures, economy and environment remains largely undetermined and so the risk assessment is difficultly performed at a large scale. An attempt to describe the socioeconomic significance of landslides has been performed by Schuster and Fleming (1986). Worldwide, the annual property damage from landslides has an estimated cost of 10 billion dollars. In Italy, one of most severely affected European country, the landslide losses are estimated to range from 1 to 2 billion of dollars annually, corresponding to about 0.15% of the national domestic product, according to Canuti et al. (2004).

In order to represent landslide risk on a global scale, a few attempts have been made to assess susceptibility, hazard and risk, with uncertain degrees of accuracy that are not always well established. Moreover, since there is no fixed standard procedure, these different studies employ different models and input data; as a consequence, they have to be only considered as general overview patterns of the potential geographic distribution of landslides.

An example is the map of the Global Landslide Hazard Distribution (GDLND), shown in Figure 5. The GDLND map is the result of a collaboration between the Columbia University Center for Hazards and Risk Research (CHRR), the Norwegian Geotechnical Institute (NGI), and the Columbia University Center for International

Earth Science and Information Network (CIESIN).The map is derived from the landslide hotspot map at global scale published by Nadim et al. (2006) and it is a representation of landslide hazard over a 2.5 x 2.5 minute grid, based on a heuristic landslide hazard model considering slope, lithology, soil moisture, precipitation, temperature and seismicity as input variables.

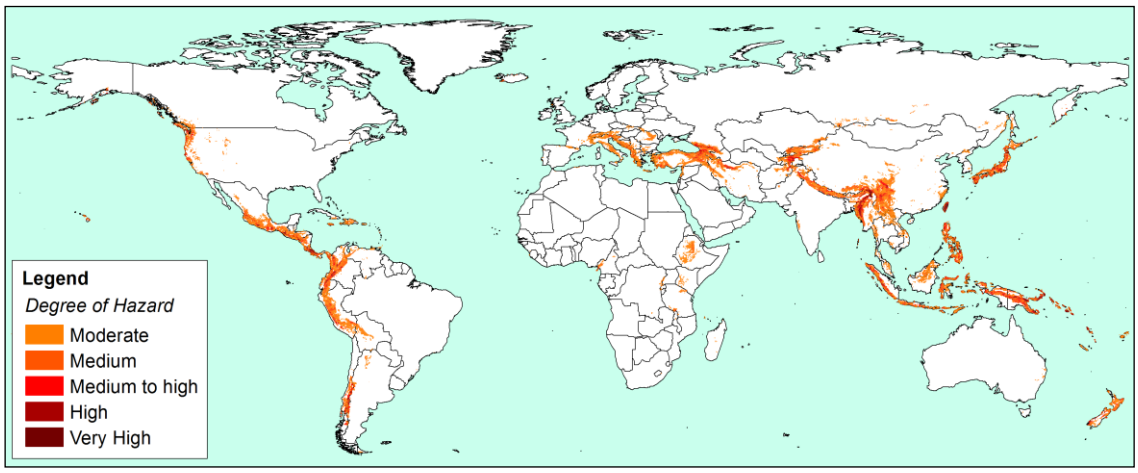

Fig. 5 - Global Landslide Hazard Distribution (GDLND) map.

Another attempt is shown in Figure 6, representing the Global landslide susceptibility map derived from surface multi-geospatial data: the susceptibility index data from Hong et al. (2007) are plotted with the 2003 and 2007 major landslide events (Kirschbaum et al., 2009).

Hong et al. (2007) used an heuristic approach based on TRMM (Tropical Rainfall Monitoring Mission) rainfall measures acquired by NASA and JAXA, and a GIS-based weighted linear combination of different landslide-controlling factors such as slope, soil type and texture, elevation, land cover and drainage density.

As shown by the outcomes of these recent studies at global scale (Fig. 5 and Fig. 6), the higher landslide hazard are prevalently concentrated along the Pacific Coasts, in the Circum-Pacific belt (e.g. Philippines-Japan regions)and in Central and South America, as well as in south-eastern Asia and in the Middle East (Turkey, Georgia, Azerbaijan, Iran). Landslide-affected areas are also found in Asia in the Himalayas ranges (India, Nepal), in the European Alps (Italy) and Pyrenees (Spain), in Balkan regions (Albania, Greece), in the Rocky and Appalachian Mountains (USA and Canada), and in some few regions of Africa (Ethiopia, Kenya, Tanzania, Cameroon).

From these data, the total area prone to landslide is estimated at 2% of the world land area.

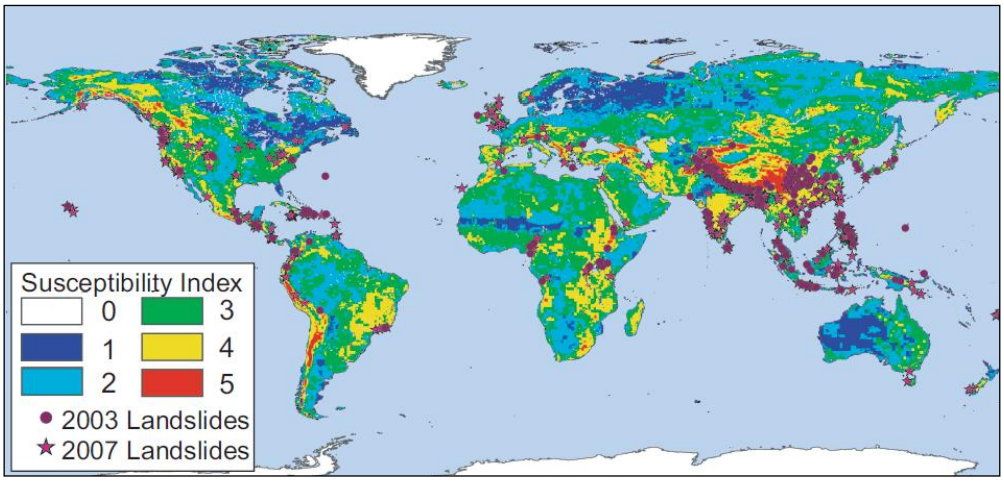

Fig. 6 - Global landslide susceptibility map proposed by Hong et al. (2007).

Considering the European territory, landslides occur in many different geological and environmental settings. Looking at the GDLND map focused on Europe (Fig. 7), we can see that the countries characterized by the highest total area prone to landslides are Italy (13% ca.), Austria (10% ca.), Balkan states (Albania, 40% ca. and Greece, 15% ca), Bosnia and Herzegovina (22% ca.), Slovenia (25% ca.), Turkey (19% ca.). Overall, regarding the spatial extent, the total area prone to landslide is estimated at 4% of the European (plus Turkey) land area.

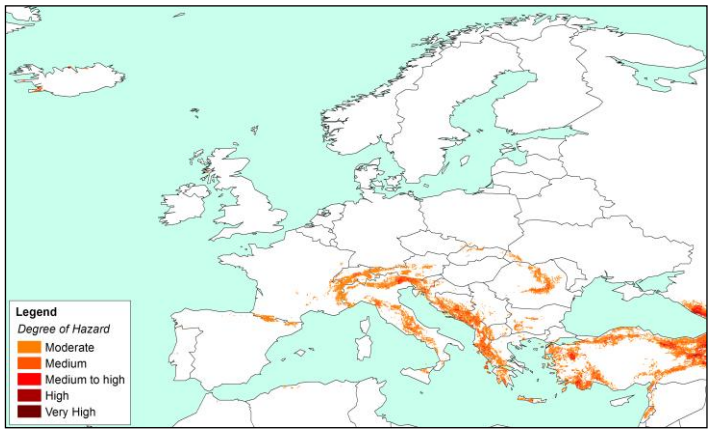

Fig. 7 - Landslide Hazard Distribution map focused on Europe

Italy is a country where the landslide risk is particularly high, due to its relief, its lithological and structural characteristics. Landslides, which are extremely widespread throughout Italy, are the most frequently occurring natural disasters and are the causes, after earthquakes, of the highest numbers of victims. There has been a significant increase in the human pressure on the country since the Second World War, with the expansion of urbanization and roads/railways construction, even in unstable areas. In this context, landslide phenomena have become a major problem with regard to the safety of the population and damage to residential areas, infrastructures, service networks and environmental and cultural heritage. Following the disastrous event at Sarno (Campania region, South Italy) on 5th May 1998, there has also been a more urgent need for a complete and homogenous overview on the distribution and management of landslide phenomena in Italy, with regard to the laws (the Law 267/1998 was promulgated after this event) and recording of information and mapping of landslides.

Within the Italian Landslide Inventory Project (*Progetto IFFI – Inventario dei Fenomeni Franosi in Italia*), 482,272 landslides have been surveyed up to 2007, covering an area of almost 20,500 km^2, which is equivalent to 6.8% of the Italian territory (ISPRA, 2008; Trigila and Iadanza, 2008). This percentage is defined as Landslide Index (LI), calculated as the ratio between landslide area to the total area. The computation of the LI for each italian Region highlights that the Regions with the highest Landslide Index over mountains-hilly territory (elevation > 300 m a.s.l.) are Piedmont, Lombardy, Emilia-Romagna, Marche, Molise and Valle d'Aosta. However, data referred to Basilicata, Calabria and Sicily regions represent an underestimate, compared with the actual instability situation because, to date, the landslide survey activities have been concentrated mainly in urban areas or zones with main road- and rail- infrastructures. A certain lack of homogeneity of landslide data, which may be noted from an analysis of Figure 8, is due not only to the different levels of detail of the previously existing inventories, but also to the greater or lesser degree of the use of the aerial photo-interpretation and field surveys, as well as to the use of the historical research and archives in the methodologies adopted by each Region and self-governing Provinces (ISPRA, 2008).

Concerning the landslide risk analysis in Italy, a preliminary evaluation of the level of attention with regard to the landslide risk on a municipal basis was carried out by using information contained in the Italian Landslide Inventory Project (IFFI) database and the Corine Land Cover Project 2000 (Fig. 8) (ISPRA, 2008; Trigila and

Iadanza, 2008). As a result, the attention level at the municipality scale was obtained overlapping landslides and vulnerable elements layer. 5708 Italian municipalities, out of a total of 8101 (70%), are affected by landslide phenomena, 2940 of which show a very high attention level (landslides intersection with urban texture and industrial-commercial settlements), 1732 a high attention level (landslides interference with lifelines, waste dump sites, construction works..), 1036 a moderate attention level (farmed land, woods, urban green areas and playgrounds), and 2393 municipalities have a negligible attention level (absence of landslide phenomena).

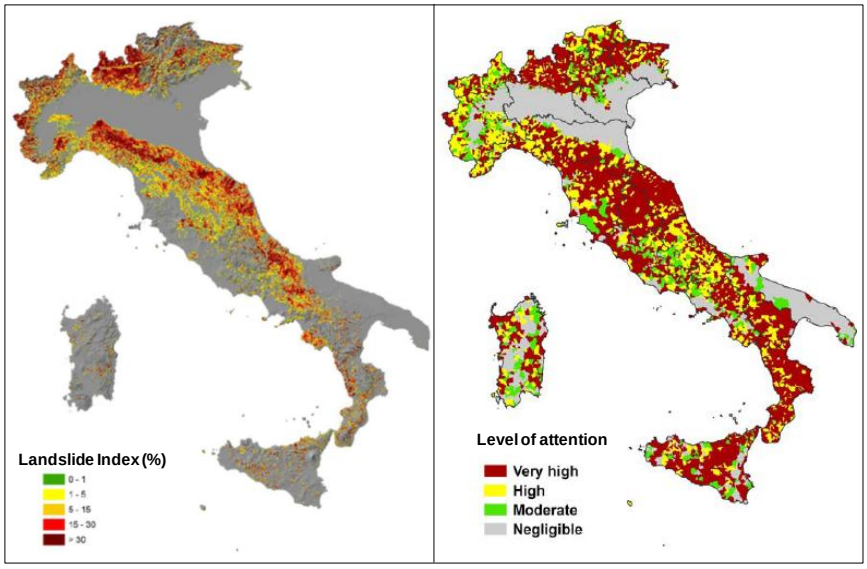

Fig. 8 - Landslide Index and risk in Italy: (left) Landslide Index (%) calculated over 1 km wide grid; (right) Level of attention with regard to landslide risk, on a municipal basis (Modified from ISPRA, 2008).

The landslide impact and risk of landslides at a national scale in Italy have been statistically analyzed also by Guzzetti (2000, 2006), Guzzetti et al. (2005) and Salvati et al. (2010), exploiting databases on occurred historical and recent landslides collected in recent years by the National Research Council (CNR). Due to its great variety of physiographical settings, landslide risk in Italy is not evenly distributed. By analyzing the period between 1900 and 2002, Guzzetti et al. (2005) find that northern Italy experienced the largest number of fatalities for landslides (especially Piedmont and Trentino-Alto Adige) mostly due to the larger territory (39.9% of the country), to the meteorological, morphological and to geological settings, and that the density of fatal events is highest in southern Italy (Campania and Calabria regions).

Despite landslides represent a widespread and a serious threat to human life all over the world, the related risk perception is very low. Consequently, knowledge of location, extent, typology, intensity, style and state of activity of landslide processes is strictly required, especially in those areas where property, infrastructures and human lives are exposed. The awareness and understanding of landslides spatial distribution and temporal evolution are mandatory both to plan mitigation works and to ensure a proper level of safety to people living in the affected areas. This information, combined with the vulnerability of the elements at risk, facilitate the knowledge of the expected losses in case of landslide occurrences, providing also an estimation of the number of people exposed to landslides.

A correct and careful knowledge of a phenomenon is the first step towards its proper understanding and for preventing potential disasters. Citizens represent the ultimate users of the hazard and risk management services, as they are affected by risk and can benefit from proper mitigation strategies, or suffer the consequences of inappropriate policies and actions. Thus, citizens can take advantage of information on where, when and to which extent the ground instabilities take place. Hence, one of the most important duties of the scientific community and responsible authorities is to make the population aware of proper behaviors

and procedures to adopt if a landslide occurs, by leading awareness and preparedness campaigns and establishing simple rules on how to prevent or minimize the damage induced by landslide phenomena.

State-of-the-art in satellite-based Earth Observation (EO) data and current global status of EO data-based landslide research and applications are included in the work reported in the **Annex 1**, edited after the International Forum on Satellite Earth Observation and Geohazards (the Santorini Conference), organized and chaired by ESA in association with the Group on Earth Observations. In this work, perspectives over the coming 5 to 10 years concerning how satellite EO data can contribute to geohazard and disaster risk reduction in landslide-prone and -affected areas are also tackled, as well as an insight into the objectives and needs of the geohazard community.

Annex 1: Ph. Bally Ed. (2012), "Scientific and Technical Memorandum of the International Forum on Satellite EO and Geohazards", 21-23 May 2012, Santorini Greece. doi:10.5270/esa-geo-hzrd-2012,59-80.

Chapter 3

Remote sensing techniques

Remote sensing and interferometric radar approach based on EO data represent a powerful tool to detect movements on the Earth's surface. Air- and space-borne Differential SAR (Synthetic Aperture Radar) Interferometry (DInSAR), which exploits the phase difference of two SAR images gathered at different times on the same area, has been widely used since late 1980s to measure surface deformation over large areas (Zebker et al., 1986; Gabriel et al., 1989). The conventional DInSAR is limited by atmospheric effects, temporal and geometrical decorrelation. Advanced multi-temporal interferometric approaches, like PSI (Persistent Scatterer Interferometry) techniques, overcome these limitations, analyzing long temporal series of SAR data, and providing annual velocities and deformation time series on grids of stable reflective point-wise targets, called Persistent Scatterers or PS (Ferretti et al., 2001). Starting from the first PSInSAR technique produced by Tele-Rilevamento Europa (T.R.E.) (Ferretti et al., 2001), many other different multi-interferogram processing approaches have been developed across time (e.g. CPT, IPTA, SPN etc.).

Moreover, some limitations associated to space-borne SAR interferometry can be overcome with the Ground Based InSAR (GBInSAR) techniques, where the radar sensor is allocated on a terrestrial instrument (Canuti et al., 2004).

Nowadays, SAR interferometry is so far a modern and well consolidated remote sensing technique. Its basic principles have been well documented and in the last decade its capabilities of measuring ground displacement have been more and more tested, implemented and improved. Being utilized as measurements tools for more than 10 years in many applications fields and benefitting from the great availability of different satellites and SAR images, radar satellite data analysis has become a reliable, standard tool within many research projects and activities. In this section, a state of the art of these radar remote sensing techniques is provided.

3.1 Radar remote sensing system and SAR (Synthetic Aperture Radar)

The word "RADAR" itself is an acronym for *RAdio Detection And Ranging.* Radar is nowadays commonly defined as an active object-detection system that operates with a beam of microwaves of the electromagnetic spectrum (Fig. 9).

Remote sensing is simply defined as the approach of obtaining information without physical contact (Lillesand and Kiefer, 1987).

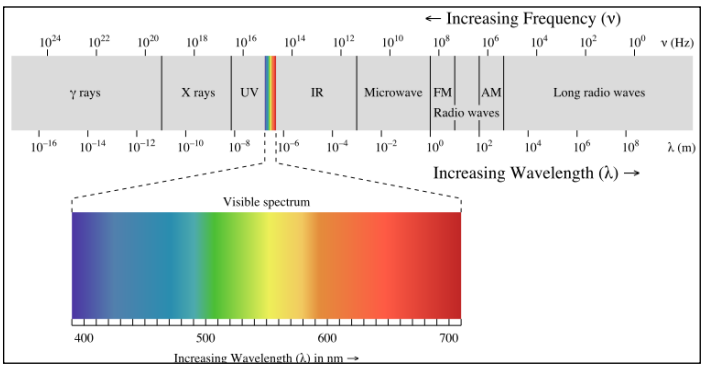

Fig. 9 - The electromagnetic spectrum. From http://en.wikipedia.org.

Radar systems were initially developed in the first half of the 20th century to determine the position or path of a moving object like an ocean-going vessel or an airplane. Pulse compression signal processing techniques have been traditionally used to improve the signal to noise ration and then locate targets with an error of few meters (Cumming and Wong, 2005).

Radar systems illuminate the source and receive back signals, characterized by lower frequency and longer wavelength with respect to the electromagnetic 'visible' range, by means of a transmitting and receiving antenna. Radar sensors are capable of penetrating clouds because they use microwaves and have day-and-night operational capabilities because they are active systems that can operate independently from weather conditions and illumination. Radar sensors are hosted on aircrafts or on satellite systems.

When detecting targets, the resolution is defined as the capability of a sensor to identify as separate two closely spaced scattering objects. Concerning radar systems, when two objects are too close each other, they are simultaneously within the same radar beam. Thus, they return reflections together and their backscattered signals are recorded by the receiving antenna at the same time. Conversely, when two targets are sufficiently far apart one another, then they are illuminated by different radar beams, so they cause reflections at different times and their echoes are received separately.

The resolution of radar sensor in the direction parallel to the flight of the satellite (azimuth direction) depends on the width of the radar beam(b), which depends on the employed wavelength (λ) and on the physical (i.e. real) length L of the transmitting antenna:

$b = \lambda / L$

Taking into account the distance (R) between the sensor and the target, the azimuth resolution ($R_{azimuth}$) for a real aperture radar system is given by:

$R_{azimuth} = R^* b$

Real aperture radars hosted by satellite platforms do not provide suitable resolution. For instance, given a beam width of 10 milliradians, at a distance of 800 kilometres, the azimuth resolution will be 8 km. For such systems, azimuth resolution can be improved increasing the length of the physical antenna used to illuminate the target scene or by using a shorter signal wavelength. The decrease of the wavelength would lead to a higher atmosphere and cloud impact on the capability of imaging radars. On the other hand, from antenna theory, the area illuminated on the ground is inversely proportional to the physical shape and dimensions of the antenna (Skolnik, 2001). Therefore, to obtain fine azimuth resolution in real-aperture radar systems (in the order of few meters), it would be necessary a very long physical antenna, e.g. some kilometers long.

SAR (Synthetic Aperture Radar) approach was developed to overcome the main limitation of real aperture system. Thus, SAR is an alternative solution to using a long physical antenna. The SAR concept separates two targets at the same range but different azimuth positions by their different relative velocities with respect to the moving platform. The reflected monochromatic waves from two different scatterers in the same illuminated beam have different Doppler shifts or phases associated with them. Using the knowledge of the path of the imaging platform, we can compute the exact phase history for every point target on the ground. We combine information from multiple echoes, effectively creating a synthetic longer aperture to separate targets within the same illuminated beam. Resolution is dependent on the total amount of phase information available for each target. The longer a target is illuminated, the better is our ability to resolve it. In other simpler words, SAR system achieves fine azimuth by using a small antenna and "long" wavelengths, on the order of few centimeters. Moreover, retrieved information is independent from the sensor-target distance. SAR is usually implemented by exploiting the forward motion of the aircraft or spacecraft. A single beam antenna, few meters long, is used. From different positions in distinct instants, the antenna repeatedly illuminates a target scene. Individual echoes, received successively at the different antenna positions, are recorded, stored, combined and then processed together, simulating a "synthetic aperture", to provide a finer azimuth resolution (Hooper, 2006) (Fig. 10).

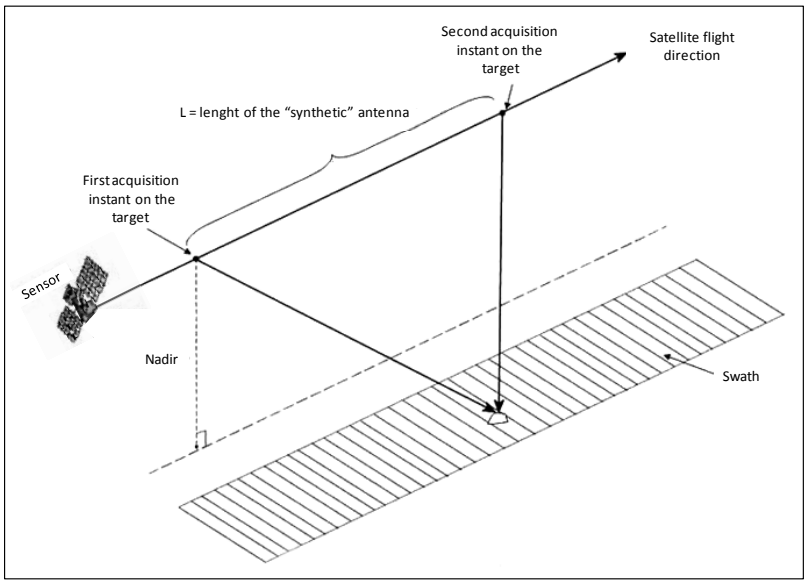

Fig. 10 – SAR system: the sensor, observing repeatedly the target and recording back the echo, reproduces a long antenna L, obtaining an high resolution image (From http://treuropa.com).

SAR is an extension of the "classical" radar techniques that create a highly directional beam using sophisticated signal processing to combine information from multiple echoes to accurately estimate the azimuth position of the target as well. The "synthetic aperture" concept allows a good spatial resolution (i.e. on the order of meters) with relatively small physical antennas.

The SAR processing is the transformation of raw SAR signal data into a spatial image. There are numerous published algorithms (Soumekh, 1999; Cumming and Wong, 2005) that can be used to process the recorded echoes to create high resolution images using the SAR concept. A review of these image processing implementations is provided by Bamler and Hartl (1998). The output from SAR processing algorithm is a single look complex (SLC) image, a two dimensional array of complex numbers, representing the brightness and phase of the scatterers on the ground. The indices of pixels in the matrix are directly related to the azimuth and range position of the scatterers with respect to a reference point on the platform's path.

SAR is an excellent tool for high resolution remote sensing of the Earth's surface from space. After experimenting with air-borne SAR instruments in the 60s and 70s, NASA launched the first space-borne SAR satellite SEASAT in 1978 for ocean studies (Fu and Holt, 1982).

A spaceborne (or airborne) SAR imaging system is sketched in Figure 11. A satellite carries a radar with the antenna pointed to the Earth surface in the plane perpendicular to the orbit. The inclination of the antenna with respect to the nadir is called "Off-nadir angle" and it is supposed to be equal to the "incidence angle" of the radiation on an assumed flat horizontal terrain. Spaceborne SAR systems typically have a fixed right side-looking antenna that illuminates an area on the ground (the "antenna footprint"), along the sensor's track, with a series of monochromatic microwave pulses. The platform's flight direction is called the "azimuth direction" and the direction of the main lobe of the transmitting antenna is called the "ground range direction". The satellite-to-target direction is usually called the "slant-range" direction (Hooper, 2006).

As the spacecraft moves, SAR sensor emits a stream of radar signals and the illuminated footprint sweeps out and traces a "swath" (area seen on the ground), in the ground range direction, on the earth surface. The imaging geometry shown in the Figure 11 is called the Stripmap mode and it s the most common one. Modern phased-array antennas implement complicated data acquisition strategies, e.g. ScanSAR and Spotlight SAR, to increase the area imaged by the radar platform, as better described below.

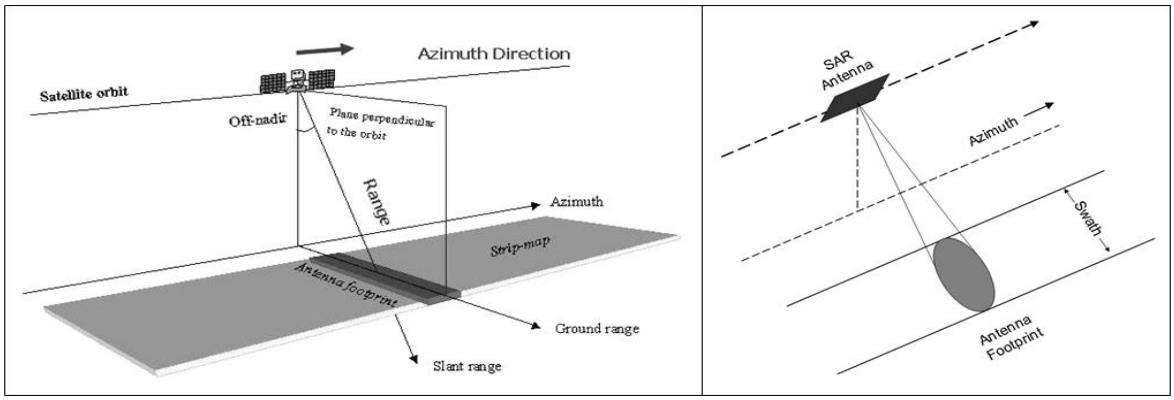

Fig. 11 – Satellite SAR system and imaging geometry (Modified from http://treuropa.com).

Radar signals are transmitted in pulses. The SAR system detects echoes of previously transmitted pulses, scattered from the Earth. The echoes are collected by the receiving antenna, which records the signal corresponding to each pulse, backscattered by the earth's surface back to the satellite. The raw data collected by the SAR are then transformed to form a spatial image. This is achieved in the direction perpendicular to the flight direction (range) through knowledge of the time delay, and in the flight direction (azimuth) through combination of echoes from multiple locations to synthesize the large antenna aperture. In range direction, bandwidth is provided by the nature of the pulse, whereas in azimuth direction, bandwidth is provided by the variation in frequency due to the Doppler effect associated with the movement of the sensor relative to the Earth.

Microwave signals emitted by SAR sensors have a specific central frequency, called "operating frequency", which characterizes signal propagation and penetration features. Hence, sensors work at specific bands of the microwave domain, corresponding to different wavelengths (λ).

Currently, the operational satellite SAR systems work in one of these microwave bands, commonly used in spaceborne radar applications: C-band (4-8 GHz, ≈5.6 cm wavelength), X-band (8-12 GHz, ≈3.1 cm wavelength) and L-band (1-2 GHz, ≈23 cm wavelength). Terrestrial radar remote sensing techniques usually use K_u band (12 – 18 GHz, ≈1.8 cm wavelength) (Tab. 3).

Band	Frequency range	Wavelength (λ)	Central λ
L	1 – 2 GHz	30-15 cm	23 cm
S	2 – 4 GHz	15-7.5 cm	10 cm
C	4 – 8 GHz	7.5-3.75 cm	5.6 cm
X	8 – 12 GHz	3.75-2.50 cm.	3.1 cm
Ku	12 – 18 GHz	2.5-1.67 cm	1.8 cm

Tab. 3 - List of commonly used microwave bands.

Satellites that carry platform hosting the SAR sensors orbit around the Earth at an altitude ranging from 500 to 800 km above the Earth's surface, following sun-synchronous, near-polar orbits, slightly inclined with respect of Earth meridians.

The angle between north-south direction (nadir) and the satellite orbit varies slightly in a range of about 10 degrees, depending on the satellite. The direction along the trajectory of the satellite is called azimuth, and the direction perpendicular to azimuth is called ground range (or across-track). The slant-range represents the direction along the sequence of rays from the radar to each reflecting point in the illuminated scene. The 'sensor to target' direction is called 'Line Of Sight' (LOS) and it is inclined of an angle 'θ' with respect to the vertical. 'θ', the off-nadir angle (or look angle or incidence angle), varies accordingly to the satellite employed

and usually can range from 23° to 45°. In Figure 12a, the geometry acquisition of ESA's ERS satellite is shown as representative example.

The satellite circumnavigates the Earth and travels northwards on one side of the Earth and then toward the southern pole on the second half of its orbit. These are called ascending and descending passes, respectively. Observation of the whole Earth's surface is achieved by combination of the orbital satellite motion along meridians (almost polar orbits) and the Earth's rotation in the equatorial plane. This possibility comes from the fact that during orbits that go from South to North (ascending geometry) and from North to South (descending geometry), the SAR antenna pointing is usually fixed to the same side of the orbital plane with respect to the velocity vector (the radar antenna is always pointed to the right side of the track). Thus, the same scene on the ground is observe by the SAR sensor from the East during the descending passes and from the West during the ascending passes (Fig. 12b).

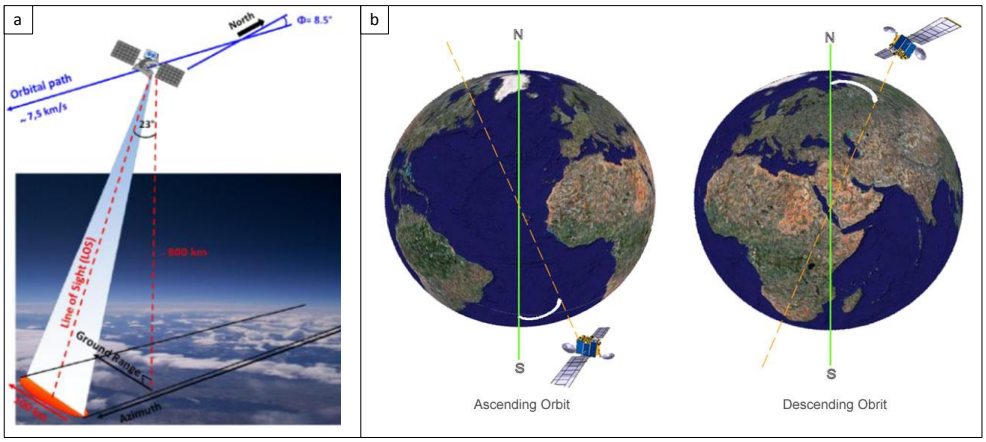

Fig. 12 - SAR sensor acquisition geometries: (a) SAR imaging geometry, example of ERS satellite (From: http://esrl.noaa.gov); (b) The two acquisition orbits (From http://treuropa.com/technique/sar-imagery)

SAR sensors can only acquire images at the frequency of the satellite repeat orbit. The time taken for a satellite to re-pass over the same area is called the 'revisiting time'. Typical repeat cycle for the main currently exploited satellites range from 44-46 days in L-band (e.g. ALOS and JERS-1), to 24-35 days in C-band, and to 16-4 days for new generation X-band modern sensors.

In the last 20 years, several different radar satellite missions have been launched providing different types of SAR images that can be used for ground movement detection and monitoring. Consequently, today many satellite interferometric data are available, including both historical archives acquired since the early 1990s (e.g. ERS 1/2 and JERS data) and images from currently operating satellites (e.g. RADARSAT 1/2, TerraSAR-X, COSMO-SkyMed). The main available past and present SAR missions and future missions are overview below, in Figure 13.

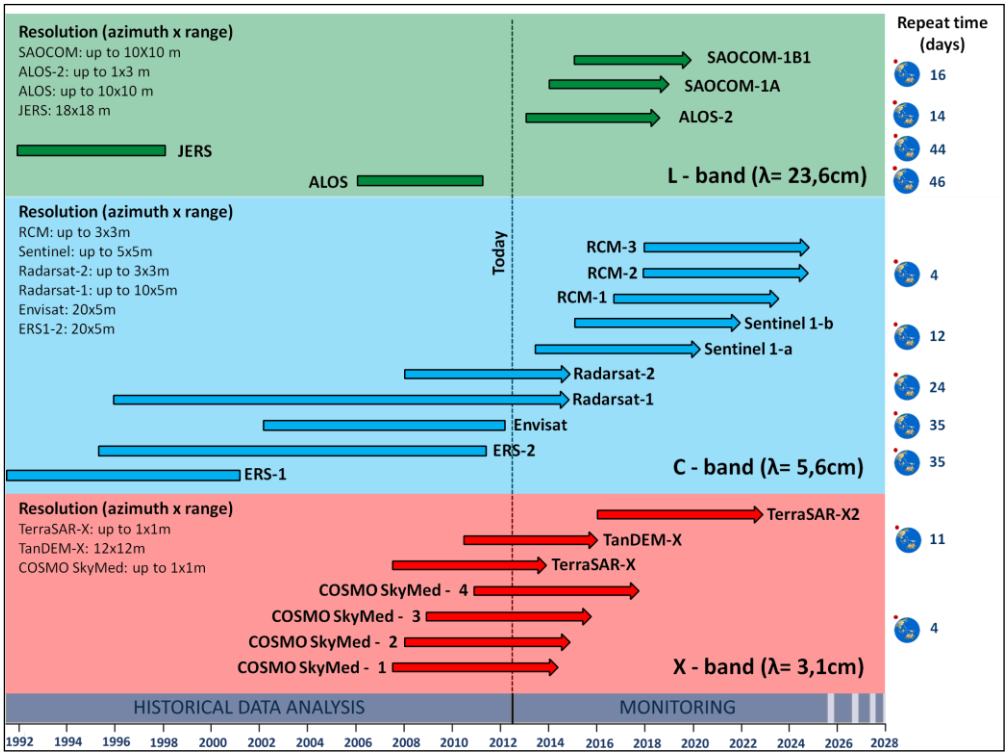

Fig. 13 - Satellite missions for interferometric applications

First SAR radar images were acquired in C-band. The main satellite systems equipped with C-band sensor are ERS-1, ERS-2, ENVISAT satellites belonging to the European Space Agency (ESA) and RADARSAT-1, RADARSAT-2 of the Canadian Space Agency (CSA). ESA missions are characterized by a wide area coverage of 100x100 km, a spatial resolution with pixel dimension of 20x5 m, a repeat cycle of 35 days and the availability of an extensive historical archives of SAR images beginning in 1992.

RADARSAT-1 (which acquires *on demand*) and RADARDAT-2 data show a greater acquisition flexibility due to variable incidence angle and swath range (depending on the 7 different acquisition modes and beams) and have a better revisiting time (24 days) with respect to ERS and ENVISAT satellites.

In the next future, the RADARSAT Constellation Mission (RCM) will be operative, consisting of three-spacecraft fleet of EO satellites, whose launch is scheduled for 2018. Sentinel-1 (ESA) is a two satellite constellation that will provide C-Band SAR data continuity following the retirement of ERS-2 and the end of the ENVISAT mission.

The X-band satellite systems are the new generation sensors. The main X-band operating satellites are TerraSAR-X and COSMO-SkyMed, launched in 2007 by the Italian Space Agency (ASI) and the German Aerospace Centre (DLR), respectively. The launch of these new sensors has improved the spatial resolution of the acquired SAR images, being up to 1x1 m the pixel dimension. Other important advantages of both the current systems are that the satellite look angle and the swath can be changed within the configuration mode, and that the acquisition frequency of SAR images is reduced, e.g. the revisiting cycle is 11 days in the case of TerraSAR-X and 16 days in the case of COSMO-SkyMed (that can be reduced to 4 days, if all the 4 satellites of the system are working).

Concerning L-band, ALOS (Advanced Land Observing Satellite) is a Japanese multi-sensor mission, built by the Japan Aerospace Exploration Agency (JAXA) for remote sensing, launched into orbit in 2006 and operating until 2011, equipped with PALSAR (Phased Array type L-band Synthetic Aperture Radar) sensor, which follows JERS-1 (Japanese Earth Resources Satellite-1) mission finished in 1998. The swath width is 20-350 km, depending on the variable incidence angle (from 10 to 60°), with a spatial resolution of 10 to 100 m both in azimuth and range.

Next future missions such as SAOCOM (SAtélite Argentino de Observación COn Microondas, Spanish for Argentine Microwaves Observation Satellite) satellite constellation by CONAE (Argentine Space Agency) and ALOS-2 by JAXA will be equipped with L-band SAR.

Basically, there are three operating acquisition modes of SAR system: Stripmap, ScanSAR and SpotLight (Franceschetti, 1999). The most simple and popular is the Stripmap mode, since has been the acquisition type of early spaceborne systems (ERS1/2, and JERS-1). In this case the radar looking angle is fixed. Antenna points along fixed direction to one side of the flight platform path (cross-track direction). As platform moves, the antenna footprint covers a relatively narrow strip (e.g. 70 and 100 km wide swath for JERS1 and ERS1/2, respectively).

The more recent family of SAR satellite platforms (RADARSAT 1/2, ENVISAT ASAR and ALOS Palsar) was designed to acquire images in both Stripmap and ScanSAR mode. Spaceborne radar applications exploiting ScanSAR images are ideally suited for mapping and monitoring large areas displacements. ScanSAR mode can achieve a wide swath coverage, periodically sweeping the antenna look angle. As platform moves, the antenna has the capability to illuminate several sub-swaths (in the cross-track direction), increasing the width of the image swath up to 400–500 km. Moreover, ScanSAR can acquire images for a given target area more frequently than Stripmap mode, significantly improving the temporal resolution of deformation mapping. Nevertheless, according to Monti Guarnieri and Rocca (1999), lower resolution images are obtained by operating in the ScanSAR mode, since the increased coverage led to a loss in the azimuth resolution. Typical swath widths of RADARSAT 1/2, ENVISAT ASAR and ALOS PALSAR images are 500, 400 and 350 km, respectively. Up to now, ScanSAR is the established mode in SAR for wide-swath imaging. However, the mode has several drawbacks caused by the focusing of the same target from different portions of the antenna (Meta et al., 2010). More accurate description of benefits and disadvantages of ScanSAR mode are included in Monti Guarnieri and Prati (1996), Moreira et al. (1996) and Holzner and Bamler (2002).

The Spotlight mode is the most modern SAR version of imaging radar and can provide imagery with high spatial resolution. Higher resolution is obtained by pointing the radar look angle to keep the target area within the illumination beam for a longer time. Thanks to a longer synthetic aperture, Spotlight SAR considerably enhances the capability of SAR sensor of acquiring high-resolution imagery, although the expense of spatial coverage. The newest X-band satellite generation (TerraSAR-X and COSMO-SkyMed) is capable of acquiring images in Stripmap, ScanSAR and SpotLight mode, achieving in the last case an image pixel resolution of up to 1 m.

Eventually, TOPS (Terrain Observation with Progressive Scan) (De Zan and Monti Guarnieri, 2006) is a further acquisition mode. It is a wide-swath mode that overcomes the limitations imposed by the ScanSAR mode. During the acquisition, the antenna is steered along the track from backwards to forwards, so that every target on the ground is observed with the complete azimuth antenna pattern. The TOPS mode was first demonstrated in orbit by TerraSAR-X (Meta et al., 2010). The TOPS mode is a promising mode of wide-swath SAR operation for future SAR satellite missions and it will be the default mode for the ESA Sentinel-1 SAR system.

A digital SAR image can be seen as a mosaic (i.e. a two-dimensional array formed by columns and rows) of small picture elements (pixel). Each pixel is associated with a small area of the earth's surface, called resolution cell. At full resolution, the value of each pixel in the image is related to the scattering properties of a resolvable path of the Earth. Specifically, it is the coherent sum of the echoes from all the individual scatterers (rocks, vegetation, buildings etc.) within the corresponding resolution cell projected on the ground. The location and dimension of the resolution cell in azimuth and slant-range coordinates depend only on the SAR system characteristics, so that the SAR image resolution depends on the sensor used and its acquisition mode. As pointed out before, oixel dimension ranges from 20x5m for ERS1/2 or ENVISAT satellites, up to 1m for the new X-band satellites (TerraSAR-X and Cosmo Sky-Med).

Each pixel value gives a complex number that has both amplitude and phase information about the backscattered microwave signal. The phase refers to the oscillation of electromagnetic waves of the radar signal and mainly depends on the sensor-to-target distance. The phase is not exploitable for a single image. The amplitude of the radiation backscattered by the objects towards the radar and contained in each SAR resolution cell depends on the reflectivity and intensity of the illuminated objects. Typically, exposed rocks or metal structures have a high capacity to reflect incident radar energy and thus the amplitude of the corresponding pixel is high. Reflectivity of smooth flat surface like water basin or soil is lower, so the amplitude of the reflected signal is lower. Besides the material, amplitude depends on the shape, size, orientation and moisture content of the scatterer, and, last but not least, on the characteristics of the radar beam (frequency, polarization and incident angle of the radar pulses).

The terrain area imaged in each SAR resolution cell (called the ground resolution cell) depends on the local topography, in the plane perpendicular to the orbit (ground range direction) and in the azimuth direction.

Distortions in radar images are frequent, especially when sensors illuminate target surfaces such as mountain slopes with high relief. These distortions are clearly visible as effects on radar images, whose appearance and information can significantly vary. The most common, well-known effects in radar images are *Foreshortening, Shadowing* and *Layover* (Fig. 14). As the terrain slope increases with respect to a flat horizontal surface (i.e. as the perpendicular to the terrain moves toward the LOS), ground resolution cell dimension in range increases. Thus, this terrain slope, facing the illumination of side-looking radar, is subject to a spatial distortion. This effect is called *Foreshortening* and it can be defined as a compression (shortening) of those slopes on the illuminated side of the beam. Shortened slopes appear bright-toned in the radar image. On the contrary, when the terrain slope is close to the radar off-nadir angle, the cell dimension becomes very large and all the details are lost. This happens when topographic surfaces on the opposite side of incoming beam generally are not illuminated and they suffer of *Shadowing* (dark-toned). The effect is more pronounced for sensors that use steeper incidence angles and for steeper slopes.

In some situations, the terrain slope exceeds the radar off-nadir angle, and so the scatterers are imaged in reverse order and superimposed on the contribution coming from other areas. In other words, the electromagnetic beam reaches the top of the slope facing the illuminating front before it reaches the foot of the slope. As a consequence, the top of the slope is reflected first to the receiving antenna and seems to be closer to the radar, in the slant range direction, than the lower portion of the slope. This is called *Layover* effect and it is most pronounced in near range field and for sensors with smaller incidence angle.

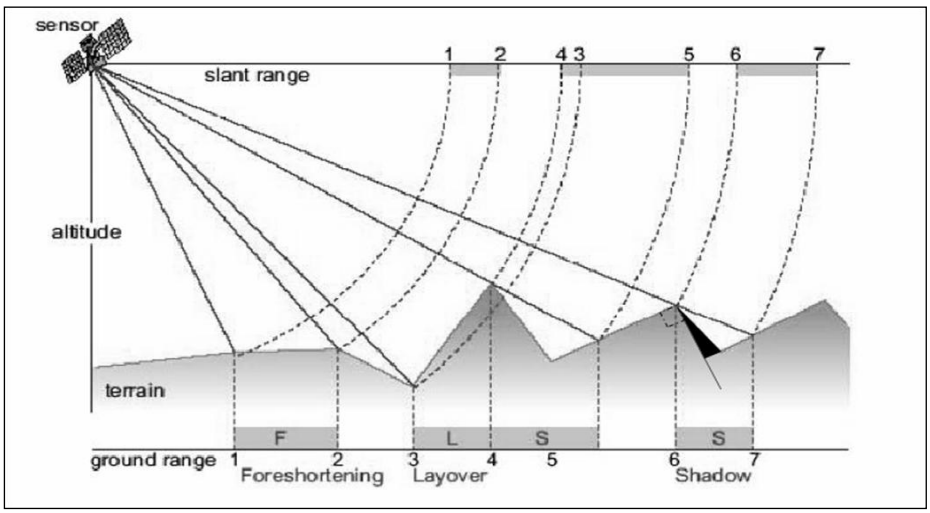

Fig. 14 – Effects of terrain topography, producing geometric distortions in SAR images.

The detected SAR image is generally visualized by means of grey scale levels, as shown in Figure 15, since available sensors operate with a single frequency. Bright pixels correspond to areas of strong back-scattered radiation (e.g. urban areas), whereas dark pixels correspond to low backscattered radiation (e.g. a quiet water basin).

Since several scatterers are present within each SAR resolution cell and since echoes can add both constructively and destructively, the amplitude values over a single image fluctuate around the nominal values for each pixel based on its radar brightness, which is known as the "speckle effect" (a visual effect of 'salt and pepper' screen) (Fig. 15).

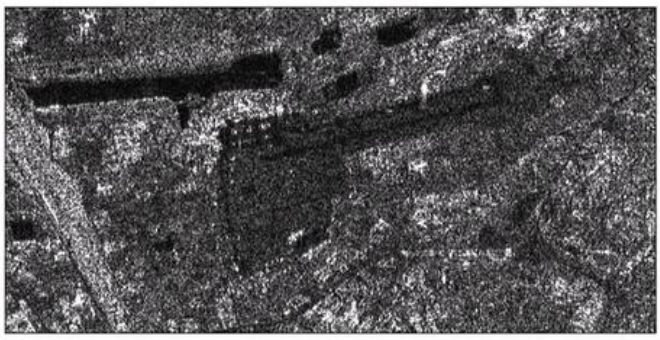

Fig. 15 - SAR amplitude image over Linate Airport, Milan. The speckle effect in the fields surrounding the airport is clearly visible (From http://treuropa.com/technique/sar-imagery).

As a result, an individual amplitude image will appear speckled. This is because each resolution cell is composed of many scattering elements, all reflecting incoming signals back to the satellite with different signal strengths and slightly different delays (phases), creating the spotty appearance.

Thus, pixel phase values for a single image are generally not useful. If a second image is acquired over the same area, either by a different sensor with similar specifications or by the same sensor at a different time, it can be "interfered" with the first image, which entails simply multiplying by the complex conjugate.

Generally, the second image is acquired from a slightly different position and it is the basis of the SAR interferometry approach, discussed below.

The principle of using space-borne SAR systems as "interferometers" dates back to early 1970s (Richman, 1971) and the first terrestrial interferometric SAR applications were in the late 1980s (Zebker and Goldstein, 1986). The launch of the ESA satellite, i.e. ERS-1 in 1991, leading to a large amount of SAR data becoming available, that made SAR interferometry widely applicable.

3.2 SAR interferometry (InSAR)

SAR imagery can be obtained either from airborne SAR systems equipped with two separate receiving antennas onboard the same platform (single-pass interferometry), or collecting data over the same test site on separate occasions, using one antenna onboard a platform that has slightly moved between two orbit acquisitions (repeat-pass interferometry). The latter approach is usually used: conventional Synthetic Aperture Radar Interferometry (InSAR) deals with the pixel-by-pixel phase difference of two acquisitions, gathered at different times with slightly different looking angles. In particular, InSAR is the measurement of signal phase change of two or more SAR images over the same scene, acquired at two different times and/or slightly different locations.

The recorded phase (ϕ) information is the key element to detect displacement occurred within the measurement time period. The phase values of a single SAR image (ϕ) depend on different contributions that can be summarized in the following equation (1):

$$\phi = \psi + (4\pi/\lambda)\,\Delta R + \alpha + \eta + \phi_{topo} \qquad (1)$$

Where:
ψ is the phase reflectivity (depending on the specific material and its geometry);
λ is the signal wavelength employed;
r is the sensor-target distance;
α is the phase contribution due to propagation of the microwave through the atmosphere;
η is a noise term of the acquisition system
ϕ_{topo} topographic distortions arising from slightly different viewing angles of the two satellite passes

The atmospheric effects (α) arise from the wavelength distortion that occurs when signals enter and leave a moisture-bearing layer. (ΔR) is any range (distance between the sensor and the target) displacement of the radar target.

If we ignore, for now, noise decorrelation effects, topography contribution and any difference in wave propagation through the atmosphere, the phase ϕ depends only on the sensor-to-target distance.

A single SAR image is of no practical use, since it is not possible to distinguish the different phase contributions related to reflectivity, topography, atmosphere and noise. The comparison of two SAR images is needed for InSAR approach and the resulting difference in phase (Δϕ) depends only on the change in path length. The difference between the two images is called *interferogram*. The SAR interferogram is generated by cross-multiplying pixel by pixel the first SAR image with the complex conjugate of the second (Rosen et al., 2000). Thus, the SAR interferogram amplitude is the amplitude of the first image multiplied by that of the second one, whereas its phase (*interferometric phase*) is the phase difference between the images. As a result, the interferogram is formed by the complex product of the two SAR images (called the *master* and the *slave*) and its phase, which is the most important information, contains contributions referred to atmosphere, topography, terrain deformation and noise.

The main purpose of InSAR is to retrieve and separate the different contributions. The resulting inteferogram represent as output very small slant range changes which can be related to topography and/or surface deformation (Klees and Massonnet, 1999). The use of InSAR technique dates back to 70s, when this approach was exploited for topographic estimation purposes (e.g. Graham, 1974; Zebker and Goldstein, 1986).

The distance between the two orbits of the satellite in the plane perpendicular to the track direction is called the *interferometer baseline*, its projection perpendicular to the slant range is the *geometrical (perpendicular or normal) baseline*: it is also the "distance" of the slave acquisition orbit with respect to the master. The difference in time between two acquisitions is the *temporal baseline* (Fig. 16).

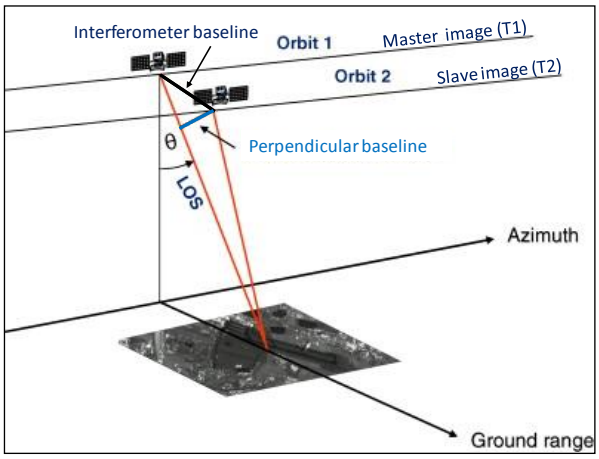

Fig. 16 - Interferometer and perpendicular baselines

3.3 Differential SAR interferometry (DInSAR)

The retrieval of the ground displacement in time that occurred between the two different SAR acquisitions can be achieved by Differential InSAR (DInSAR) within the repeat-pass interferometry method (Zebker and Goldstein, 1986; Gabriel et al., 1989; Massonnet and Feigl, 1998; Rosen et al., 2000). This approach is used when a pair of images is subjected to interferometric analysis for identifying terrain displacement and, afterward, for quantifying this movement (Fig. 17).

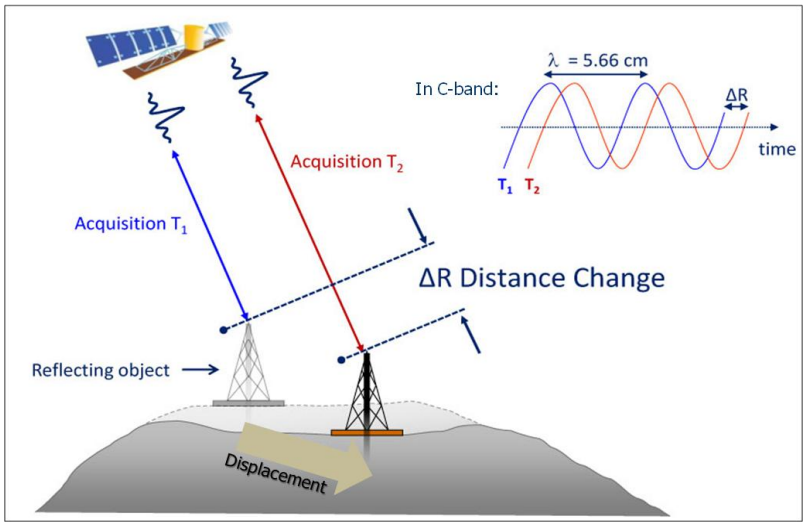

Fig. 17 - Schematic picture showing basic principle of DInSAR and the relationship between ground displacement and signal phase shift (Modified from http://treuropa.com/technique/insar-evolution).

Since in this case the ground displacement over time is the goal, topographic effects are removed and compensated by using a Digital Elevation Model (DEM) of the area of interest, creating what is referred to as a *differential* interferogram (the word "*differential*" here refers to the subtraction of the topographic phase contribution from the SAR interferogram) (Fig. 18). The equation can then be represented as follows:

$$\Delta\phi = \Delta\psi + (4\pi/\lambda)\,\Delta R + \Delta\alpha + \eta + \phi_{topo\text{-}res} \qquad (2)$$

$\Delta\phi$ is the *differential* interferometric phase; ΔR is the incremental distance from the sensor to the ground and back; α is the atmospheric contribution to phase shift. η is the noise and $\phi_{topo\text{-}res}$ is the residual topographic phase contribution, due to inaccuracy in the reference DEM used to retrieve information on ground surface.

DInSAR is the commonly used term for the production of interferograms from which the topographic contribution (ϕ_{topo}) has been removed.

Whenever the noise, reflectivity and atmosphere effect are low (i.e. decorrelation effects are negligible) and the phase contribution due to the local topography is accurately compensated for (i.e. ϕ_{topo} is negligible as well), then the remaining phase will be only due to any deformation of the Earth's surface between the two acquisitions (Fig. 17). This means that the interferometric phase can be referred only to the solely displacement occurred between the first and the second SAR acquisitions.

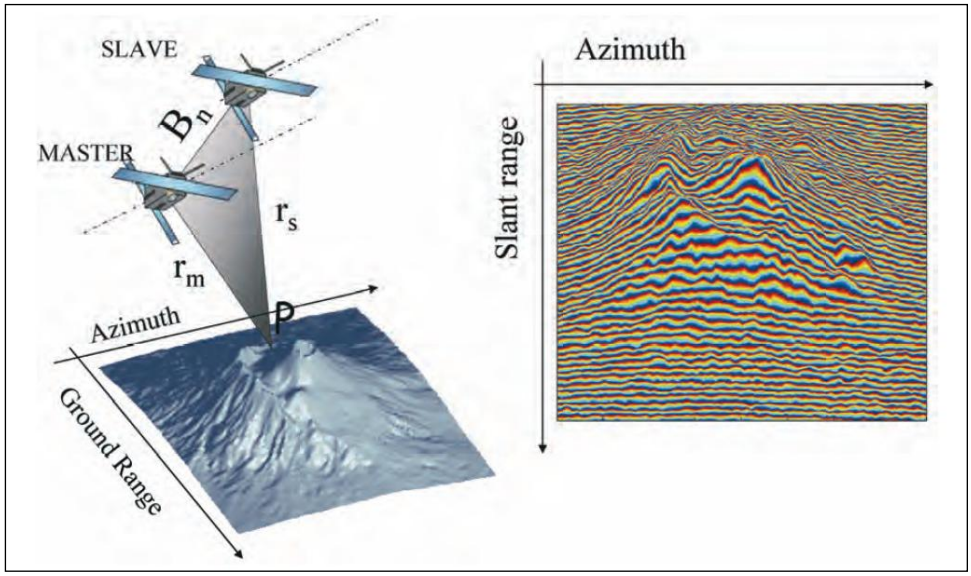

Fig. 18 Generation of a synthetic interferogram (right) based on a DEM (left) and on the knowledge of the sensor orbits and timing (Modified from Ferretti et al., 2007).

This is true only for very short temporal intervals and represent almost "ideal" conditions. Otherwise, the different, not negligible, factors can reduce or even compromise the quality and reliability of DInSAR results.

Firstly, the most significant limitation of conventional DInSAR is the atmospheric phase delay. There is a variation in the delay of the signal as it propagates through the atmosphere, which leads to the phase term ($\Delta\alpha$) that varies over the image, and that cannot be estimated through conventional DInSAR.

Additionally, differential interferograms suffer from temporal and spatial (geometric) decorrelation, due to the variation of the phase reflectivity ($\Delta\psi$) of some kinds of radar targets that are not coherent in time. Electromagnetic properties of natural terrain change more rapidly than urban areas or rocks. As the time lag between the two SAR acquisitions increases, the reflectivity cannot be considered identical in the two SAR image acquisitions, and so decorrelation increases. For example, vegetation shows scattering properties that change with time, leading to a loss of interferometric coherence ("temporal decorrelation"). Decorrelation also results from variations in imaging geometry. If the perpendicular baseline between the two spacecraft positions at the two time acquisitions is non-zero, this difference alters the measurement that does not repeat exactly. This phenomenon is called "spatial decorrelation" and increases as the spatial baseline increases.

Despite these limitations, Classical DInSAR has been widely used since late '80s to detect and quantify surface deformations occurred over large or small (i.e. few kilometres) areas within relatively short temporal period (Berardino et al., 2003; Catani et al., 2005; Strozzi et al., 2005). DInSAR analysis is useful to study relatively fast ground deformation and dynamic phenomena occurred in a short period of time, when compared to the satellite revisiting time (e.g. co-seismic displacements). The best results are achieved using several pairs of interferograms and restricting the analysis to small areas e.g. up to a few square kilometers.

Figure 19 depicts a simple scheme of how two images of the same area gathered from two slightly different across track positions, interfere and produce phase fringes that can be used to accurately determine the variation of the LOS distance.

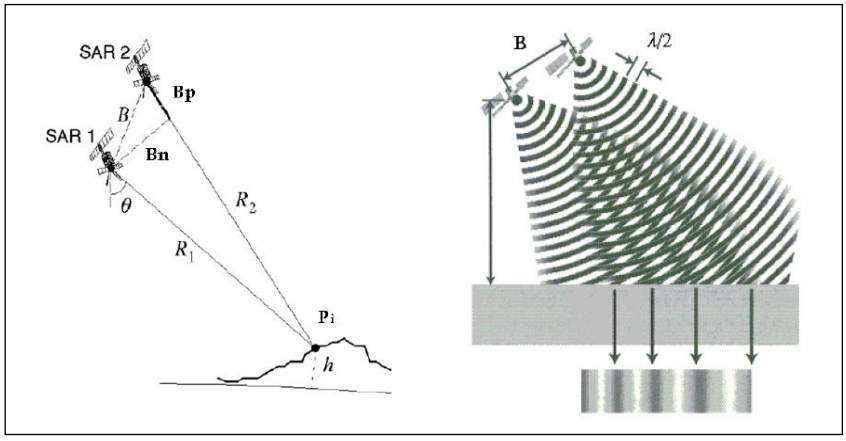

Fig. 19 - (Left) InSAR geometry. The along the track direction is perpendicular to the graph plane. (Right) the rationale of the fringes formation due to baseline (Modified from Sang-Ho, 2008).

Interferometric fringes can only be observed where image coherence prevails. When an area on the ground appears to have the same surface characterization in all the acquisition images, then the images are said to be coherent. If the ground surface is disturbed between two acquisitions (e.g. an agricultural field has been ploughed, tree leaves have moved positions etc.), then those sub-areas will result in noise and no information can be obtained. The term 'noise' is frequently used, standing for non-coherence, or decorrelation. The fringes visible in Figure 20 reveal areas with high coherence while the speckled areas represent very low coherence and noise.

The coherence of an interferogram is affected by several factors, including: topographic slope angle and orientation (steep slopes lead to low coherence), terrain properties, the time between image acquisitions (the longer the time interval the lower the coherence), the distance between the satellite tracks during the first and second acquisitions, also referred to as the baseline (larger baselines lead to lower coherence). Typical sources of decorrelation can be referred for instance to vegetation and rapid movements, as already mentioned before.

Coherence is measured by an index ranging from 0, when the area completely decorrelates, to 1, when the area is completely coherent. Overall, DInSAR analysis is successful, within an accurate deformation measurement, when the coherence index is between 0.5 and 1.0. Meaningful SAR results with coherence levels < 0.5 can also be obtained, but results will display increasing levels of noise and may show erratic deformation patterns from scene to scene, although movement trends are visible and generally reliable.

Wherever fringes occur, it is possible to calculate deformation by calculating the number of fringes and multiplying them by half of the wavelength. In the case of Figure 20 on L'Aquila site after the 2009 earthquake, C-band SAR was used and therefore each fringe should be multiplied by 28mm (one-half of the wavelength) to calculate the total apparent displacement (Fig. 20).

Comprehensive reviews of different DInSAR applications are provided by Massonnet and Feigl (1998), Rosen et al. (2000), Hanssen (2001), Crosetto et al. (2005).

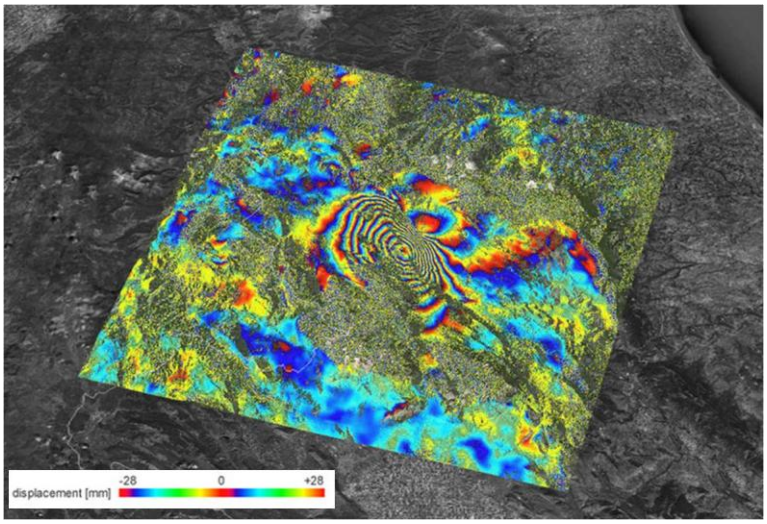

Fig. 20 - Co-seismic interferogram (using 2 satellite images) of the L'Aquila earthquake (Italy) on the 6th April 2009. Ground displacement is represented on a cyclic scale, with one full color circle representing 28mm of displacement. Data: ENVISAT (Feb. 2009 – Apr. 2009). Background image: Google Earth. (Modified from: http://treuropa.com/technique/insar-evolution).

3.4 Persistent Scatterer Interferometry (PSI

Effects of various decorrelation phenomena can be reduced by combining multiple SAR observations using what is called Advanced Multi-temporal DInSAR techniques. Thus, in order to overcome the limits of single-pair interferogram analysis (i.e. conventional SAR interferometry approach), namely the phase decorrelation and atmospheric effects, the multi-temporal inetrferoemtric approach such as Persistent Scatterer Interferometry (PSI) technique was developed in the late 1990's.

PSI can be seen as a multi-interferogram algorithm for DInSAR analyses. Atmospheric impacts on the estimated displacement values are removed or, at least, reduced using long temporal series of SAR imagery. The core purpose of long-term interferogram approach, i.e. PSI analysis, is to reconstruct the terrain topography and to monitor deformation phenomena by exploiting long series of SAR data acquired under different geometries and time lags.

The first PSI technique to appear, in 1999, was the PS Technique™, based on the PSInSAR™ produced by the Politecnico di Milano (Polimi) and licensed exclusively to Tele-Rilevamento Europa (T.R.E.) for commercial development.

PSI techniques need many multi-temporal spaceborne SAR images (at least 15-20), which are co-registered, and acquired on the same target area in many different acquisition dates, with a sampling depending on the repeat cycle of the employed satellite. The larger is the number of SAR images, more precise and robust are the results.

PSInSAR™ technique is a long-term multi-image interferometric approach firstly proposed and well explained by Ferretti et al. (2000, 2001). This approach is able to overcome major disadvantages of classical DInSAR (e.g. temporal decorrelation and atmospheric disturbances). Long temporal series enable the decoupling of height and deformation. Meanwhile, atmospheric artifacts can be estimated and moved out.

The main idea is to analyze the radar signal backscattered from an observed scene, identifying ground elements characterized by temporally stable electromagnetic features and by high reflectivity. These elements are called PS (*Permanent Scatterers* o *Persistent Scatterers*) (Ferretti et al. 2001). The accuracy of the height estimate depends on the normal baseline dispersion of the acquisitions. The wider is the range of the baselines, the better is the digital elevation model (DEM) estimate. High values of normal baseline are also a

source of decorrelation in correspondence of the Permanent Scatterers; thus, only almost-point-like scatterers are identified because they keep on being coherently imaged (Perissin et al., 2006) (Fig. 21).

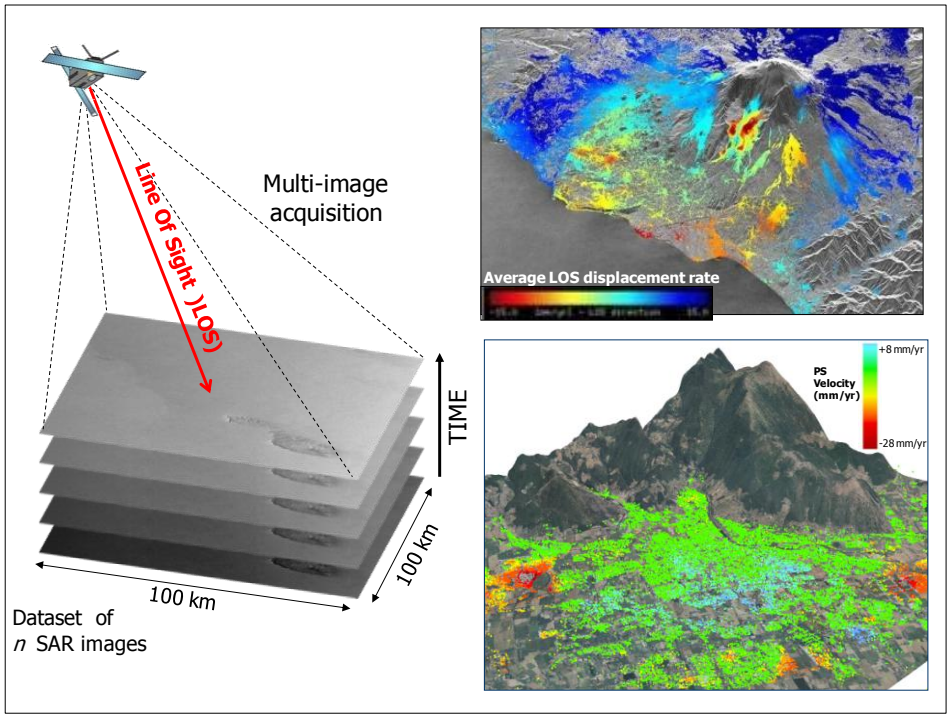

Fig. 21 – Basic principle of Advanced Multi-temporal DInSAR techniques.

Thus, for the development of PSI, the main need is to overcome the errors introduced into signal phase values by atmospheric artifacts. By examining multiple images, usually a minimum of 15 scenes, many interferograms are generated by selecting one of the scenes as a "master" to which all the other scenes become "slaves".

The process by which removal of atmospheric effects is achieved involves searching the imagery and interferograms for pixels that display stable amplitude and coherent phase throughout every image of the data set. They are referred to as Permanent, or Persistent, Scatterers. Thus, a sparse grid of these point-like targets characterized by high signal to noise ratios is identified across an area of interest on which the atmospheric correction procedure can be performed. Once these errors are removed, a history of motion can be created for each target.

Once removed the atmospheric effects, the interferometric data that remain are displacement values (measured along the satellite LOS) and noise, dependent on the quality of the reflector.

A Persistent Scatterer (PS) is defined as a radar target that reveals stable amplitude properties and coherent signal phase within a resolution cell, throughout all of the SAR images within a data stack. Thus, a PS corresponds to a resolution element containing a single dominant scatterer. PS point-wise targets exhibit reduced temporal decorrelation due to their high electromagnetic reflectivity and their coherent and stable scattering behavior. Having a stable radar signature, PS are only slightly affected by decorrelation effects and the backscattered radar signal is much higher than the noise of the sensor.

Amplitude data of backscattered signal are analyzed computing the so-called amplitude stability index, i.e. the ratio between the average amplitude referred to each pixel and its standard deviation (Ferretti et al., 2001). Identification of a grid of Permanent Scatterers Candidates (PSC, i.e., points that are expected having a PS behavior) is performed simply thresholding the amplitude stability index (Ferretti et al., 2001).

The interferometric phase is analyzed on a pixel-by-pixel approach. Stable radar benchmarks, namely the PS, are identified using a coherence map. Objects that make good PS are usually man-made structures (e.g.

buildings, dams, bridges, pylons, street lights, above-ground pipelines, any rectilinear structure that can create a dihedral signal reflection back to the satellite), as well as natural reflectors (e.g. rock outcrops, hard un-vegetated surfaces, boulders etc..).

The velocity of each single PS point target can be estimated by performing a statistical analysis on amplitudes of electro-magnetic returns. Signal analysis of the network of coherent PS radar targets, exhibiting high phase stability over the entire observation time period, allow estimating the displacements, acquisitions by acquisition, by distinguishing the different contributions related to ground motions from those due to atmosphere, topography and noise.

Referring to equation (3):

$$\Delta\phi = \Delta\psi + (4\pi/\lambda)\,\Delta R + \Delta\alpha + \eta + \phi_{topo} \qquad (3)$$

the subtraction of topographic information (ϕ_{topo}) from each interferogram can be performed through a conventional InSAR DEM that can be reconstructed thanks to the Tandem pairs (i.e. ERS-1/2 data with a temporal baseline of 1 day), or that can be taken from an already pre-existing DEM (e.g. such as the Shuttle Radar Topography Mission, SRTM or the ASTER Global DEM) and resampled on the master image grid (Ferretti et al., 1999). Then, in the equation (3), for each identified PS, the terms $\Delta\psi$ and η can be neglected. Therefore, the only problem to overcome is the assessment of atmospheric effect contribution. $\Delta\alpha$ is a term strongly correlated in space but not in time. Spurious atmospheric effects ($\Delta\alpha$) are estimated and removed throughout a statistical analysis of the signals and by applying specific algorithms:. The detailed description of PSInSAR^{TM} technique can be found in Ferretti et al. (2000, 2001, 2005) and in Colesanti et al. (2003a).

PSI techniques have been primarily exploited for the analysis of ground movements over urbanized areas, where the presence of man-made structures (i.e. buildings, roads, bridges, pylons) allow identifying a dense network of strong reflectors (up to several hundred per square kilometer). These stable targets allow retrieving estimates of the displacements along the satellite LOS, with unprecedented accuracy. Thank to this multi-interferometric approach, the LOS velocity for each PS can be estimated with millimeter precision that is fraction of the operating signal wavelength.

It is worth to highlight that all the measurements are made in the satellite's LOS radar beam and that are "relative" (not "absolute") measurements, both in space and time. This is because each measurement is referred temporally and spatially to respectively an unique reference image ("Master" image) and to a stable point ("reference point") supposed motionless. The master scene is chosen in order to maximize the total coherence of the interferometric stack and to keep the dispersion of the normal baseline values as low as possible. The selection of the reference point is made within a stable sub-area of the investigated area of interest.

The accuracy for the average LOS displacement rate on each PS is 0.1-1 mm/yr. Displacement time series can be retrieved, acquisition per acquisition, with accuracy on single measurements usually ranging from 1 to 3 mm.

The geocoding accuracy of PS points depends on the ground pixel resolution (a few meters, depending on the used satellite). For instance, the positioning precision for C-band ERS1/2 (pixel dimension: 20x5 m) is about ±7m in Easting direction, ±2m in Northing direction, and ±1.5m on the vertical axis. For X-band TerraSAR-X (pixel dimension: up to 1x1 m) accuracy is ±4m in Easting and ±1m in Northing and the vertical axis (Colesanti et al., 2003a).

As mentioned before, PSI started with the so-called Permanent Scatterer technique proposed by Ferretti et al. (2000). After this initial work, many other multi-temporal interferometric processing approaches were proposed for this technique in the following years in order to extract long-term stable benchmarks as PSI point

targets from multi-interferogram analysis of SAR data (Berardino et al., 2002; Arnaud et al., 2003; Mora et al., 2003; Werner et al., 2003; Hooper et al., 2004; Lanari et al., 2004; Kampes, 2006).

Although these advanced multi-temporal techniques were initially called "Permanent Scatterer techniques", now all of them, including the original Permanent Scatterer technique, are usually called "PSI techniques" (Persistent Scatterer Interferometry techniques), while the term "Permanent Scatterers" is exclusively associated with the original technique patented by Ferretti et al. (2001). PSI techniques are also called "Advanced multi-temporal DInSAR" to distinguish from the "Classical differential DInSAR" (Fig. 22).

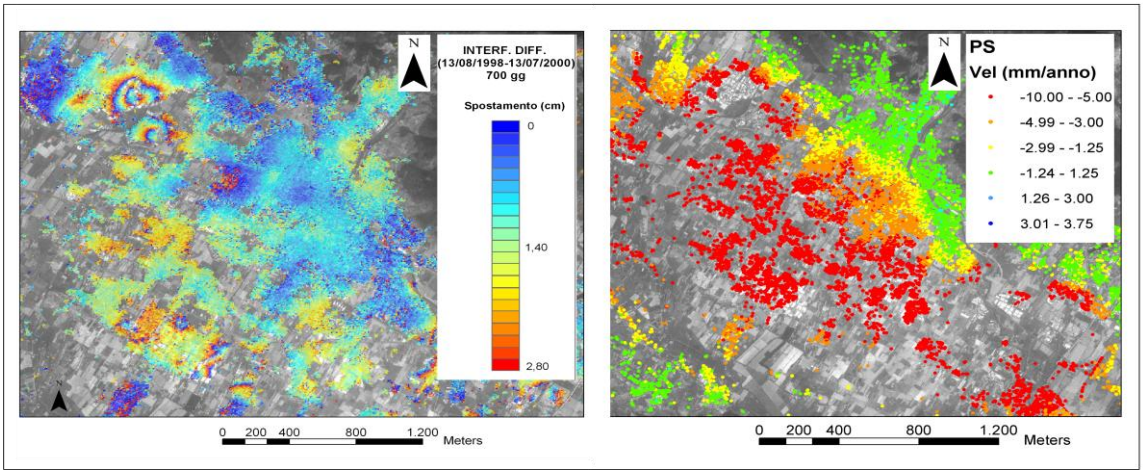

Fig. 22 – Classical DInSAR (differential interferogram, on the left) and Advanced multi-temporal DInSAR(PS targets, on the right) obtained from ERS SAR images on Firenze- Prato-Pistoia basin (Italy).

Actually, all the advanced multi-temporal interferometric approaches can be briefly classified into two groups: Persistent Scatterer (PSI) and Small Baseline (SB) methods.

PSI methods work by identifying image pixels in a stack of interferograms generated with the same master that are coherent over long time intervals (Ferretti et al., 2000; Hooper et al., 2004; Kampes, 2006). On the other hand, SB methods use SAR image combinations with a short spatial baseline to reduce the effects of spatial and temporal decorrelation (Berardino et al., 2002; Lanari et al., 2004) and they are used for processing long series of SAR imagery.

Each of these methods has its advantages and limitations, and they have both proved to be effective in successfully estimating deformation time series in various regions (e.g. Hilley et al., 2004; Hooper et al., 2007). In multi-temporal InSAR processing, both the PS and SB approaches are optimized to obtain ground displacement rates with a nominal accuracy of millimeters per year.

PSInSAR

Permanent Scatterer Interferometry (PSInSAR), proposed by Ferretti et al. (2001) and improved by Colesanti et al. (2003b), distinguishes itself from other SAR interferometric processing by the use of a single master image to generate a stack of differential interferograms without limitations in temporal or spatial baselines. PS candidates, which *a priori* carry reliable phase information across the interferogram stack, are selected based on their backscattering properties. On these points, the PS approach adopts essentially a model-based, temporal unwrapping strategy. Accordingly, *a priori* information on the displacement is necessary, from which a deformation model can be established. In general, the average linear displacement velocity and the DEM error are considered as the two major parameters of 2D linear regression of the wrapped phases. As temporal unwrapping is performed on local phase differences, the PS approach includes schemes to integrate in space relative displacement rates and DEM errors (Fig. 23).

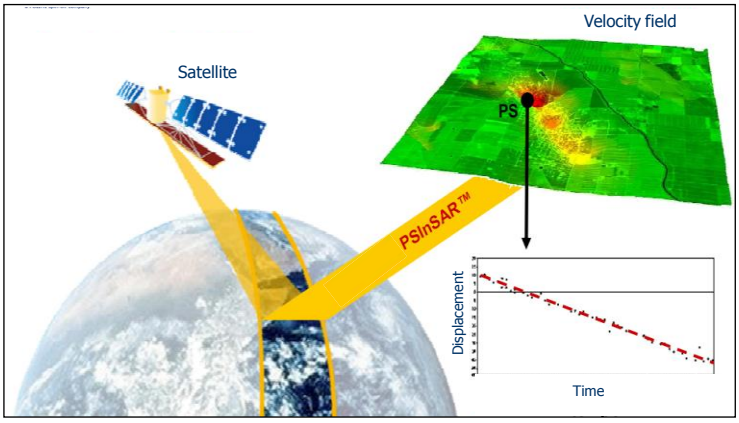

Fig. 23 - Representation of PSInSAR technique (From http://treuropa.com).

SBAS

The Small-BAseline Subset (SBAS) technique developed at IREA-CNR (Institute for Electromagnetic Sensing of the National Research Council of Italy) is a SB processing approach. The SBAS (Berardino et al., 2002; Lanari et al., 2004; Casu et al., 2006) computes the interferograms only for image pairs separated by small temporal and spatial baselines, in order to maximize the coherence. The spatial coverage is increased by taking into account the speckle properties of most targets in SAR images. Decorrelation noise in the interferograms is partly removed by range filtering of the non-overlapping part of the spectrum and by applying a spatial filter, thus reducing the interferogram spatial resolution. Unwrapped differential interferograms are combined through the Singular Value Decomposition (SVD) method (Berardino et al., 2002).

PSInSAR partially fails on rural and natural environments due to complete decorrelation of the great majority of scatterers. In order to extend the ability of PSI to natural settings, two different approaches have been developed: the SqueeSAR and the StaMPS techniques.

SqueeSAR

In 2010, T.R.E. developed the new SqueeSAR™ algorithm, which is an advance on the PSInSAR™ algorithm. SqueeSAR™ is a second generation PSInSAR™ analysis, exploiting both 'point-wise' PS and 'spatially distributed scatterers' (DS). DS are areas corresponding to rangeland, pastures, bare earth, debris fields and desert or dry soils. These targets do not produce the same high signal-to-noise ratios of PS, but are nonetheless distinguishable from the background noise and their reflected radar signals are less strong, but statistically consistent.

The SqueeSAR™ algorithm was developed to process the signals reflected from these low-reflectivity homogeneous areas, but it also incorporates PSInSAR™, hence no information is lost and movement measurement accuracy is improved (Ferretti et al., 2011). SqueeSAR™ also produces improvements in the quality of the displacement time series and has been successfully used in some works for analyzing ground motion (e.g. Raspini et al., 2013).

StaMPS

The Stanford Method for Persistent Scatterers (StaMPS), proposed by Hooper et al. (2004, 2007), utilizes the spatial correlation of interferogram phase to find persistent benchmarks. The StaMPS method was the first technique designed to extend the applicability of InSAR to non-urban environments and it is applicable to low-amplitude natural target (e.g. Sousa et al., 2011).

Other processing approaches (e.g. IPTA, PSP, CPT, SPN, STUN…) have been recently developed and extensively tested on SAR data, and are here briefly presented.

IPTA

The Interferometric Point Target Analysis (IPTA) was introduced by Werner et al. (2003) and Strozzi et al. (2006), developed at the GAMMA Remote Sensing Research and Consulting (Gümligen, Switzerland). This approach has the advantage in finding persistent benchmarks in low-coherence regions and can use large baselines for phase interpretation. A specific software, called IPTA GAMMA SAR, has been implemented (Werner et al., 2000) and devoted for processing raw data for both conventional DInSAR and PSI.

An important feature of IPTA is that even scene pairs with larger baselines can be used to obtain a more complete and reliable data on deformation history (Wegmuller et al., 2004; Strozzi et al., 2005; Strozzi et al., 2006).

PSP

The Persistent Scatterer Pairs (PSP) is a PS processing technique for the identification and the analysis of persistent scatterers in series of full resolution SAR images (Costantini et al., 2000). The central idea of the PSP method is to both identify and analyze PS working only with pairs of points ("arcs"). In this technique, atmosphere phase artefacts are effectively eliminated by exploiting their spatial correlation, but without using model based interpolations to remove orbital and atmospheric phase artefacts. This approach allows efficiently identify the persistent scatterers, and to retrieve the corresponding terrain height and displacement velocity.

CPT

The Coherent Pixel Technique (CPT) is a SB approach introduced by Mora et al. (2003) and Blanco-Sanchez et al. (2008). The CPT algorithm has been developed at the Remote Sensing Laboratory (RSLab) of the Universitat Politecnica de Catalunya (UPC). CPT enables an estimation of linear and non-linear components of ground deformation and can extract the displacement evolution over wide areas across time from a stack of differential interferograms. The CPT technique has been successfully applied to monitor subsidence and terrain deformation episodes (Tomàs et al., 2005; Duque et al., 2007).

SPN

The Stable Point Network (SPN) technique is a PSI technique developed by Arnaud et al. (2003) and Duro et al. (2005). It is the finding of a research projects between the CNES (French Space Agency), ESA and Altamira Information.

SPN focuses on pixels with stable and high-quality behaviour in SAR amplitude and in interferometric and spectral coherence. For any selected point, the temporal evolution of the displacement is extracted. Thanks to its ability of analyzing interferograms at reduced resolution (multi-look operation: 40×40 m pixel dimension), SPN algorithm is also suited for investigations in non-urban areas. Some examples of SPN algorithm in landslide or subsidence analysis can be found in Herrera et al. (2009a,b; 2011), Notti et al. (2010) and Crosetto et al. (2008a).

STUN

The Spatio-Temporal Unwrapping Network (STUN) algorithm was proposed by Kampes et al. (2006) for estimating displacement and topography at persistent scatterer points using an interferometric single-master data stack. In particular, it combines displacement model with spatial network for phase unwrapping, based on single-master interferograms.

WAP

The Wide Area Product (WAP) mapping was developed by the German Space Agency (DLR) in the framework of the ESA GMES Terrafirma project (Adam et al., 2011). The WAP technique was adapted by DLR for the processing of "wide areas". The WAP uses full frame ERS acquisitions with dimensions of about 100km by 100km and up to 1,000,000 points as a building block. The final product is a mosaic of full frames and can cover a country or even continents.

The WAP PSI-based approach is foreseen to be a standard level 1 product for the future Sentinel-1 mission with its TOPS mode acquisition scenario.

These main advanced multi-temporal interferometric processing approaches are summarized in Table 4.

Technique	Developer	References
Persistent Scatterer SAR Interferometry, **PSInSAR**	Tele-Rilevamento Europa (T.R.E.), Italy	Ferretti et al., 2000, 2001; Colesanti et al., 2003a, b
Small-BAseline Subset, **SBAS**	CNR-IREA, Italy	Berardino et al., 2002; Lanari et al., 2004; Casu et al., 2006.
SqueeSAR	Tele-Rilevamento Europa (T.R.E.), Italy	Ferretti et al., 2011
Stanford Method for Persistent Scatterers, **StaMPS**	Standford University, USA	Hooper et al., 2004, 2007
Interferometric Point Target Analysis, **IPTA**	Gamma Remote Sensing, Switzerland	Werner et al., 2003a; Werner et al., 2000.
Persistent Scatterer Pairs, **PSP**	Tele-Rilevamento Europa (T.R.E.), Italy	Costantini et al., 2000
Coherent Pixels Technique, **CPT**	Universitat Politecnica de Catalunya, Spain	Mora et al., 2003; Blanco et al., 2007.
Stable Point Network, **SPN**	CNES, ESA and Altamira Information	Arnaud et al. 2003; Duro et al. 2005
Spatio-Temporal Unwrapping Network, **STUN**	German Aerospace Center (DLR), Germany	Kampes et al., 2006
Wide Area Product, **WAP**	German Aerospace Center (DLR), Germany	Adam et al., 2011

Tab. 4 - List of the main advanced multi-temporal interferometric processing approaches.

3.5 GBInSAR

The Ground based SAR interferometry (GBInSAR) also referred as Terrestrial Synthetic Aperture Radar Interferometry (TInSAR) is based on the SAR technique similar to the one used on satellites, but implemented in a ground-based platform and usually transmitting/receiving radar signal in Ku microwave band. By the movement of the radar sensor along a linear scanner (i.e. a rail that allows precise micrometric movements of the sensor), 2D SAR images are derived. GBInSAR monitoring can be performed by installing the equipment at a stable location in a panoramic position, and it does not require the installation of contact sensors or reflectors in the monitored area.

At the end of the last century, the first prototype of this terrestrial technology was elaborated by the Joint Research Center (JRC) and licensed by LISA (LISA system) for landslide monitoring (Tarchi et al., 2003; Casagli et al., 2010), consisting of a coherent transmitting and receiving set-up, a mechanical guide, a PC based on data acquisition and a control unit (Tarchi et al., 1997). The transmitter and the receiver are mounted beside one another in a quasi-monostatic configuration on a mechanical linear rail, which is computer-controlled, synthesizing a linear aperture along the azimuth direction. The high-frequency front-end is based on a coherent up and down frequency conversion and can perform measurements in the C and Ku bands (Rudolf and Tarchi, 1999). The processing includes a coherent SAR algorithm and interferometric techniques. The sensor is characterized by an high degree of operative flexibility, in terms of acquisition frequency (i.e. few minutes), geometry, polarisation and easiness of installation.

In the last years, other different ground-based radar instruments have been realized, improving frequency and stability capabilities (Fig. 24), such as GBInSAR LiSALab instrument, IBIS-L instrument produced by IDS society (Noferini et al., 2005), which is able to generate microwave signals at definite increasing frequencies sweeping a radiofrequency band, the GAMMA portable interferometer produced by GAMMA Remote Sensing (Werner et al., 2008). Another new generation instrument is the Multiple-Input and Multiple-Output (MIMO) radar, based on the fact that independent signals are transmitted through different antennas, and that these signals, after propagating through the environment, are received by multiple antennas (Bliss and Forsythe, 2005; Sammartino et al., 2010; Tarchi et al., 2012).

The GBInSAR technology has been successfully used in several application fields, especially for unstable slope and single landslide monitoring (e.g. Leva et al., 2003; Luzi et al., 2006; Casagli et al., 2006; Bozzano et al., 2011). A valuable example can be found in the **Annex 2** (Bardi et al., to be submitted), in which GBInSAR data from the instrument installed at San Fratello site (Sicily) are integrated with PSI data.

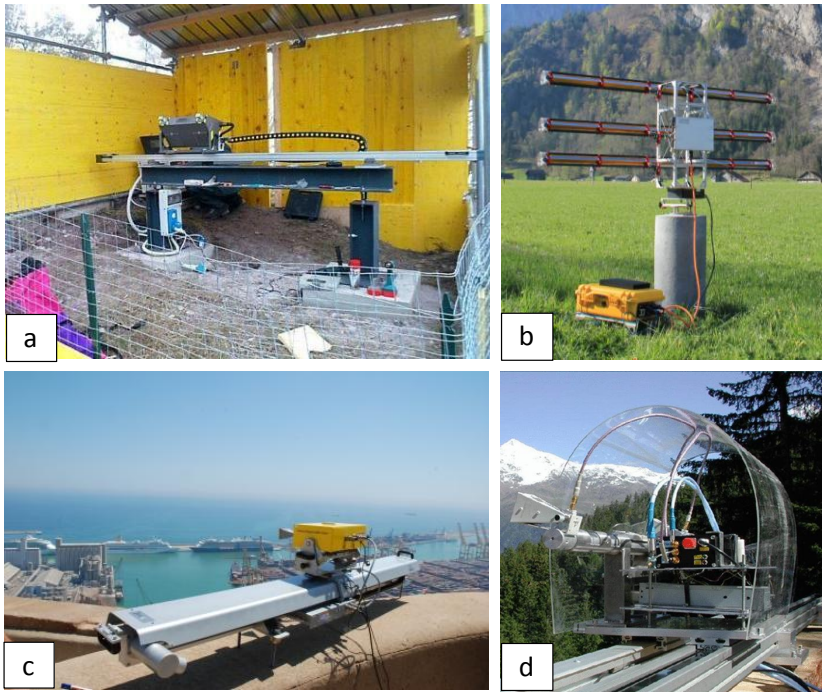

Fig. 24 - Different ground-based radar instruments: (a) GBInSAR LiSALab instrument; (b) GAMMA portable interferometer; (c) IBIS-L instrument; (d) Multiple-Input and Multiple-Output (MIMO) radar instrument.

Annex 2: Bardi F., Frodella W., Ciampalini A., Bianchini S., Del Ventisette C., Gigli G., Fanti R., Moretti S., Basile G., Casagli N. (to be submitted) Integration between ground based and satellite SAR data in landslide mapping: the case study of San Fratello (Sicily, Italy).

Chapter 4

Remote sensed applications for geo-hazard investigations

SAR interferometric technique, since its first applications dated back to the beginning of '90s, has demonstrated to be a powerful technique to retrieve precise measurements of ground displacements induced by different geophysical and geological phenomena, such as slow moving landslides, land subsidence, tectonic motions, and volcanic activity (Massonnet and Feigl 1998; Rosen et al., 2000). The reason of the technique success relies on its appeal mainly connected to the capability of measuring ground displacements with a millimetric-to-centimetric precision even over wide areas (Farina et al., 2006).

Landslide studies can greatly take advantage from remote sensing techniques, which allow systematic and easily updatable acquisitions of data over large areas, reducing costs and optimizing field work, thanks to their non-invasiveness, low cost-benefit ratio, wide area coverage and high precision.

The use of remote sensing data, whether air-, satellite- or ground-based radar, especially if combined with traditional geomorphological tools (field surveys, orthophotos analysis, *in situ* observations, ground monitoring systems etc..) can give a valuable and useful effort to the landslide-related studies, i.e. mapping, monitoring, and prediction.

Several European research projects exploit traditional and innovative Earth Observation (EO) combined with ground based (non-EO) data and technologies to improve analysis and understanding of ground displacement phenomena and to deliver products tailored on the needs of national, regional and local Civil Protection Authorities for managing the risks posed by these ground deformations.

In the last decades, several different satellite missions have been launched, providing different types of SAR images that can be used for ground movement detection and monitoring. Consequently, today many satellite interferometric data are available, including both historical archives acquired since the early 1990s (e.g. ERS 1/2, ENVISAT, JERS data) and images from currently operating satellites (e.g. RADARSAT 1/2, TerraSAR-X, COSMO-SkyMed), spanning a time interval of more than 20 years and allowing the analysis of both past and recent ground displacements of the observed scenes with millimeter precision.

In this section, a general review of remote sensing techniques for landslide studies is presented, as well as applicability and application examples. Then, the main research scientific community background at European level exploiting EO SAR data is briefly mentioned, followed by an overview of the activities and uses of these data by the National Civil Protection Department in Italy.

4.1 Review of remote sensing technologies for landslide studies

The first application of SAR Interferometry to the study of natural phenomena was in the 1970s. Afterwards, it has been successfully applied to the observation of different geophysical and geological processes and dynamics, which induce terrain deformation, such as volcanic activity, earthquakes and land subsidence (Zebker et al., 1994; Peltzer and Rosen, 1995; Fornaro et al., 1996; Massonnet and Feigl, 1998). This trend has grown, especially during the last 10 years, due to the availability of a large amount of SAR data acquired from different systems and satellite sensors. The interest in applying InSAR for environmental studies is related to its capability of remotely obtaining two-dimensional deformation maps of the area under observation.

Exhaustive review on the application of remote sensing techniques for landslide investigations during the 90s is given by Mantovani et al. (1996), who argued that among the several available remote sensing techniques for the study of landslides, even in the late 1990s only stereoscopic air photo-interpretation was actually fully

exploited, being the most frequent remote sensing tool applied in the mapping and monitoring of landslide characteristics.

A further more recent review is provided by Metternicht et al. (2005), who analyzed the use of remote sensing data in landslides studies during the 1980s, 1990s and 2000s. Metternicht et al. (2005) stated that the remote sensing data give a valuable and useful effort to the three main stages of landslide-related studies, i.e. (i) detection and mapping, (ii) monitoring, and (iii) spatial analysis and hazard prediction. For the (i) landslide detection and identification, the most significant remote sensing tools include optical (multi- and hyper-spectral) and infrared (IR) sensors, active VNIR sensors (e.g. LASER altimetry), active microwave sensors (e.g. SAR interferometry). The (ii) monitoring of landslides is mostly undertaken applying InSAR and DInSAR techniques (satellite or ground-based). For the (iii) spatial analysis and hazard prediction, the remote sensed data, such as SAR interferometry, aerial photographs, HR satellite imagery, topographic profiles collected by laser altimeter, and digital photogrammetry, can provide landslide diagnostic features for heuristic, statistical, deterministic or inventory methods for landslide hazard works. In particular, remote sensing is useful in landslide hazard and risk assessment for hazard identification, spatial extent prediction and triggering factors detection (Metternicht et al., 2005).

Overall, for the landslide studies, Singhroy and Molch (2004) divided the remotely sensed approaches into two different groups: the satellite or air-borne imagery and photo-interpretation, for determining more 'qualitative' phenomena characteristics (e.g. distribution and type) and the SAR interferometry or LASER altimetry, for estimating more 'quantitative' features (e.g. length, thickness, velocity).

Interferometric SAR techniques are suitable for measuring very slow movements of slopes and individual objects. The main advantage over other techniques is the possibility of very precise and repeated displacement measurements over large areas at reasonable costs (Rott, 2004; Singhroy, 2002). In particular, the pixel-by-pixel character of the Persistent Scatterers technique enables exploiting individual radar targets in low-coherence areas, making space-borne interferometric measurements possible in vegetated areas, if a sufficient density of natural stable ground reflectors (e.g. man-made structures, exposed rocks) is present (Metternicht et al., 2005).

4.2 Applicability of SAR techniques to landslide phenomena

Nowadays, EO data and new technology, both satellite and ground-based remote sensing techniques, are widely used to detect, map, monitor and forecast ground deformation for different types of landslides and land subsidence.

On one hand, space-borne SAR sensors are used at different scales for the detection of unstable landslide-prone and -affected areas, and for the assessment of the long-term behaviour of the detected phenomena. On the other hand, ground-based SAR is used to zoom in a specific area of interest, improving the spatial resolution of the measurements and reducing the sensor revisiting time. This brings SAR technology in the near real-time monitoring, which is necessary during catastrophic events.

Capabilities, applicability and accuracy of remote sensing technologies to detect and study ground displacements depend on the technical parameters and precision of the technique, as well as on the characteristics of the investigated phenomena.

In particular, the classical DInSAR analysis is useful to study ground movements and dynamic phenomena, e.g. co-seismic displacements, that occurred in a short period of time and relatively faster if compared to the satellite revisiting time, (Carnec et al., 1996; Catani et al., 2005; Biescas et al., 2007; Crosetto et al., 2011). The best results are achieved using several pairs of interferograms and restricting the analysis to small areas e.g. up to a few square kilometers.

Multi-temporal DInSAR analysis produces important information on mass movements, their velocities and dynamics (Colesanti and Wasowski, 2004; Hilley et al., 2004; Strozzi et al., 2005; Wasowski et al., 2008). Such analysis, also called "Advanced DInSAR", has been successfully used to map not previously detected landslides or to update the geometry of already mapped landslides (Ferretti et al., 2005; Meisina et al., 2008; Notti et al., 2010; Lu et al., 2010, 2011; Bianchini et al., 2012a). Multi-temporal DInSAR analyses are very useful for long term spatial-temporal monitoring of slow movements (Catani et al., 2005; Colombo et al., 2006; Farina et al., 2006), permitting to obtain measurements on ground displacements with millimetric accuracy. In order to properly apply these techniques, the distribution of the retrieved radar targets within the boundaries of the identified potentially unstable areas should be validated throughout field checks, *in situ* survey or other ground-truth data, in order to confirm the remote sensed information and increase the confidence degree (See Chapter 7).

GBInSAR analysis has proved its potential for measurement of surface ground displacements of different landslide types, in terms of failure mechanism, involved materials, kinematics, water content and deformation rates (Luzi et al., 2006; Casagli et al., 2010; Bozzano et a., 2011). In specific conditions, such as within relatively faster-moving phenomena and inaccessible areas, the technique can be employed directly as a monitoring tool, providing multi-temporal displacement maps of the observed area.

The following Table 5 describes the capabilities of the above-mentioned different EO analyses, i.e. Classical DInSAR, Advanced DInSAR (Multi-interferometric analysis, e.g. PSI), GBInSAR, for detecting and monitoring landslides related to the velocity classes, according to Cruden and Varnes (1996).

Landslide class	Typical velocity	Classical DInSAR analysis	Multi-temporal PSI analysis	GBInSAR analysis
Extremely	< 16 mm/yr	NO	YES	PARTIALLY
Very slow	0,016 – 1,6	YES	YES	YES
Slow	1,6 m/yr - 13	NO	NO	YES
Medium	13 m/yr - 1,8	NO	NO	PARTIALLY
Rapid	1,8 m/h - 3	NO	NO	NO
Very rapid	3 m/min - 5	NO	NO	NO
Extremely	> 5 m/s	NO	NO	NO

Tab. 5 - Application of satellite DInSAR, PSI and GBInSAR analyses related to the landslide velocity scale as proposed by Cruden & Varnes (1996).

Comparing satellite and ground-based radar interferometry techniques, it is worth to highlight that they deal with different spatial and temporal scale applications. Satellite SAR frames cover areas up to 100 km per 100 km with resolutions of a few tens of meters. The revisiting time of the present satellites over the same area range between 46 and 4 days. The area covered by a ground-based radar interferometry (GBRI) systems depends on the distance from the point of observation, but it is usually limited to a few hundreds of meters up to a few kilometres, corresponding to a patch-landscape scale. The GBRI systems can presently acquire an image up to about every 40 ms and they are consequently more suitable for faster slope movements which require a close series of successive measurements. Hence, satellite data allow the monitoring of "extremely slow" or "very slow" movements only, whereas the GBRI device allows also the assessment of "slow" and "moderate" velocity landslides (Canuti et al., 2004; Metternicht et al., 2005). In addition, the spatial coverage of satellite images is limited by the peculiar SAR imaging geometry, which result in layover and shadow distortions on large mountainous areas. On the other hand, a terrestrial radar system can be placed also in front of steep walls which are in most cases not visible from space.

Focusing on the Advanced Multi-temporal SAR Interferometry, i.e. PSI, for natural hazards and, in particular landslide processes, this technique is largely being carried out in the last years, demonstrating its applicability to different environments and its flexibility to different landslide typologies and dimensions.

The applicability of the PSI technique to the landslide phenomena can be assessed in relation with their velocity, their material type and movement type, as classified by Cruden and Varnes (1996) (Tab. 5 and Tab. 6).

PSI measures are extremely vulnerable to phase aliasing effects, due to their ambiguous nature caused by the 2π phase-wrapping. Thus, phase unwrapping problems limit to a quarter of the wavelength, $\lambda/4$ the maximum displacement between two successive acquisitions and two close PS of the same dataset (Ferretti et al., 2000, 2005; Hanssen, 2005; Raucoules et al., 2009; Crosetto et al., 2010).

Depending on the spatial pattern of ground displacements (with respect to PS density) and their velocity (with respect to the temporal SAR sampling), some deformational phenomena that are intrinsically fast-moving e.g. fall and topple landslide types, cannot be detected or they are often underestimated due to phase unwrapping errors (Cigna et al., 2011) (Tab. 6). Advanced InSAR technique has been successfully applied to analyze slides, either rotational and translational phenomena (Strozzi et al., 2005; Farina et al., 2006). Regarding flows, InSAR potential applicability varies depending on the involved material type: rock flows, characterized by slow movements and regularly distributed in the dislocated mass without a well defined slip surface, can be effectively monitored throughout SAR multi-interferometric analysis. Earth flows can be investigated only if they are very slow-moving and poor water-bearing (Squarzoni et al., 2003). Debris flows cannot be monitored by means of InSAR techniques, because they are too rapid to be observed by the on-going satellite systems. Spreads can be partially analyzed by the satellite sensors, since only the sub-vertical component of the motion can be measured, related to the sinking of the upper coherent layers and induced by the lateral or sub-horizontal spreading of the lower fine-grained layers (Meisina et al., 2007). Lateral spreads due to liquefaction cannot be monitored by satellite interferometry because of their rapid occurrence.

Movement type	Material type	Advanced DInSAR (e.g. PSI)
Fall	Rock/debris/earth	NO
Topple	Rockdebris/earth	NO
Slide	Rock/debris/earth	YES
Flow	Rock	YES
	Earth	PARTIALLY
	Debris	NO
Spread	Rock/debris/earth	PARTIALLY

Tab. 6 - Applicability of Advanced InSAR to landslide phenomena in relation to the material type and movement type, as classified by Cruden and Varnes (1996).

4.3 Compared evaluation of different wavelength SAR data

The use of SAR data acquired in different microwave lengths from the different satellite sensors requires a comparative assessment and illustration of the advantages for landslide detection and monitoring.

The choice of the best radar data stacks for a given test site is usually and mainly driven by the spatial and temporal coverage of these data. However, since many SAR images are available today, including both historical and recent data, the use of the more suitable dataset and of the best appropriate satellite geometry

(ascending or descending) is fundamental for a correct PSI analysis, depending on satellite acquisition parameters, local topography and phenomena types of the area,.

The applicability of satellite InSAR for the three microwave bands, i.e. L-band, C-band and X-band, is summarized in Table 7 and Table 8, in relation to different phenomena and environment characteristics that have to be taken into account.

C-Band satellites (e.g. ERS, ENVISAT or RADARSAT) that operate at a 5.6 cm wavelength, cover wide areas at a low cost and provide data since the 1990s. They are good for the regional analysis and "back-monitoring" (concept proposed by Cigna et al., 2011) of very slow-moving landslides. X-band sensors (e.g. TerraSAR-X, COSMO-SkyMed) that operate at 3.1 cm wavelength with the highest temporal and spatial sampling, allow the detection and monitoring of recent movements affecting small areas with great detail. L-Band satellite (e.g. ALOS PALSAR) which operates at a 23 cm wavelength, permits to detect faster landslides even in vegetated areas (Tab. 7).

Land use (Level 1, CORINE Land Cover, 2000)	Satellite SAR data		
	L-band	C-band	X-band
Artificial - built-up	YES	YES	YES
Rural - agricultural	YES	YES	YES
Forests and semi-natural	YES High radar signal penetration	PARTIALLY Moderate radar signal penetration	NO Low radar signal penetration
Damp zones and water	NO	NO	NO

Tab. 7 - Applicability of different microwave bands SAR data in relation to the land use class.

Regarding the velocity of the considered phenomena, according to the landslide velocity classification of Cruden & Varnes (1996) and IUGS/WGL (1995), the acquisition parameters of the currently available SAR sensors do not enable the estimation of deformations faster than few tens of cm/yr, which would compromise the results of the PSI processing. Thus, due to the phase ambiguity of SAR data processing and satellite acquisition parameters in all L-, C- and X-bands, the PSI analysis of mass movement is limited to landslide phenomena ranging from "extremely slow" (velocity < 16 mm/yr) to "very slow" (16 mm/yr < velocity < 1.6 m/yr) (Cruden & Varnes, 1996). (Tab. 8).

Landslide class	Typical velocity	Satellite SAR data		
		L band	C band	X band
Extremely slow	< 16 mm/yr	Yes	Yes	Yes
Very slow	0.016 – 1.6 m/yr	Yes	Yes	Yes
Slow	1.6 m/yr - 13 m/month	No	No	No
Medium	13 m/month – 1.8 m/h	No	No	No
Rapid	1.8 m/h - 3 m/min	No	No	No
Very rapid	3 m/min - 5 m/s	No	No	No
Extremely rapid	> 5 m/s	No	No	No

Tab. 8 - Applicability of different microwave bands SAR data in relation to the landslide velocity class (Cruden and Varnes, 1996).

Overall, as pointed out before, aliasing effects limit to a quarter of the wavelength the maximum displacement between two successive acquisitions and two close PS of the same dataset due to the ambiguous nature of the 2π-wrapping of interferometric phase (e.g. Hanssen, 2005; Crosetto et al., 2010). Velocities compromising the PSI processing depend on the employed SAR wavelengths and satellite revisiting times; they are about 15 cm/yr for ERS/ENVISAT data (C band), 21 cm/yr for RADARSAT (C-band), 17 cm/yr for COSMO-SkyMed (X-band), 25 cm/yr for TerraSAR-X (X band), 46 cm/yr for ALOS/JERS (L-band). In presence of very high deformation rates of the phenomena, there is a loss of stable reflective radar benchmarks within any PSI technique capacities (Herrera et al., 2011). Thus, higher motion rates cannot be tracked and/or interpreted correctly. Improvements of the PSInSAR can be achieved by exploiting Ground-Based InSAR techniques (e.g. Leva et al., 2003; Luzi et al., 2003; Tarchi et al., 2003; Antonello et al., 2004; Werner et al., 2008; Casagli et al., 2010), which can extend the velocity range of applicability to slightly faster phenomena.

The use of new X-band SAR sensors, i.e. TerraSAR-X and COSMO-SkyMed with high spatial resolution up to 1 meter (1-3 m in azimuth and 1.5-3.5 in range, depending on the acquisition mode and incidence angle) and reduced revisiting time (11 or 16 days up to 4 days) enhanced PSInSAR capability for land motions mapping and monitoring, allowing the identification of more recent ground movements affecting small areas with improved precision. Thus, X-band radar data turn out to be particularly suited for local detection of earth surface processes at small scales, since high resolution and density of PS point targets in X-band permit to better understand and accurately describe deformation phenomena, entering at the level of the site-specific ground motions investigation.

These advantages improve the level of detail of the analysis and allow studying highly localized surface displacements and their dynamic evolution patterns. Although temporal decorrelation is more problematic at X-band compared to longer wavelengths like C-band, the high resolution data permit more coherent targets to be identified in even in case of long time intervals, and more and faster phenomena to be detected.

Despite the potential of X-band data for detecting greater deformation gradients benefitting from their high resolution, the shorter revisiting time compensates only partially the higher temporal decorrelation in vegetated areas; additionally, the atmospheric delay features take a greater portion of shorter X-band wavelength. So, decorrelation noises from vegetation and atmospheric effects are of greater importance in X-band.

Significant differences can be observed within the number and the density of C- and X-band radar targets. The PS density obtained from TerraSAR-X/COSMO-SkyMed datasets is significantly higher than the one of ERS/ENVISAT datasets, due to the cell size effect.

Regarding the temporal occurrence of the investigated phenomena, C-band PS data provide historical archives dating back to 1992. Conversely, X-band PSI analysis can update phenomena mapping up to 2011 and 2012, as operating TerraSAR-X and COSMO-SkyMed satellite systems are working since 2007 and are still ongoing. Therefore, X-band SAR data can analyze and investigate recent deformation, while C-band data can perform a back-monitoring of past and present displacements and can reconstruct the deformation history of the investigated areas.

The displacement time series of X-band data are better than the C-band ones, due to the shorter revisiting time. Thanks to the higher temporal sampling of TerraSAR-X and COSMO-SkyMed, it is possible to analyze the evolution of the non-linear terms of the displacement such as acceleration or deceleration. This facilitates the detection of the non-linear trends that are somehow characteristic of landslide or subsidence kinematics. From a geological point of view, non-linear behaviours can take place as a consequence of the nature itself of the deformation phenomenon, e.g. subsidence processes due to sediment compaction that generally show quadratic trends; a slow change in the predisposing or triggering factors, e.g. intense or prolonged rainfall that can cause acceleration for landslide processes or water level changes; loading due to new constructions, urban

excavations etc; the occurrence of a rapid deformation event, e.g. reactivation, sudden sinkhole, seismic events.

Concerning the map scale of the analysis, radar remote sensing techniques can be exploited to observe subsidence and landslide-induced ground deformations, ranging from regional to local scale, i.e. 1:250,000-1:25,000 and 1:25,000-1:5,000, respectively (Fell et al., 2008).

From a spatial point of view, X-band data are more suitable for analysis at local scale, covering restricted phenomena and affecting small areas. The comparison of X- and C-data demonstrates the capability of X-band data for localized infrastructure and local motions monitoring, thanks to their advantages of dense PS sampling and high temporal frequency. On the other hand, C-band data are more suitable for regional investigation due to their wide coverage and medium resolution; thus, at regional scale, the use of C-band SAR images is envisaged because these data cover wide area at low cost.

The use of L-band allows a feasible investigation on rural areas, due to its higher penetration coefficient on the ground and the consequent lower volumetric and temporal decorrelation in vegetated zones with respect to C- and X-band radar data.

Besides the lower sensitivity to temporal decorrelation, especially for the another advantage of the use of L-band data, e.g. ALOS-PALSAR data, is that it allows detecting faster ground movements e.g. related to landslides or sudden subsidence events that have occasionally occurred in the recent past. Assuming the orbital repeat cycle δt of 46 days of ALOS, we have a maximum detectable displacement rate along the LOS $V_{max} = \lambda / 4\delta t = 45.6$ cm/yr, compared to the value of 14.6 cm/yr valid for the C-band of ERS/ENVISAT missions, where the orbital repeat cycle is 35 days, and to the value of 25.7 cm/yr for X-band TerraSAR-X data, where the revisiting time is 11 days.

Overall, it can be concluded that X-band, L-band and C-band InSAR could play synergic roles in deformation mapping and monitoring, especially in view of the following considerations:

(i) The use of X-band imagery significantly improves the level of detail of analysis and extends the applicability of space-borne SAR interferometry to faster ground movements, due to higher spatial resolutions (up to 1 m), higher PS targets density and shortest repeat cycles of X-band satellites with respect to the medium resolution SAR sensors (11/16 days up to 4 days in respect to 35 or 46 days);

(ii) C-band data allow detecting lower displacement rates. Availability of long historical datasets enables applications of C-band PSI techniques over large areas with a single-pixel precision at medium resolution and low cost;

(iii) L-band data are more sensitive to strong deformation episodes, for which C-band is beyond the aliasing limit. The reduced geometrical decorrelation in L-band allows easier application of conventional differential interferometry where PSI methods fail.

4.4 Review of some applications of PSI techniques to landslide studies

In the last decade, satellite radar interferometry has become a very useful remote-sensing tool for the detection and monitoring of active geological processes such as landslides and subsidence. The application of space-borne InSAR to landslide research has been particularly improved by the development of the Persistent Scatterers Interferometry, as well as by the increasing availability of SAR data from different satellite sensors.

Advanced InSAR approaches generating radar benchmarks using a multi-interferogram analysis of SAR images like PSI technique, enable detection and mapping of ground instability even in not accessible areas, thus reducing times, costs and efforts of traditional geomorphological tools and field surveys.

The rapid dissemination of remote sensing products during the last two decades have been facilitated by the great number of different airborne and satellite sensors and by their synergies with the Geographical Information Systems (GIS) (Rengers et al., 1992), that allow a wide range of users to manage geospatial datasets, essential task when dealing with environmental issues.

PSI is suitable for studying slow-moving landslides in several aspects, due to its millimeter precision. As mentioned before, only "very slow" and "extremely slow" phenomena can be investigated (Cruden and Varnes, 1998), due to the current satellite technical acquisition parameters such as the revisiting time and the signal wavelength.

In literature, many works rely on the use of PSI for detection of slow-moving landslides (e.g. Berardino et al., 2003, Prati et al., 2004). Bovenga et al. (2006) combined PS information with ground-data and monitoring systems to detect landslides in the Daunia Apennine Mountains in Southern Italy. PSI shows its usefulness in landslide mapping and inventory updating (Strozzi et al., 2013). PSI was successfully used for landslide investigation at regional scale by combining radar data with the visual interpretation of optical images (Farina et al., 2006). PS can also refine the boundaries and the state of activity of landslides for updating inventory maps and for understanding the deformation pattern and relation with triggering factors (Cascini et al., 2010; Righini et al., 2012). Cascini et al. (2009) used PSI to check and update a existing landslide inventory at 1:25,000 scale and to test the reliability of inventory based on geomorphologic criteria. Cigna et al. (2013) employed a PSI-based matrix approach to evaluate the state of activity and intensity of slow-moving landslides. Besides, landslides can be potentially detected by the PSI "*hotspot mapping*" (Bianchini et al., 2012a**: Annex 3**; Lu et al., 2012).

PSI provides an effective tool also for landslide monitoring. This can be fulfilled by integrating PS with instrumentation data such as topographic leveling, GPS, inclinometers, piezometers or rain gauge data for ground deformation monitoring (Colesanti et al., 2003b; Tofani et al., 2013).

Cigna et al. (2013) and Greif and Vlcko (2012) used the transformation of line-of-sight (LOS) displacement rates to slope vector direction (Colesanti and Wasowski, 2006; Cascini et al., 2010) respectively to analyze the instability of a slope in Southern Italy (Calabria) and to monitor the post-failure behavior of landslides in Central Slovakia. The monitoring capacity was further improved by Herrera et al. (2013) to figure out different moving directions, to measure different velocity patterns within the same moving mass and to identify triggering factors. Additionally, Bovenga et al. (2012) indicated that X-band sensors, which have higher spatial resolution and shorter revisiting time, can estimate the surface displacement using fewer images and the monitoring can be done in shorter time for high risk cases.

Multi-band PSI data acquired by different satellites can be used and integrated to obtain a multi-temporal and more robust interpretation of landslide phenomena. For instance, Bovenga et al. (2013) integrated X-band COSMO-SkyMed, C-band ENVISAT and GNSS measurements for landslide investigation in Assisi, Italy. Herrera et al. (2011) detected and monitored the Portalet landslide in Spain using a combination of X-band TerraSAR-X data and C-band ERS and ENVISAT data.

PSI has potential in landslide mechanism understanding. For quantitative estimation, PS are suggested to be combined with ground truth, field survey and analysis of acquisition geometry to understand landslide dynamics (Colesanti and Wasowski, 2006). The seasonality of ground acceleration revealed by PS can be combined with the precipitation data to analyze the dynamics of slow-moving landslide (Hilley et al., 2004; Zibret el al., 2012; Tofani et al., 2013). Zhao et al. (2012) show that by comparing PS velocity with precipitation record, landslide displacements can be correlated with rainfall peak for further investigation of landslide mechanism and for defining rainfall threshold for early warning purposes.

In some cases, PSI has been also applied for quantitative landslide hazard and risk assessment in order to quantify the potential hazard, susceptibility and risk resulting from slow-moving phenomena (Catani et al., 2005; Piacentini et al., 2012; Lu et al., 2013).

4.5 Geohazard scientific community background

The scientific community carries out prediction and prevention research activities for knowledge development on landslides, and collaborates at both functional and operative levels with the responsible authorities to

provide mapping, monitoring, surveillance and alert systems for hydrogeological risk, mainly in the deferred time and, partially, in near-real time (**Annex 1**). Its activities include technical-scientific training and assistance for the civil protection agencies and local authorities, in the framework of simulated events, as well as the development of methodologies for the identification of landslide triggers, forecasting models, assessment of hydrological thresholds and dangerousness of landslide processes, definition of operative procedures and protocols for the identification of risk scenarios in agreement with national and/or local authorities.

In particular, in the last decade, ESA (European Space Agency), EC (European Commission), Civil Protection Departments (DPC) and many other entities in charge of risk management initiated a range of projects contributing to the understanding, mitigation, preparedness and management of hydro-geological risks.

In the European context, hydrogeological services and applications exploiting EO satellite technologies are widely accepted; they are mature in Italy, Switzerland and Spain and are becoming consolidated also in Greece, Slovakia, Hungary, Lithuania, Germany, Netherlands, Norway, Poland and France.

The main EO capacities dealing with landslide services and applications are strongly promoted by projects such as SLAM (Service for LAndslide Monitoring) project (2003-2005) and Terrafirma (2003-2012) in the framework of ESA Global Monitoring for Environment and Security (GMES), now called European Earth Observation Programme Copernicus, and EC projects such as Framework Programme (FP), e.g. FP6 PREVIEW (2005-2008), FP7 PanGeo project (2011-2013), SAFER (Services and Applications for Emergency Response) project (2009-2011), SafeLand (2009-2012), DORIS (Ground Deformation Risk Scenarios: and Advanced Assessment Service) project (2010-2013) and LAMPRE (LAndslide Modelling and tools for vulnerability assessment Preparedness and Recovery management) project (2013-2015).

These projects contributed significantly to the development of the European EO capacities for geo-hazard inventory, mapping, monitoring and forecasting. They have shown how the exploitation of EO data can reply to most of the user needs for landslide identification and monitoring, through the rapid detection of unstable areas, detecting their spatial extension and temporal evolution to support the emergency management process and the environmental planning strategies.

In Europe, thanks to the efforts made and time spent by the scientific community in the last decade to make EO-based applications accepted among users and practitioners, 50 geological surveys have became users of EO-based terrain deformation services.

Several national initiatives in Switzerland and Spain also contributed significantly to the development and acceptance of the EO capacities for detecting, mapping and monitoring hydrogeological instability events: the Swiss authority FOEN (Federal Office for the Environment) has adopted EO as a method for monitoring landslide risks, while the spanish IGME (Instituto Geologico y Minero de España – Geological Survey of Spain) widely use InSAR data within the Geohazard group.

Recent national initiatives in Italy funded by the Italian National Civil Protection Department, e.g. SAR.net1/2 projects in 2005-2012, were carried out to improve the acceptance of EO-based services and applications for landslide risk. These projects provided successful examples on how applications based on EO data can operatively support the DPC in the definition of operative procedures for the rapid assessment of risk during emergencies.

Moreover, in Italy, the government has purchased continuous InSAR coverage for the national territory: the Extraordinary Plan of Environmental Remote Sensing (Piano Straordinario di Telerilevamento) (MATTM, 2010) is an agreement program between different levels of government. Its main objective is to provide and share a national database containing measures of ground motions obtained by SAR interferometry for the creation of a synoptic view of the instability phenomena (potential and/or in progress) throughout the country, in support to authorities involved in land use planning activities and hydro-geological risk management.

These examples demonstrate that within the geo-hazard community including both scientific community, local/national authorities and the other end-users (Space Agencies, research institutes, operational users, civil

protection agencies, geological surveys), the topic on how EO data can contribute to geo-hazard and disaster risk reduction is very significant and still ongoing. A milestone in this discussion has been marked within the International Forum on Satellite Earth Observation and Geo-hazard held in May 2012 in Santorini (Greece) organized by ESA and GEO (Group on Earth Observations). The publication of the Scientific and Technical Memorandum on the Santorini Conference (**Annex 1**) represents a landmark in the international efforts to apply satellite EO, by reviewing current status of application of satellite EO to geo-hazard risk management, by defining objectives for each of the actors of the geo-hazard communities for many years to come, and by defining a vision for the implementation of strategies to achieve these objectives.

4.6 InSAR data in the Civil Protection Emergency Cycle in Italy

The National Civil Protection Department (DPC) in Italy operates according to the lines of prevention, forecast and assessment, early warning and alerting, emergency response and recovery from emergency (Pagliara et al., 2014). The work of italian DPC are daily supported by research efforts on the assessment of vulnerability and exposure to landslides and hydrogeological risk of population, buildings and critical infrastructures.

The new and emerging technologies (EO, non-EO, aerial) integrated with the conventional analysis and methods greatly support the landslide risk management activities through all the emergency cycle phases, performed both in real- and deferred-time (Fig.25).

Fig. 25- Sketch image representing the three phases of the emergency cycle.

During the Preparedness/Prevention phase, products dealing with disaster risk reduction are performed in the form of overview and detailed maps or inventories (e.g. landslide inventory maps, ground deformation maps based on InSAR data) of areas that are, or might be, at risk.

During the Emergency Response phase, products are provided in “rush” mode that means an high-priority service delivery. These products can include analyses of the landslide impact and extent; event maps to evaluate the magnitude of the phenomenon; damage assessment for providing an indication of the affected infrastructure and population; velocity maps based on EO data for residual risk evaluation, monitoring and early warning, in order to define the preliminary stabilization measures based on the characterization of landslides.

During the Recovery phase, products are intended to be used for analyzing landslides in a statistical way, and to identify residual landslide risk zones. Medium or long term monitoring using satellite images allows the progress of reconstruction work to be followed, possible changes in land cover to be observed, and landslide risk to be evaluated and monitored. GBInSAR and Satellite InSAR data can be used for the evaluation of the recovery measures (e.g. Montaguto landslide) and to assess the geomorphological hazard for new settlements (e.g. San Fratello in Sicily and Cerzeto in Calabria).

Chapter 5

Spatial characterization of landslide phenomena by means of PSI data

The spatial scale for landslide phenomena ranges from regional to local, i.e. varies from studies of landslide mapping over very wide areas (up to a few thousands of square kilometres) to analysis of single phenomena. Hence, on one hand the technologies supporting landslide studies should guarantee to cover territories of huge extension, but on the other hand be able to provide access to detailed information for the understanding of phenomena occurring over very small areas (e.g. a few square meters), and for the characterization of ground motion with high accuracy.

Remote sensed data, currently used both in near-real time and deferred time work, can give support for the creation and updating of landslide inventory maps over large areas, as well as for the local long-term monitoring of single unstable slopes. In many cases, EO satellite data can provide precise estimates of ground motion and indicators of landslide geometry and activity, without requiring the installation of any targets or instrument on the ground. In particular, the Persistent Scatterers Interferometry (PSI) technique has become a widespread tool for landslide mapping, properly combined with traditional geomorphological survey techniques and other monitoring instruments.

In this chapter, the spatial characterization of landslide phenomena is discussed, focusing on the landslide detection and mapping procedures by means of PSI data.

5.1 Landslide inventory mapping

Spatial detection and mapping of mass movements are the basis for all assessments and activities related to geological risk management and mitigation activities, at both regional and local scale.

Preparing landslide maps is important to document the extent of landslide phenomena in a region, to investigate the location, types, pattern, recurrence and statistics of slope failures, to determine landslide susceptibility, hazard, vulnerability and risk, and to study the evolution of landscapes dominated by mass-wasting processes (Guzzetti et al., 2012).

The Landslides Inventory Maps (LIM) date back to the 1970's (Carrara and Merenda, 1976) and can be defined as representations of the distribution, typology, and, if possible, the date of occurrence of those mass movements that have left detectable evidence on the affected areas.

Landslide inventory maps show the spatial distribution of both past and current landslides, represented as polygons or points and often include also information about their state of activity (Wieczorek, 1984).

Mapping for landslide inventory is scale dependant, with generally three scales of spatial analysis being defined (Mantovani et al., 1996; Fell et al., 2008): a regional scale (<100,000), a medium scale (1:50,000 - 1:25,000) and a large scale (>1:10,000). Thus, landslide inventory map can range from regional to local scale.

Landslide mapping activities can be performed by using a purely convention approach (i.e. stereoscopic interpretation of aerial photography) or exploiting modern and emerging technologies, mainly relied on remote sensing. Recently, Guzzetti et al. (2012) provided a review about the various approaches for landslide identification and mapping, both the conventional and the new recent techniques.

The traditional methods most commonly used for preparing inventory maps are based on historical archives, local databases, photo-interpretation of stereo aerial photos and geomorphologic surveys (Crozier, 1984; Soeters and Van Westen, 1996). Thus, these conventional methods rely chiefly on the visual interpretation of stereoscopic aerial photography, aided by field checks. These methods are well-established, but are time-consuming and resource-intensive (e.g. Brabb, 1991; Galli et al., 2008). Moreover, the inventory maps created

with only these traditional techniques are usually subject to uncertainties and limitations related mainly to difficulties in the recognition and the subsequent mapping of morphological features and evidences related to ground instability, especially in highly vegetated and urbanized/built-up areas (Brardinoni et al., 2003). Even more problematic is the assessment of the state of activity, for which various but not resolving approaches have been proposed, such as stereoscopic multi-temporal analysis of aerial photos (Canuti and Focardi, 1986).

New and emerging techniques are mainly based on satellite, airborne, and terrestrial remote sensing technologies. These techniques have demonstrated to be valuable for the recognition of landslides (Rengeres et al., 1992) and other geomorphological features, and so for facilitating the production of landslide maps, reducing the time and resources required for their compilation and systematic update (Guzzetti et al., 2012).

These modern and promising techniques for the analysis of surface morphology include the exploitation of (i) very-high resolution digital elevation models (DEMs) (i.e. VHR digital representations of surface topography obtained by LiDAR sensors), (ii) SAR images processed through DInSAR and PSInSAR techniques, and (iii) different types of satellite optical images (monoscopic and/or stereoscopic analysis of panchromatic multispectral and hyperspectral satellite imagery). A visual and semi-automated classification and interpretation method for creating and updating landslides maps through optical images analysis (i.e. "Multiple Change Detection") has been recently carried out by Mondini et al. (2011). From the late 90s, airborne and satellite SAR data have been successfully used to detect, characterize, and map single or multiple landslides (Singhroy et al., 1998). Space-borne SAR Interferometry offer great support in the implementation of landslide inventory maps, because it provides rapid and easily updatable ground displacement measurement over large areas with very high accuracy (millimetre) and spatial resolution (up to 1 m), good temporal coverage (starting from 1992 up to present) and sampling (monthly acquisitions), reducing field work and costs.

Today, all the EO technologies are widely used by now, and more and more a landslide mapping is often performed through a combination of many techniques. The different technologies are quite commonly employed by the researchers and operational communities of some countries (mainly Italy, Spain and Switzerland), for a preliminary map of the most critical and hazardous landslide-prone areas or for a rapid production of landslide event-inventory in the emergency phase following a disaster.

In this thesis research, the attention is focused on the PSI (Persistent Scatterer Interferometry) that has recently demonstrated its valuable suitability for the spatial detection and characterization of slow-moving landslides, and their complementarity with on-site measurements, at both regional and local scales (e.g., Strozzi et al., 2005, Farina et al., 2006; Colesanti and Wasowski, 2006; Guzzetti et al., 2012).

In particular, the so-called "*radar-interpretation*" conceived by Farina et al. (2003) (and then improved and integrated by Farina et al., 2006, Casagli et al., 2008, Farina et al., 2008) consists in assigning a geomorphological meaning to the scattered point-like ground displacement measurements coming from the Persistent Scatterers (PS) targets.

This analysis is possible due to the integration of PSI measures with conventional optical data (ortophotos, multi-temporal aerial photos, and VHR optical satellite images) and further ancillary geo-thematic data (e.g. topographic and geological maps). Thus, the procedure combines the photo-interpretation of aerial and satellite images with the 'radar-interpretation' of PSI data (Farina et al. 2008; Cigna et al. 2011; Righini et al. 2012), allowing the spatial extension of the point-wise ground motion measures provided by satellite data and the identification of geomorphologic and kinematic evidences related to landslide activity.

On one hand, the conventional photo-interpretation permits to recognize terrain features and landslide evidence in natural environments such as vegetated and rural areas, but not in urbanized areas where landslide-induced geomorphologic features are instead difficult to be identified, due to dense urban fabric. On the other hand, radar-interpretation is very suitable for mapping ground displacements in urbanized and artificial areas where much more PS benchmarks (e.g. buildings, other reflective structures and urban

infrastructure) are retrieved; whereas, in vegetated areas, the vegetation coverage prevent a high density of PS targets to be identified (Bianchini et al., 2012a). Thus, radar- and photo-interpretation are integrable and complementary tools to get complete information on slope instability and to map landslides (e.g. Farina et al., 2006, 2008; Meisina et al., 2007).

This approach based on the radar- and photo-interpretation chain has been successfully and widely exploited and validated by several scientific applications during last years (e.g. Casagli et al., 2008; Meisina et al., 2008; Herrera et al., 2009a; Cigna et al., 2010; Notti et al., 2010; Righini et al., 2012; Bianchini et al., 2012a; Cigna et al., 2013).

The methodology generally operates at regional or medium scales (i.e., 1:100,000–1:25,000 and 1:25,000–1:5,000, respectively, according to Fell et al., 2008), and its contributions to the creation of new landslides inventory maps or to the updating of pre-existing inventories consist in: (i) detection of landslide phenomena not emerged from conventional geomorphological analyses; (ii) verification or modification (better definition) of landslide boundaries; (iii) assessment of representative ground displacement velocity for each landslide; and (iv) evaluation of state of activity (explained more in detail in the next section, i.e. par 5.2) (Fig. 26).

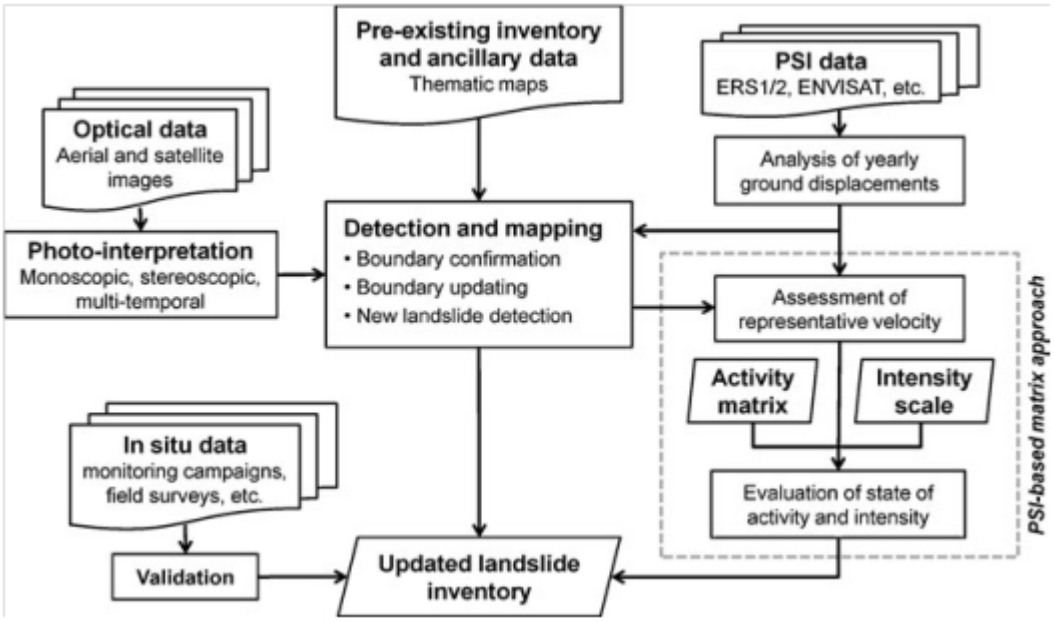

Fig. 26 - Flow chart describing the mapping of landslides and the evaluation of their state of activity and intensity. Modified from Cigna et al. (2013).

In particular, as pointed out by Bianchini et al. (2012a) and Cigna et al. (2013), on the basis of pre-existing inventory map and PS distribution, the combined radar-interpretation and photo-interpretation procedures allow the modification of boundaries (usually enlargement) of pre-mapped phenomena and the identification of new landslides which were not previously mapped through conventional geomorphological studies.

Generally, in order to make radar-interpretation more robust, the analysis is focused on groups of at least 3-4 radar targets (Meisina et al., 2008; Bianchini et al., 2012a), since measures recorded on single targets may often not be representative or indicative of a mass movement, but tied to local instability of a single infrastructure (e.g. structural fractures or settlement of building).

Moreover, the integrated analyses of InSAR PS measures, along with ancillary data, thematic maps and photo-interpretation, should always be supported by field investigation and surveys, in order to confirm or even to improve all the information and evaluations performed through radar-interpretation, to verify damage on buildings and infrastructures and other geomorphologic evidences and features connected to ground instability.

One of the most successful work for the updating of landslide inventories by means of PSI using the radar-interpretation procedure, is the so-called *"hotspot mapping"* approach (Lu et al., 2012; Bianchini et al., 2012a): this approach couples and integrates PSI displacement measures with thematic maps and optical data, for the detection of slow-moving mass movements over large areas of interest. This methodology, which is well explained in the **Annex 3** (Bianchini et al., 2012a), scans wide areas to identify "*hotspots*", which correspond to those sites that are characterized by high hydro-geological hazard. These narrow areas are assessed as the most critical ones, for the type or extent of identified instability phenomena, for the high exposure of the element at risk and/or for the measured displacement velocities. To these hotspots, priority has to be given when planning *in situ* validation and field surveys, in order to optimize work efforts and time and to save economic resources.

Landslides inventories are crucial for further analysis, e.g. assessing landslide hazard, susceptibility and risk within an area (Aleotti and Chowdhury, 1999; Dai et al., 2002). However, landslide databases may have different spatial resolution and detail, according to the different goals, scale and data collection methods (Pereira et al., 2012). Quality and accuracy of these landslide databases depend strongly on the scale of resolution (Guzzetti, 2006).

In Italy, official landslide inventories exist, provided by local authorities and based on documental sources, historical archives, aerial ortophotos analysis and geomorphologic surveys (Crozier, 1984; Soeters and Van Westen, 1996). The IFFI project (Inventory of Landslide Phenomena in Italy, Inventario dei Fenomeni Franosi in Italia), carried out by ISPRA (Istituto Superiore per la Protezione e la Ricerca Ambientale) (ISPRA, 2008) and the Regions and self-governing Provinces, and PAI (Hydrogeological setting plan, Piano di Assetto Idrogeologico) are projects carried out to supply detailed picture of the distribution of landslide phenomena within Italy, aiming at identifying and mapping landslides over the whole national territory, based on standardized criteria.

Figure 27 shows an example of landslide representation within IFFI project, in which landslide areas are depicted as polygons (or lines, if phenomenon is too narrow, i.e. < 10,000 square meters), and geo-referenced points located at the highest point of the crown. The mapping scale is 1:10,000 in the most part of Italian territory. However, less resolution scale (i.e. 1:25,000) has been used in mountainous and sparsely areas.

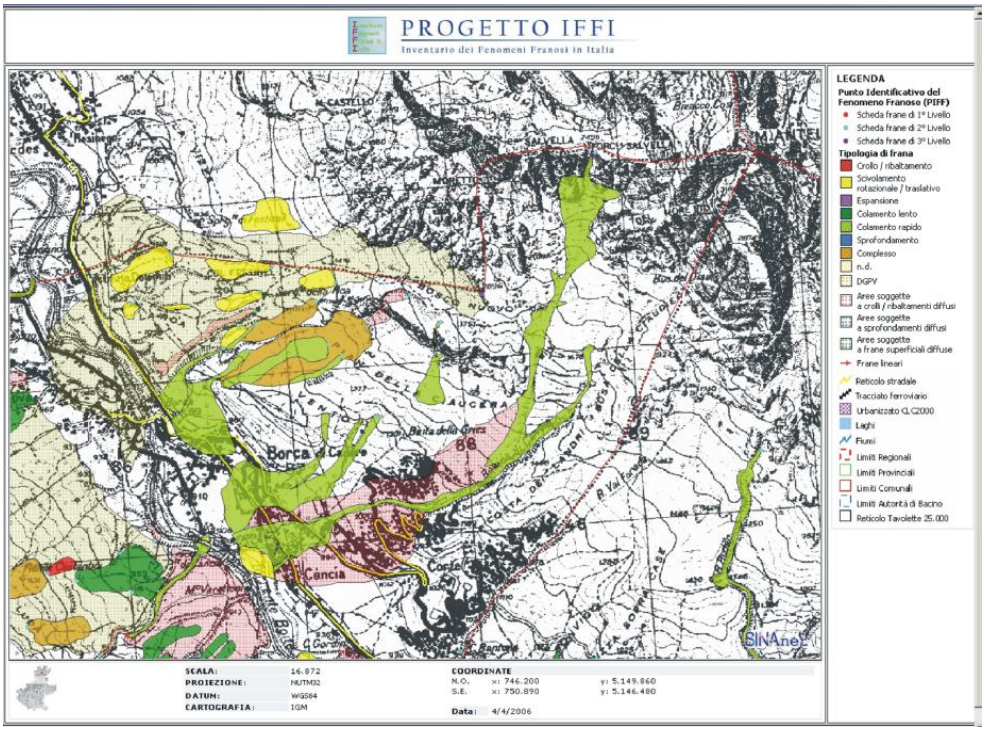

Fig. 27 – Example of landslides visualization within IFFI project database (From ISPRA, 2008).

By the way, the landslide spatial extensions are often not up to date within these PAI or IFFI databases and, moreover, landslides classification and validation strategies need to be optimized for phenomena assessment procedures at regional and local scales (Agnesi et al., 2012; Guzzetti et al., 1999).

The **Annex 4** (Frangioni et al., 2013) and **Annex 5** (Cigna et al., 2010) present an updating of pre-existing landslide inventory map by means of PSI data, at regional scale in Calabria (Italy) and at a basin scale in Emilia-Romagna (Italy), respectively.

5.2 PSI-based evaluation of landslide state of activity

When preparing or updating a landslide inventory map, once mapped the spatial distribution of landslides, then the state of activity of phenomena can be evaluated.

The classification of the activity of landslides proposed in the Multilingual Landslide Glossary (WP/WLI, 1993) includes the following states (Fig. 28): (i) "active", for a landslide that is currently moving; (ii) "suspended", for a landslide that has moved within the last 12 months (i.e. last seasonal cycle), but is not active at present; (iii) "Reactivated", for a phenomenon that is now active, after being inactive; (iv) "inactive", for a landslide that is not moved within the last 12 months and can be divided into 4 more states: "Dormant" (an inactive landslide, which can be reactivated by its original causes or other causes) "Abandoned" (an inactive landslide, which is no longer affected by its original triggering causes), "Stabilized" (an inactive landslide, which has been protected from its original causes by remedial measures, naturally or artificially) and "relict" (an inactive landslide, i.e. which developed under climatic or geomorphological conditions considerably different from those at present, i.e. a "paleo-landslide").

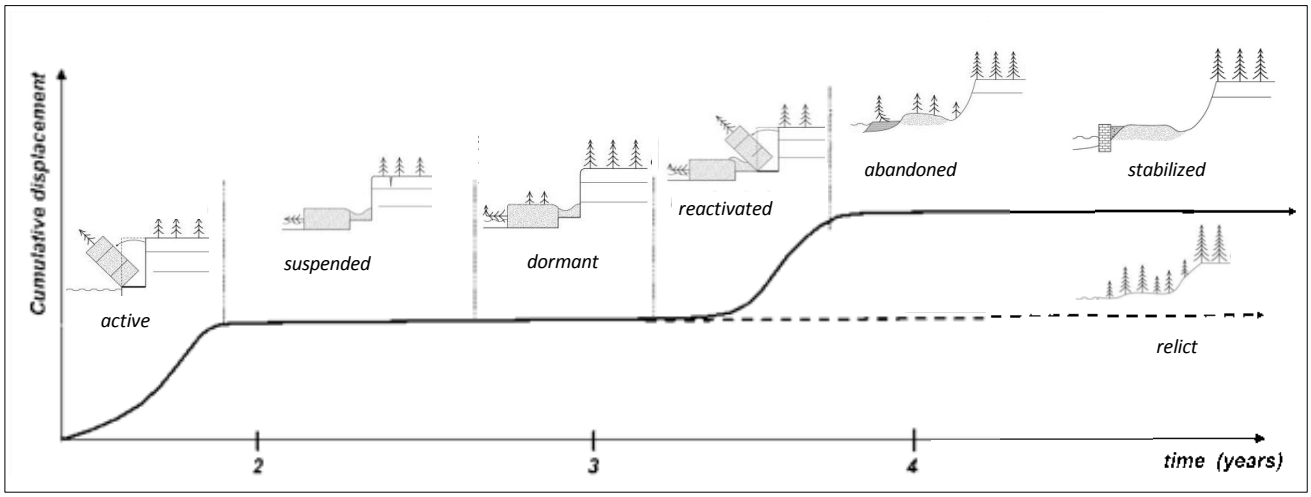

Fig. 28 - Landslide state of activity across time. Modified from Cooper (2007) and from Agliardi et al. (2012).

An innovative methodology for the evaluation of the "state of activity" and "intensity" of slow-moving landslides is the matrix approach, based on the use of PS measurements, which has been initially conceived within the Earth Sciences Department of the University of Firenze, and applied on several test sites in the framework of national and international projects, such as ESA SLAM (Service for LAndslide Monitoring), Terrafirma and PREVIEW (Farina et al., 2006; Casagli et al., 2008).

This approach is based on the classification of the "state of activity" provided by the Multilingual Glossary for Landslides (WP/WLI, 1993) and its applicability is limited to extremely slow (velocity < 16 mm/yr) and very slow landslides (16 mm/yr < velocity < 1,6 m/yr), according to Cruden and Varnes (1996).

The "intensity" of a landslide is a difficult parameter to be evaluated since many features must be accounted. Hungr (1997) defines the intensity as the destructiveness of a landslide, in terms of energy volume, area,

depth, movement velocity or total displacement, etc.). Intensity expresses the geometrical and mechanical severity of a landslide, associated with its destructive power (Einstein, 1988). The intensity is considered depending upon kinetic energy, mass and/or velocity (Hungr, 1995). At basin scale, the intensity is not easily measurable, due to the lack of detailed information on volume and expected velocity for a large number of landslides (Catani et al., 2005). Usually, the landslide intensity assessment refers to range scales based on possible consequent damages (Canuti and Casagli 1996, Cruden and Varnes 1996). Hungr (1981), in his scale, provides specific velocity thresholds associated with the different classes, modified by Cruden and Varnes (1996) and adopted by the IUGS/WGL (1995).

In this context, the landslide intensity can be is assessed by PSI data in terms of movement velocity (Righini et al., 2012).

The operational methodology, which has been recently used within several scientific works (Cigna et al., 2010; Righini et al., 2012; Bianchini et al., 2012a), is performed by a "PSI-based matrix", integrating qualitative (state of activity) and quantitative information (intensity) of the phenomenon at hand.

Firstly, a representative ground displacement velocity value is determined, for each landslide, through the analysis of available PS data. These representative values, in terms of LOS deformation velocity (mm/yr), are referred to the coverage time of satellite acquisitions; for each landslide the values are determined by calculating the average velocity of all the PS included within its boundary. Then, the representative ground motion rates of each landslide are compared to some displacement thresholds (e.g. ±2 mm/year in the LOS direction, away or towards the satellite), whose values depend on the characteristics of each application (landslide main typology, InSAR data, measurement accuracy, distance from reference point, etc.), for distinguishing 'moving' from 'not moving' phenomena. Finally, the state of activity and intensity are assigned through the use of one matrix and one scale (for activity and for intensity evaluations, respectively), which are defined in terms of velocity and acquisition time and consist of cell grids with different velocity combinations, whose inputs are past or present PS velocities or/and information coming from pre-existing inventories.

The first attempt of activity matrix was exploited by Righini et al. (2012) and makes use of an activity cell-grid, whose inputs are InSAR measurements of past (ERS 1/2) and present (ENVISAT) displacement. Representative ground motion values of each landslide are compared to the velocity threshold of 2 mm/yr, and finally, by means of the matrix, the state of activity is determined (Fig. 29). The threshold of 2 mm/yr is precautionary chosen as the minimum value exceeding the precision of the PSI technique, as found also within other works (Meisina et al. 2007, 2008; Cascini et al., 2009; Cigna et al., 2010; Righini et al., 2012).

The intensity scale is defined in terms of mean yearly velocity and consists of three different classes: 'negligible', 'extremely slow' and 'very slow' (Cruden and Varnes, 1996). It is worth to highlight that the deformation threshold discriminating the two classes of extremely slow and very slow movements is adjusted from 16 mm/year (defined by Cruden and Varnes, 1996) to a lower value, e.g. 10 mm/year (Cigna et al., 2010; Righini et al., 2012; Bianchini et al., 2012a) due to the underestimation of real movements produced by PSI techniques, which estimate the displacement rates along the LOS direction. Thus, LOS measured displacements generally differ from the actual direction of landslide motion. Moreover, a further underestimation of landslide movements occurs during the assessment of landslide representative rates, which are computed as average velocities, both spatially (averaging the measures from different PS within the same landslide area) and temporally (assessing yearly rates) (Bianchini et al., 2012a).

An explanation and application of these first activity and intensity matrixes are carried out in the **Annex 4** (Frangioni et al., 2013).

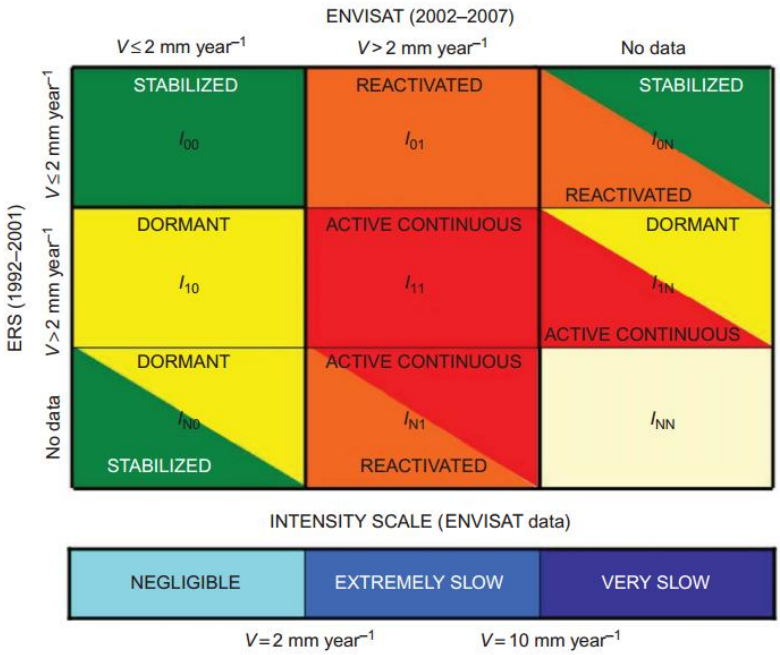

Fig. 29 - First attempt of activity matrix and intensity scale, according to Righini et al. (2012).

The second version of the activity matrix has been implemented by Cigna et al. (2010) **(Annex 5)** and Bianchini et al. (2012a) **(Annex 3).** While previous studies (Righini et al., 2012) used PSI measures derived from two different satellites providing interferometric data for two distinct time intervals, e.g. historical ERS and recent ENVISAT measurements, this development of the activity matrix is based on the information coming from the pre-existing inventory map and PS average yearly velocity extracted from a single PSI dataset (Fig. 30). Thus, this matrix can be used when interferometric data are only available for a single period of acquisition (e.g. ENVISAT data). In order to determine the state of activity of each phenomenon, the representative landslide velocity is firstly compared to the velocity threshold. The result is eventually combined with the landslide information extracted from the pre-existing inventory (i.e. state of activity referred to the time of updating of the pre-existing inventory) and the state of activity of each phenomenon is evaluated.

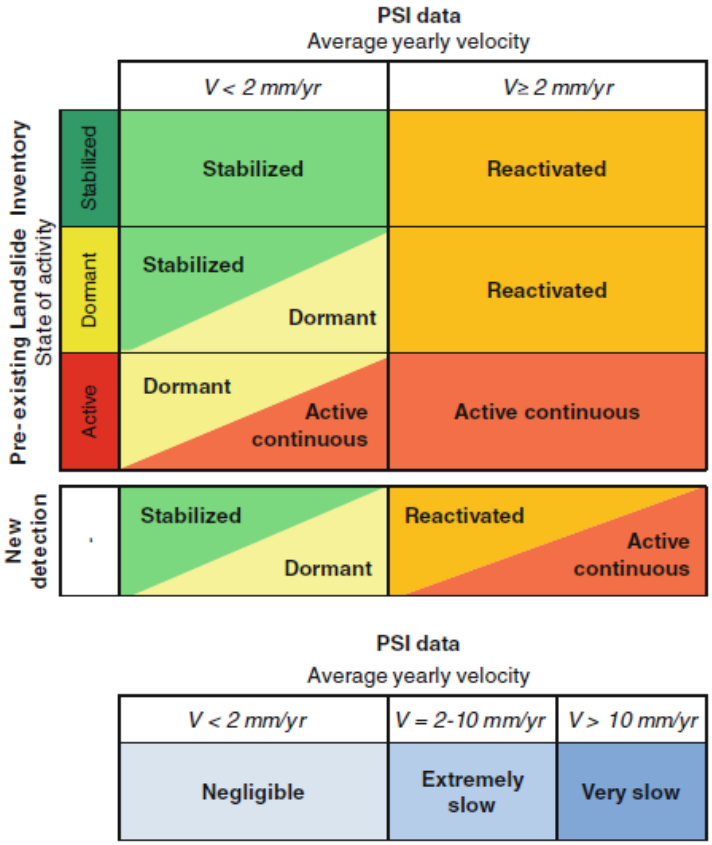

Fig. 30 - Second version of the activity matrix as implemented by Cigna et al. (2010) (Annex 5) and Bianchini et al. (2012a) (Annex 3).

Subsequently, the matrix-based procedure for the evaluation of landslide activity has been improved by Bianchini et al. (2013a) (**Annex 6**) and Cigna et al. (2013) (**Annex 7**). In this third version, the evaluation of activity and intensity is computed by analyzing separately present and historical PS data for each landslide, and by calculating the average velocity of the PS identified within its boundary. Thus, present and historical velocities, called VP and VH, which are referred, respectively, to the two temporal coverages, present (D_{P1} – D_{P2}) and historical [D_{H1}–D_{H2}] ones. These representative velocities (VP and VH) are then compared with the activity and intensity thresholds (±2 mm/yr and ±10 mm/yr). In this further development, the state of activity of landslides is assigned through two activity matrices (Fig. 31): the first one is used for already pre-mapped phenomena and it is based on the information coming from the pre-existing inventory map (reference data: D_{INV}) and present PS measures (D_{P1} – D_{P2}). The second one is used for newly mapped phenomena and it is based only on the exploitation of historical [D_{H1}–D_{H2}] and present [D_{P1}–D_{P2}] PSI data (Fig. 30b). Third column of this matrix (Fig. 31a) may be substituted with (Fig. 31b) to refer all the assessments to the past date [D_{P2}]. The reference year of the classified activity is pointed out in every cell-grid of the matrices.

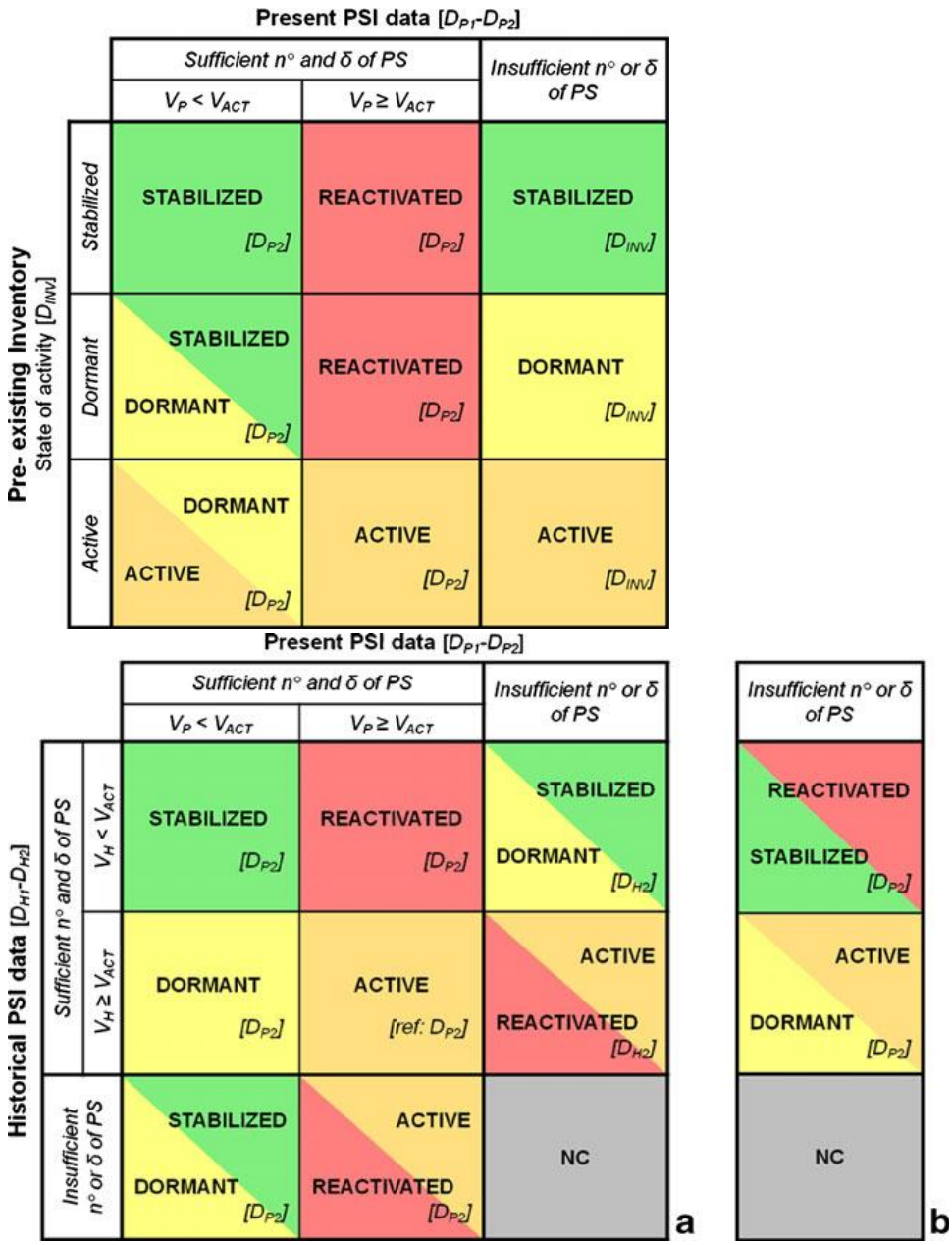

Fig. 31 - Landslide activity matrixes according to Bianchini et al. (2013a) (Annex 6) and Cigna et al., (2013) (Annex 7).

It is worth to highlight that the PSI-based matrix approach use a simplified version of the official classification of the landslide states of activity defined in the multilingual landslide glossary (WP/WLI, 1993), and the following four different states of activity are distinguished: 'reactivated' (moving after being inactive), 'active continuous' (currently moving; includes also suspended phenomena), 'dormant' (inactive, but potentially being reactivated), 'stabilized' (not affected anymore by original causes; includes artificially and naturally stabilized phenomena).

The ambiguous (double) classification in the lowermost-left cells of the activity matrix for pre-mapped phenomena and in the cells of the matrix for new detections, reflects the uncertainty in the assessment of the state of activity. This is because, as pointed out by Bianchini et al. (2012a) **(Annex 3)**, the activity matrixes are based on a 'conservative' or 'cautionary' approach: even if PSI data register low movement rates, the state of activity recorded in the pre-existing inventory is not lowered, unless field evidences and *in situ* monitoring data confirm an actual lowering of activity. This explains the double names of some cells (i.e. the two lowermost-left cells in the matrix for pre-mapped phenomena), resolvable only through field validation. For

new detections, despite the availability of recent deformation measurements, the lack of sufficient present or historical PS ground displacements prevents to discern between stabilized and dormant, or between active and reactivated phenomena (i.e. the two lowermost and two left cells in the matrix for new phenomena).

Cigna et al. (2013) (**Annex 7**) provide a comprehensive step-by-step analysis and discussion of the whole above-explained 'PSI-based matrix approach'.

As mentioned before, the following Annexes are some examples of PSI technique for landslide inventory detection and mapping, at regional or basin scale. These applications reveal how PSI can be an effective tool to identify slope instability, by combining satellite-based ground displacement estimates with conventional geomorphologic tools, e.g. field survey, photo-interpretation of aerial or satellite optical imagery, and other auxiliary geo-thematic data. The final goal of these applications is the creation of landslide inventory maps or the updating of a pre-existing one, through the delivery of qualitative (e.g. state of activity) and quantitative (e.g. velocity) information of each mapped phenomenon and the detection and mapping of those phenomena not previously identified through conventional means or new unknown potential landslide hazard areas.

Annex 3: BIANCHINI S., Cigna F., Righini G., Proietti C., Casagli N. (2012a) Landslide HotSpot Mapping by means of Persistent Scatterer Interferometry. *Environmental Earth Sciences*, vol. 67(4), pp. 1155-1172, ISSN:1866-6280.

Annex 4: Frangioni S., BIANCHINI S., Moretti S. (2013) Landslide inventory updating by means of Persistent Scatterer Interferometry (PSI): the Setta basin (Italy) case study. Accepted in *Geomatics, Natural Hazards and Risk.* doi: 10.1080/19475705.2013.866985

Annex 5: Cigna F. BIANCHINI S., Righini G., Proietti C., Casagli N. (2010) Updating landslide inventory maps in mountain areas by means of Persistent Scatterer Interferometry (PSI) and photo-interpretation: Central Calabria (Italy) case study". In: Malet JP, Glade T, Casagli N (eds) *Mountain Risks: Bringing Science to Society, Proceedings of the International Conference,* CERG Editions, Florence, Italy, November 24-26, 2010, pp 3-9.

Annex 6: BIANCHINI S., Cigna F., Casagli N. (2013a) Improving landslide inventories with multi-temporal measures of ground displacements retrieved through Persistent Scatterer Interferometry. *Proceedings of The Second World Landslide Forum - WLF2*, Rome (Italy), October 3th-9th, 2011.

Annex 7: Cigna F., BIANCHINI S., Casagli N. (2013) How to assess landslide activity and intensity with Persistent Scatterer Interferometry (PSI): the PSI-based matrix approach. Landslides, vol. 10 (3), pp. 267-283, doi: 10.1007/s10346-012-0335-7.

Chapter 6

Temporal characterization of landslide phenomena by means of PSI data

Thanks to the long-time monitoring over some tens of years, the multi-temporal continuous data availability and the monthly (or less) acquisition sampling, satellite interferometric techniques are able to successfully help and integrate ground-based analysis, not only to identify and map ground instabilities, but also to study their temporal evolution.

The monitoring and temporal characterization of landslide phenomena can be provided by exploiting PSInSAR displacement time series, which supply precise measures of ground motions without any physical contact with the unstable slopes nor necessity of positioning any targets on the ground.

6.1 PS time series analysis

InSAR time-series estimate the temporal evolution of deformation over large areas by incorporating information from multiple SAR interferograms (Shanker et al., 2011).

PS displacement time series (TS) show the measured LOS velocity at each acquisition within the entire acquisition temporal range, with millimeter (mm) precision. Thus, TS represent a very interesting PSI product, since they provide the whole deformation history over the satellite observed period, with one estimate per SAR acquisition, which is fundamental information for many applications.

It is important to remind that the TS are not a cumulative displacement: the position of each acquisition is referred to the master image and not to the previous image (Notti et al., 2011).

Despite the great potential of the PSInSAR technique, radar interpretation of slope movements is generally based on the sole analysis of average displacement velocities, while the information embraced in multi-interferograms time series is often overlooked if not completely neglected. The underuse of PS time series is probably due to the detrimental effect of residual atmospheric errors, which makes the PS time series characterized by erratic, irregular fluctuations, and also to the trouble of performing a visual analysis of the time series for a large dataset (Berti et al., 2013). As a result, PSI time series are somewhat noisy and difficult to interpret, because of the noise errors and problems related to phase aliasing. For these reasons a linear regression model is generally fitted to the data and the average displacement rate is used to describe the entire time series.

Crosetto et al. (2009) assess that the real information content of the PSI deformation time series has not been entirely understood so far. Even if excellent time series examples have been published in the literature (e.g. Colesanti et al., 2003b; Parcharidis et al., 2010; Cigna et al., 2011; Tofani et al., 2013), their problematic has been not fully clarified yet.

As pointed out by Crosetto et al. (2010), TS product has two important limitations to account for: first, it is particularly sensitive to phase noise. Additionally, its interpretation can be affected by the (linear) deformation model assumption, made within many PSI approaches.

Concerning the linear deformation model assumption, until recently many PSI techniques made use of a linear deformation model in their estimation procedures. The linear model assumption can have a negative impact on the PSI estimates for all deformation phenomena characterized by non-linear temporal deformation behaviour, i.e. where the assumption is not valid. In areas where the deformation shows “significantly non-linear motion”, the PSI products may lack PSs, due to the fact that the PSI phases (i.e. the observations) do not fit the (incorrect) linear model. This may represent a critical limitation because PSI may be unable to provide displacement measurements precisely over the most interesting deformation area (Crosetto et al., 2010).

Figure 32 shows an example of PS time series with a linear evolution in time. Each PS has a quality index called coherence. This index describes how well the interferometric phase observations fit the used temporal displacement model (usually linear model), or, in other words, it represents the "degree of fit to the (linear) model". From the interpretation point of view, coherence values close to 1 (e.g. 0.96 in Fig. 32) corresponds to a good fit and so to a good PS with small phase noise; low coherence values can be due to "bad" PS with noisy phases, or misfit with the linear deformation model because the real deformation is not linear.

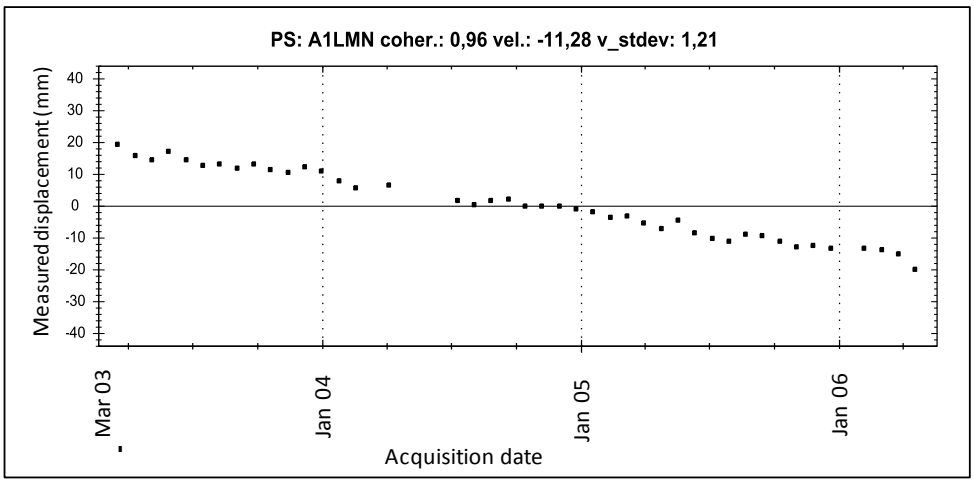

Fig. 32 - Example of a PS time series, showing a linear deformation evolution in time.

On one hand, until recent times, the most successful analysis on slow-moving ground displacements over regional areas by means of PS data provided good results only in the evaluation of the average yearly rate of movement (along the LOS) over the investigated satellite acquisition period.

On the other hand, the estimation of phase variation across time for producing deformation time series (TS), was firstly made with a linear model, so it was very difficult to have a time series that fit well with the real trend of deformation of a natural process. Using PSInSAR™, it was possible to use a non linear model only with a local advanced analysis scale (Ferretti et al., 2001).

In the last years, the development in the processing of SAR PSI data has allowed an improvement in time series precision, also over wide areas at regional scale. Nowadays, the more recent data are elaborated also with non-linear models and this allows studying also the temporal variation in the evolution of a natural process, even if some restrictions and problems arise (Notti et al., 2014).

For instance, the new SqueeSAR™ processing permits to elaborate a non-linear time series also on regional areas with a huge number of PS/DS (Ferretti et al., 2011).

In addition, the higher density of data (PS+DS) allows reducing the effects of noise (i.e. atmosphere) for the time series of SqueeSAR respect to PSInSAR.

Some methodologies for TS data interpretation have been proposed in literature, in order to improve the quality of the time series analysis and to obtain as much information as possible, as well as the study of few relevant time series for providing useful information on slope dynamics (e.g. Meisina et al., 2008; Cigna et al., 2011; Berti et al., 2013; Tofani et al., 2013). It is worth to highlight that these methods don't work on the TS generation processing, but only on the already processed data.

Cigna et al. (2011), in particular, manually sub-sample and classify the time series of several radar targets, in order to identify the change in deformation rate caused by a specific slope instability event with a known occurrence date.

The visual analysis and supervised manual classification of time series, however, is a tedious, time-consuming and subjective work which cannot be carried out for large datasets. Hence, criteria and methods for an objective, automated classification of time series included in large datasets are needed for enhancing radar

interpretation capabilities at the regional scale and for providing, at a glance, a comprehensive picture of the evolution of slope movements over the period covered by the interferometric analysis.

Some PSI-based studies have brought to light the importance of automatically calculating additional TS indexes, which are able to better characterize the information stored within each PS time series (Cigna et al., 2011; Berti et al., 2013). The extraction of these descriptors can facilitate the recognition of nonlinear components, accelerations, decelerations and – more generally – any kind of deviation from a trend defined *a priori.*

In order to analyze the TS and to identify different trends in time series, some works (Cigna et al., 2011; Notti et al., 2014) mathematically "derive" the time series of velocity. The velocity is the gradient of time series (*dx*/*dt*) calculated over an interval of at least 6 months to reduce variability noise effects. The method of Deviation Index (DI) indicates how a trend after an event at time x is different from previous trend; the index includes variability corrections. The variability (or noise) represents the dispersion of the time series. The greater the DI, the more different are the trends. Other works (Milone and Scepi, 2011) propose a classification of TS using models.

Cigna et al. (2012) proposed a semi-automated extraction of two different Deviation Indexes (DI), to improve the radar-interpretation of PS time series. These indexes, distinguished with regard to the typology of natural hazards at hand, are capable of recognizing deviations of the LOS displacements from the deformation model defined *a priori* during the PSI processing. Moreover, the added value of these DI lies in their practicality to facilitate the trend deviation identification while handling huge volumes of PS data (up to several thousands of targets per square kilometer), as those being increasingly provided after new high resolution satellite PSI processing.

Cascini et al. (2013) introduces the A-index, which can be computed for each PS time series, in order to complement with the mean velocity value; the A-Index represents the second order derivative of the second order polynomial curve best fitting the PS displacement time series. The combination of the velocity value and the A-Index of each PS can provide useful information on the trend of measured displacements. In particular, Cascini et al. (2013) find out that when the signs of the A-Index and the velocity are concordant (i.e. both negative or positive), then the trend of the time series can be considered increasing, while it can be considered decreasing if signs are discordant (Fig. 33).

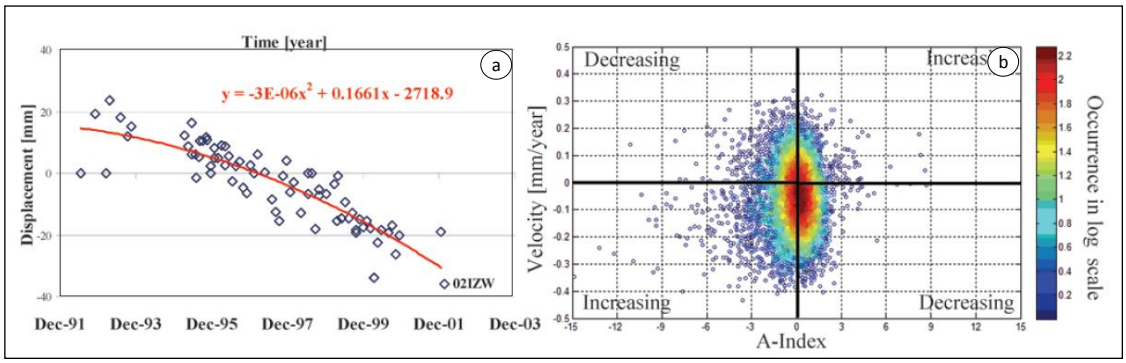

Fig. 33 - A-index value, representing the coefficient of x squared in the second order polynomial equation fitting the time series; (b) A-index vs. LOS-velocity diagram for the ERS PSI data; the color bar shows the occurrence in log-scale (Modified from Cascini et al., 2013).

Berti et al. (2013) present a procedure for automatic classification of PS time series based on a series of statistical characterization tests. The procedure allows classifying the time series into six distinctive target trends (0=uncorrelated; 1=linear; 2=quadratic; 3=bilinear; 4=discontinuous without constant velocity; 5=discontinuous with change in velocity) and retrieves, for each specific time series, descriptive parameters which can be efficiently used to characterize the temporal changes of ground motion. The results of the

analysis, tested in North Italy, show that even with a rough-quality dataset affected by a significant noise to signal ratio, the automated classification procedure can greatly improve radar interpretation of mass movements. Berti et al., (2013) assess that the spatial distribution of classified time series is also consistent with respect to the known distribution of flat areas, slopes and landslides in the tests area. Classified time series enhances the radar interpretation of slope movements at the site scale, pointing out significant advantages in comparison with the conventional analysis based solely on the mean velocity. Overall, in the work of Berti et al. (2013) uncorrelated PS (type 0) are concentrated in flat areas such as fluvial terraces and valley bottoms, and along stable watershed divides; linear PS (type 1) are mainly located on slopes or near the edge of scarps or steep slopes; non-linear PS (types 2 to 5) typically fall inside landslide deposits or in the surrounding areas. The spatial distribution of classified PS allows detecting deformation phenomena not visible by considering the average velocity alone, and provide important information on the temporal evolution of the phenomena such as acceleration, deceleration, seasonal fluctuations, abrupt or continuous changes of the displacement rate.

Notti et al. (2011) introduce two further methodologies for TS interpretation (Fig. 34). "The spatial averaging" consists in averaging the PS/DS time series in an area characterized by the same process (i.e. landslide or subsidence) that presents a wide extent and similar type of targets and where a cluster of PS/DS shows a homogeneous rate of displacement. This is a simple way to partially reduce the effect of noise, or local effect that can affect the single scatterer. The result of averaging is usually a smooth TS that fits well with the natural trend of process. It is worth to highlight that this averaging must be performed for TS of PSs over a single landslide with a same range of velocity or within the same geomorphological setting (Fig. 34a).

Another methodology proposed by Notti et al. (2011) is the "partial slope of TS" that consists in calculating the rate of the velocity for periods with homogeneous trend of displacement. This procedure is similar to the sub-sampling procedure, but applied to linear time series, purposed by Cigna et al. (2011). The "partial slope" can be obtained by a visual interpretation of the plotted TS. In this case, the main problem is to separate real variation and trends from errors, since each natural process usually presents its singular deformation behaviour, so that the analysis must be performed at local scale (Fig. 34b). If the TS is fragmented and periods of a certain number of observations (at least 4 - 5) are considered, the temporal trends are more regular and can be explained with a real variation of landslide movement. However, the variation on short period (1-2 satellite revisits) is not for sure related to a real variation and in some cases changes could be related to a possible phase unwrapping (Notti et al., 2011, 2014).

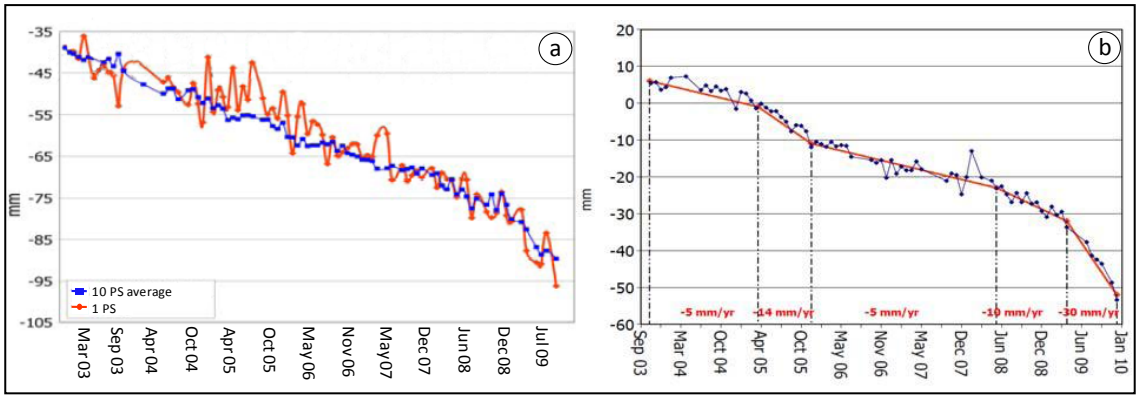

Fig. 34 - Methodologies of TS data interpretation: (a) "Averaging": time series of a single PS compared with average TS of 10 PS/DS over landslides in Oltrepò Pavese; (b) "Partial slope": Time series of landslides in Po Valley, Piemonte. It is possible detect different trend of velocity (Modified from Notti et al., 2011).

Notti et al. (2014) developed interesting post-processing tools in order to solve some problems affecting the time series, i.e. the detection of false trends, and the resolving of phase unwrapping.

Regarding the detection of false trends, it can be observed that TSs may be affected by temporal patterns or anomalous measures that not related to real ground movement of landslides, but to other factors. These trends usually affect the whole PS dataset: for instance, if the effect of thermal dilatation or other local effects (like single building settlement) are affecting the chosen reference point, then all the TS should be noised. Another problem may be related to an anomalous and spatially diffuse value of TS caused by atmospheric events that can affect SAR image. In order to detect this kind of problems, Notti et al. (2014) suggest to analyze very stable and high coherence TS on some stable areas, so if more than 1/3 of TS shows a high dispersion value (> +/- 5 mm than standard TS) at the same date, then it is an indicator of probable noise of SAR image.

In order to detect and correct potential phase unwrapping mistakes in the time series by only analyzing consequential displacement, Notti et al. (2014) propose the equation (4). If the displacement (D) between two consecutive acquisitions (tx, tx+1) is major or equal than + λ/4 (the phase ambiguity) (e.g. 14 mm for C-Band) we correct the series by introducing a shift of -λ/2 (e.g. -28 mm for C-Band).

$$\text{IF } D(t_{x+1}) - D(t_x) \geq \lambda/4 \text{ mm} \rightarrow D(t_{x+1}) - \lambda/2 \text{ mm} \qquad (4)$$

It is important to remark that the phase unwrapping is only an hypothesis of solution of the phase ambiguity. In order to validate the unwrapping it is necessary to have other available monitoring data or clear evidence from further sources (e.g. historical reports, rainfall, literature) that the landslides had relevant accelerations in the same period of potential phase unwrapping mistake (Notti et al., 2014).

6.2 PS time series quality and validation

Time series validation methods and results can be assessed and tackled in order to better understand the information they provide.

Considering large PS datasets coming from ERS and ENVISAT data, Crosetto et al. (2008b) reported the degree of similarity of the TS patterns estimated, over common PSs, by different working teams. This was measured by the correlation coefficient between TS pairs. A generally low degree of similarity was observed, raising doubts on the actual information contained in the analyzed TSs. According to Crosetto et al. (2010) the information content of the C-band TSs has yet to be fully studied. Even though excellent TS examples have been published in the literature (e.g. Cigna et al., 2011; Shanker et al., 2011; Herrera et al., 2013), the global performances of large TS datasets have not been fully understood.

In order to validate and better analyze the landslides kinematics by means of PS temporal patterns, the time series can be compared with data histories of other monitoring techniques and instruments

This comparison is important to make a cross-validation, so that the errors of both the monitoring systems can be detected. One of the advantages of PS time series is the sample frequency (e.g. 34 or 24 days for C-band satellites up to 16-4 days for X-band sensors) that is higher than other non-continuous monitoring systems like GPS or inclinometers (usually no more then 2 - 3 measures per year). Another advantages is the possibility to compare time series that cover the same time intervals for many landslides and so it is easier to detect regional events and compare the different behaviour of landslides in relation with triggering events (Colesanti et al., 2003b; Herrera et al., 2013; Notti et al., in press).

The main con of time series of SAR data is related to the impossibility of increasing the number of measures during critical events of landslide accelerations. Other disadvantages are related to the small range of detectable velocity (up to few tens of cm per year) and to the already known PSI limitations (Notti et al., in press).

Concerning the cross-comparison time series and inclinometers or GPS data, it is important to consider that the displacement is calculated in two different ways by the two monitoring techniques: the inclinometers register the cumulated displacement along the line of maximum movement and they are referred to a stable surface under the sliding surface, while the PS time series are not cumulative displacement curves because each measurement is the difference with the original master image (usually at the first image of the sequence). Moreover the target points of measurement (PS) are usually placed on buildings, debris and other objects that can be affected by other movements, and the reference point is a motionless benchmark located outside the investigated landslide. Colesanti et al. (2003b), Herrera et al. (2013) and Tofani et al. (2013) are some examples of successful results in comparing inclinometers and time series data for landslides analysis.

Within the European project DORIS, a procedure to determine the PS time series confidence degree was experimented. This method was implemented for evaluating the quality of a specific SAR dataset to perform a PSI processing. This information can be very useful to understand the quality of the PS time series based on the SAR images availability. In order to assess this confidence degree the following parameters have to be considered (Fig. 35): (i) the number and dates of SAR acquisitions and the theoretical revisiting time; (ii) the spatial baseline distribution; and (iii) the SAR satellite sensor used for the processing (e.g. ERS/ENVISAT, Radarsat-1/2, ALOS, TerraSAR-X or Cosmo-SkyMed).

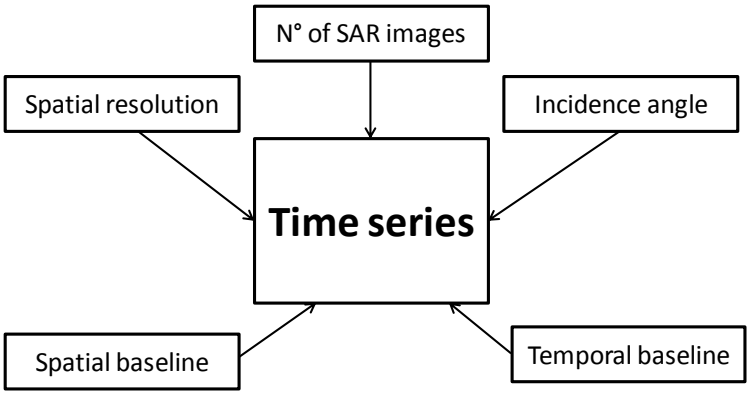

Fig. 35 - Parameters for assessing the quality of TS.

Firstly, a classification based on the number of SAR images and the acquisition satellite is proposed (Tab. 9). In this case we are considering the quality of a dataset with respect to the wavelength. Accordingly, due to the temporal de-correlation that increases with the wavelength, we need a larger number of acquisitions for X band than for C-band to guarantee the same quality values.

Value	Nº. Images L-band	Nº. Images C-band	Nº. Images X-band
1	1-7	1-15	1-20
2	7-14	15-30	20-35
5	>14	>30	>35

Tab. 9 - Quality values based on the Number of images and different SAR satellites.

Secondly, the acquisition frequency is evaluated considering the mean temporal baseline (TB) between each acquisition and the following one. This value gives an estimation of the temporal "density" of the SAR dataset (Tab. 10).

Value	TB L-band (days)	TB C-band (days)	TB X-band (days)
1	> 360	> 120	> 60
2	180-360	60-120	30 -60
3	1-180	1-60	1-30

Tab. 10 - Quality values based on the mean temporal baseline (TB).

Next parameter evaluates the geometrical de-correlation, which depends on the spatial perpendicular baseline, the incidence angle and the spatial resolution, according to the critical spatial baseline definition (equation 5):

$$Bperp_{critical} = \frac{\lambda}{2\Delta r} r' \tan \vartheta \qquad (5)$$

Where λ is the wavelength, r' is satellite height, ϑ is the incident angle and Δr is the slant range resolution.

The mean spatial baseline (SB) is computed on the generated interferometric pairs and evaluated according to Table 11.

Value	SB L-band (m)	SB C-band (m)	SB X-band (m)
1	> 1500	> 500	> 300
2	750-1500	250-500	150 -300
3	1-750	1-250	1-150

Tab. 11 - Quality values based on the spatial baseline distribution (SB).

The incident angle and the spatial resolution (slant range) is evaluated according to Table 12.

Value	Incident angle (IA)	Spatial resolution
1	<25	>6
2	25-35	3-6
3	>35	<3

Tab. 12 - Quality values based on the spatial resolution and incidence angle.

Finally, all the values obtained in Tables 9 to 12 are combined (addition) to generate Table 13 where 3 levels (low, medium and high) are provided about the potential quality of the PS time series, i.e. the PS time series confidence degree.

Value	Confidence Degree (CD)
Low	5-9
Medium	10-13
High	14-17

Tab. 13 - PS time series confidence degree.

The analysis of the PS time series related to some geological processes permits to identify the main factors that have an influence on the time series and, at the same time, to evaluate the reliability of TS to describe natural processes.

In Figure 36 the main factors that should have an influence on TS patterns are represented, taking into account only the factors related with natural processes. Besides the chosen sensor (and the quality of its SAR images), the chosen algorithm for processing, and the residual noise effects (e.g. atmosphere), temporal patterns of TS can be related to deformation of single scatterer (i.e. thermal effects or building deformation) or deformation on large scale (i.e. landslides or subsidence), as well as to the phase unwrapping problems (Notti et al., 2014).

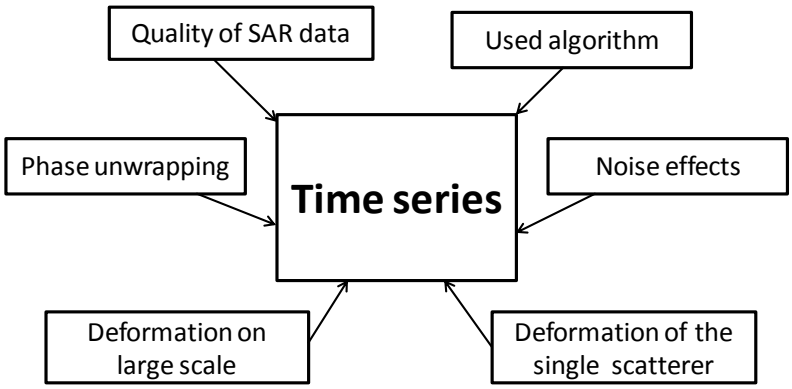

Fig. 36 - Factors that influence TS.

Over wide areas it is important separating the deformation of the single persistent scatterer from the main deformation. One of the effects to take into account at single scatterer scale is the thermal dilatation (Crosetto et al., 2010; Notti et al., 2011). This effect usually affects large metal structures and other hand- made objects. The natural scatterers (debris or rock) are less affected by this problem. If this process affects the target used as reference point the oscillation may affect (with an opposite oscillation) the other time series and cause misunderstanding in the interpretation.

For studying deformation and natural processes like subsidence or landslides on large scale, PS time series can be compared with other monitoring data (e.g. rain gauges, GPS, leveling, inclinometers) to see how TS match with them (Colesanti et al., 2003b, Tofani et al., 2013). However, as mentioned before, it is difficult to compare TS with inclinometers data, due to the different time sampling, the period of measure, the direction of measure. Usually it is better to do a qualitative comparison than a quantitative. For instance it is important to verify that both the systems detect the same temporal trend of deformation like accelerations or stops, instead of comparing the absolute rate of movement.

A landslide with a displacement rate at the limits of PSI detection can be well described only if its movement is linear. Also slow-moving landslides that present a rapid acceleration are not good for analysis through PS time series that may be affected by phase unwrapping effects.

The landslides usually do not have a regular and linear trend, but the rate of movement can change during the year, due to the external conditions (rainfall, snow melting, ground water etc.).

In many cases related to landslide or subsidence with slow and constant movement, it is possible to detect different trends in the period of measurement. Long term trends are usually easy to identify and sometimes also seasonal trends may be detected. The displacement rate is usually related to rainfall or groundwater table variation.

The non-linear time series can detect quite well the smooth change in the rate of movement, like a seasonal or long terms trends, but not the rapid acceleration. If a landslides (or other process) move more than $\lambda/4$ between two acquisitions (e.g. 14 mm with C band) it is not possible, without any other information, to determine the real displacement. If the movement is very fast, then coherence is lost and any PS/DS can be retrieved, but if the movement is in the order of 1/2 phases shift, then the PS can be probably identified, even if we underestimate the real movement.

Sometimes it is possible to detect processes that are moving more than λ/4 between two acquisitions by applying a phase unwrapping, but, to confirm this, it is necessary to compare TS with other monitoring data, and consider this data with extreme caution (Notti et al., 2014).

6.3 PSI-based interpretation of landslide time series

Besides the simple use of the average annual rates of motion, local scale applications and analyses of single landslide phenomena can frequently benefit from the information stored within the deformation history of each PS (e.g. Tapete et al., 2012), where ground motions are recorded with millimeter precision at each satellite acquisition. In these cases, the characterization of the deformation behaviour and the quality of a set of radar targets are often insufficient, if only based on the yearly velocities, their standard deviation and the coherence of the available targets (Cigna et al., 2011).

The exploitation of PS time series of displacement provide valuable information about the temporal evolution of landslides, allowed a more realistic detection and classification of the phenomena and a better understand of the deformation pattern across time.

The availability of a large number of satellite SAR images derived from the ESA archives in the microwave C-band (ERS and ENVISAT), permits to analyze the historical evolution of the displacements from 1992 up to present.

The temporal continuity and the geometric compatibility among time series of ERS 1/2 and ENVISAT data represent an unprecedented opportunity to generate very long time series of ground deformations. This provides exclusive information for an improved understanding of the long term behavior of slow and very-slow ground displacement phenomena.

In the **Annex 8** (Del Ventisette et al., 2013), the catalogues of multiple C-band SAR sensors (e.g., ERS-ENVISAT) are extensively exploited to finally provide, via a joint analysis, additional information on ground movements in different test sites in Europe, in the framework of DORIS projects. The paper shows a detailed description on the potential of generating very long deformation time series (almost 20 years) by properly merging the ERS-1/2 and ENVISAT datasets, throughout different interferometric techniques (i.e. SBAS, PSInSAR, IPTA, SPN techniques).

The investigation and temporal characterization of landslide phenomena can be successfully performed at local scale by means of accurate PS time series analysis. In the **Annex 9** (Bianchini et al., 2013b) and **Annex 10** (Bianchini et al., 2012b), the detection and monitoring of landslide phenomena across time is carried out over a village (Gimigliano site) in Calabria region (Italy). In the paper, X-band data and time series show a remarkable and useful quality improvement with respect to the C-band, especially for investigating non-linear motions at a detailed scale, due to the higher resolution and shorter temporal revisiting time, up to 4 days.

Time series turn out to be a valuable and reliable tool for studying natural ground motion, especially through the integration with *in situ* monitoring instrumentation and ground truth, e.g. rainfall data (Hilley et al., 2004; Zhao et al., 2012; Zibret et al., 2012; Tofani et al., 2013).

Annex 8: Del Ventisette C., Ciampalini A., Manunta M., Calò F., Paglia L., Ardizzone F., Mondini A., Reichenbach P., Mateos R.M., BIANCHINI S., Garcia I., Füsi B., Villő Deák Z., Rádi K., Graniczny M., Kowalski Z., Piatkowska A., Przylucka M., Retzo H., Strozzi T., Colombo D., Mora O., Sánchez F., Herrera G., Moretti S., Casagli N., Guzzetti F. (2013) Exploitation of Large Archives of ERS and ENVISAT C-Band SAR Data to Characterize Ground Deformations. *Remote Sensing,* 5 (10), 3896-3917; doi:10.3390/rs5083896.

Annex 9: BIANCHINI S., Cigna F., Del Ventisette C., Moretti S., Casagli N. (2013b) Monitoring landslide-induced displacements with TerraSAR-X Persistent Scatterer Interferometry (PSI): Gimigliano case study in Calabria Region (Italy), *International Journal of Geosciences*, 4(10).

<u>Annex 10:</u> BIANCHINI S., Cigna F., Del Ventisette C., Moretti S., Casagli N. (2012b) Detecting and monitoring landslide phenomena with TerraSAR-X persistent scatterers data: the Gimigliano case study in Calabria region (Italy). In: IEEE International Geoscience and Remote Sensing Symposium. Remote Sensing for a Dynamic Earth - IGARSS2012, Munich, Germany, 22-27 July 2012, pp. 982 - 985, ISBN: 978-1-4673-1160-1.

Chapter 7

Implementation of remote sensing data

PSI techniques have recently demonstrated to be a valuable and successful tool to detect slope instability and map geomorphological processes such as slow-moving landslides (Mantovani et al., 1996; Hilley et al., 2004; Ferretti et al., 2001; Farina et al., 2006; Meisina et al., 2008; Herrera et al., 2009a; Righini et al., 2012; Cigna et al., 2012; Crosetto et al., 2010; Bovenga et al., 2012) with improved resolution and precision.

Nevertheless, they hold some limitations, mainly due to the acquisition geometry of the satellite systems. PSI-based displacement data are mono-dimensional along the satellite LOS (Line Of Sight); consequently, they are dependent on the relationships between sensor acquisition geometry, the local topography and the real direction of movement (Colesanti and Wasowski, 2006; Plank et al., 2010; Notti et al., 2010). This is critical when dealing with landslides, since only a fraction of slope movement component can be captured in the LOS. Additionally, the same ground movement can be estimated with opposite sign and different module from ascending and descending orbits, making the slope dynamics interpretation not immediately intelligible.

The suitability of PSI technique for investigating landslide phenomena on a given area depends on the geomorphological features of the area itself, as well as on the characteristics of the employed satellites, i.e. the acquisition parameters of the radar sensors.

Pre- and post-PSI processing implementations can be performed to increase the affordability of interferometric data for landslide analysis, by analyzing the geometrical visibility of the area of interest we are investigating, and by evaluating the radar data suitability. PS data derived from different satellite sensors and orbits can be homogenized, for instance, by re-projecting LOS velocities along the local steepest slope (assumed as the most probable direction of movement) and/or further validated throughout field surveys or other additional ground-truth data. Moreover, the confidence degree of the landslide inventory, or what else is the PSI-based product-map, can be assessed, in order to determine how truthful and reliable it is, on the basis of the availability and use of radar data and other external information sources. In this section, all these facets are tackled and discussed, taking into account the most important topics, and past and recent literature works.

7.1 Visibility and radar data suitability

The geometrical visibility of an area to perform PSI analysis is related to the combination of the local topography in respect with the satellite acquisition mode. Thus, the suitability of a slope to be investigated through PS data depends on its aspect and inclination, with respect to the LOS orientation.

The choice of the proper SAR dataset for studying surface ground motions within a given area must be taken into account for a correct visibility of the phenomena on the slopes; the use of the appropriate satellite orbital geometry (i.e. ascending or descending) is also fundamental for a truthful analysis.

Observation of the PS distribution with respect to the aspect map reveals that the number and percentage of PS significantly depend on the orientation of the slopes. Generally, radar data collected in ascending orbits are suitable for detecting E-facing slopes, while descending passes are more appropriate for W-facing slopes.

The role played by the aspect angle and the slope inclination on the feasibility of SAR deformation monitoring has been discussed in literature in the last years (e.g. Colombo et al., 2006; Cascini et al., 2010; Notti et al., 2010). In these works, the geometrical visibility for PSI analysis in a given area of interest was performed by forecasting the PS density of the area, through the combination of the effects of radar geometry with local topography and land use. In particular, Colombo et al. (2006) predict the PS targets density of an area by

merging the geometrical distorsion effects produced by radar acquisition with topographical characteristics. Cascini et al. (2009, 2010) produce an "*a priori* DInSAR landslide visibility zoning" to address the choice of the most suitable image datasets. Notti et al. (2010) introduce the visibility indexes (i.e. R-index, L-index and the resulting RC-index) generated by an equation that takes into account land use, slope and aspect as visibility factors for forecasting the PS number of the area of interest.

In particular, the effect of the topography can be assessed through the "R-Index" (RI), firstly proposed by Notti et al. (2010). The R-Index is calculated through equation (6) that represents the ratio between the slant range and the ground range, considering the acquisition geometry of the radar (i.e. incidence angle = θ; angle from North of the satellite track = α) and the geometry of the ground surface (slope and aspect layers, S and A respectively, derived from DEM:

$$RI = -\sin(S \cdot \sin(A - \alpha + 90) - \vartheta) \qquad (6)$$

The RI ranges from the maximum value +1 to -1. It assumes the maximum value when the suitability of the area to be investigated through the selected PS dataset is the highest: this means that the slope direction of the area is approximately parallel to the satellite LOS direction. On the contrary, the R-index assumes negative values when no PS can be detected or when geometrical distortions (i.e. layover and the shadow effects) prevent an acceptable visibility of the area. The R-index is around 0 where the area is affected by foreshortening effect.

Regarding the Land use, Notti et al. (2010) assigned a unique land use index, "LU index" (LU), for each land use class of the CORINE land use information, which varies from 0 (no PS can be detected) to 100. Finally, a resulting RC-index is evaluated on the combination of RI and LU-indexes (Notti et al., 2010, in press).

The radar "ranging" mechanism induces a slope dependent resolution along ground range, leading to geometric distortion effects which need to be taken into account before attempting the exploitation of SAR data. Satellite acquisition with a looking angle θ causes perspective deformations due to the terrain conformation. Therefore, the combination of the local incidence angle with the local terrain slope can cause significant underestimation of land motions, or can even prevent the identification of PS within the observed scene, due to geometric effects of the ground, i.e. foreshortening, layover and shadowing.

Cascini et al. (2009) and Colesanti and Wasowski (2006) addressed considerations on the assessment of suitability of PS data with respect to the inclination of the orbit and to the aspect of the slope and determined zoning masks of each distortion effect (foreshortening, layover, areas with enhanced resolution and areas in shadow) for every available PS dataset.

Table 14 summarizes the main geometrical constraints dealing with incidence angle and slope angle on the feasibility of SAR data, after Cascini et al. (2010). Available satellite systems have a quasi-polar orbit and are side-looking, therefore they have no sensitivity along the platform flight direction (azimuth) and any deformation occurring along the north-south direction has a very small LOS projection. Thus, translational displacements along the north-south direction are characterized by a low system sensitivity and turn out to be visible with difficulty, whatever acquisition geometry is used.

Best resolution for visibility is obtained on slopes dipping away from the sensor (i.e. areas facing west, northwest and southwest for descending passes and areas facing east, northeast and southeast for ascending passes) and exhibiting slope angles lower than 90° - Θ. However some visible areas could be in shadow due to the presence of nearby peaks with local slope inclinations higher than 90° - Θ. Slopes dipping towards the sensor are considered not well visible because of foreshortening and layover effects. In particular, foreshortening distortion occurs on slopes facing the sensor with slope angle lower than the satellite incidence angle ($0 < \alpha < \Theta$): these areas are compressed in a few image pixels with bright reflectivity, representing a sum of signal contributions referred to scattering elements spread in a larger sampling cell. Such slopes show a

significantly bad resolution, also worse than flat terrain. Slopes with inclination exceeding the incidence angle ($\alpha > \Theta$) are affected by layover effect, as the top and bottom of the slope appear inverted on the SAR image.

Orientation of slope	Satellite sensors (L-, C-, X-band)	
	Ascending passes	Descending passes
Slope facing E	Best range resolution if $\alpha < (90 - \Theta)$ ---------- Shadow if $\alpha > (90 - \Theta)$	Foreshortening if $\alpha < \Theta$ ---------- Layover if $\alpha > \Theta$
Slope facing W	Foreshortening if $\alpha < \Theta$ ---------- Layover if $\alpha > \Theta$	Best range resolution if $\alpha < (90 - \Theta)$ ---------- Shadow if $\alpha > (90 - \Theta)$
Slope facing N or S	Visible with difficulty	Visible with difficulty

Tab. 14 - Main geometrical constraints dealing with incidence angle (Θ) and slope angle (α) on the feasibility of SAR data (Modified from Cascini et al., 2010).

Notti et al. (in press) (**Annex 11**) and Bianchini et al. (2013c) (**Annex 12**) have improved these facets by enhancing the methodology for deriving visibility indexes and thus for assessing the suitability of an area to be investigated by PSI analysis.

In Notti et al. (in press) a new formula for deriving the R-Index is exploited:

$$\begin{aligned} RI &= -\sin((S \cdot \sin(A + \omega)) - \alpha) \cdot Sh \cdot L \\ \text{Where: } \omega &= 4.712 - \theta \\ Sh: \text{ Yes} &= 0 \text{ No} = 1; \\ L: \text{ Yes} &= 0 \text{ No} = 1; \end{aligned} \quad (7)$$

Where the shadowing (Sh) and Layover (L) effects are also taken into account. Four main R-index classes are determined and in particular RI values from 0.66 to +1 are estimated when the suitability of the area to be investigated through the PS dataset is the best: this means that the slope direction of the area is approximately parallel to the satellite LOS direction (class 4). RI values from 0.33 to 0.66 include either PS located on slopes with an acceptable geometry with respect to the satellite LOS or PS located in flat areas. RI values between 0.00 and 0.33 indicate that the slope geometry is not favourable for the satellite acquisition geometry and a lower PS number is retrieved.

Bianchini et al. (2013c) calculate the Land Use Index (LU-index) for analyzing the effect of the land coverage on PS detectability and five main categories of land use are defined, based simply on the theoretical radar signal penetration properties. Bianchini et al. (2013c) (**Annex 12**), differently from Notti et al. (2010, in press), evaluated RI and LU separately, since the two indexes are not merged together, due to the different calculation and kind of information they rely on.

Moreover, visibility indexes in Bianchini et al. (2013c) are calculated not as predictors of PS, but to give a "quality" index to each PS in relation to the slope geometry and land characteristics of the area of interest (respectively R- and LU- indexes). Thus, the R- and LU-indexes are calculated and then assigned to each PS and to every landslide, assessing how good the ground surface is to backscatter the satellite radar signal in relation to its relief and land use.

Complete findings of the performed work are presented within the two papers (**Annex 11** and **Annex 12**) and also within the proceeding Bianchini et al. (2013d) (**Annex 13**), written in Spanish and presented to the Simposio Nacional sobre Taludes y Laderas Inestables, held in Palma de Mallorca in June 2013.

7.2 Homogenization of satellite acquisition modes

Post-processing homogenization of radar data measured along the satellite LOS can be necessary within the PSI analysis for landslide investigations.

In order to homogenize PS data derived from different satellite sensors and from different acquisition orbits (i.e. ascending and descending), some PSI post-processing procedures have been tested and applied in literature to the original radar datasets before using them for ground motion mapping (Colesanti and Wasowski, 2006; Cascini et al., 2010; Raspini et al., 2012; Plank et al., 2012; Greif and Vlycko, 2012).

In particular, two significant operative procedures for homogenizing PS data aim at obtaining integrated datasets in which the displacement can be referred to the local slope movement and/ or to the horizontal planar and the vertical directions (Fig. 37).

The first one can be applied when only a single orbit of a satellite is available and leads to the re-projection of PS LOS velocities along the slope direction. The second one is applied when the two acquisition geometries (i.e. ascending and descending) are available for the same satellite sensor and allows combining velocities obtained from the two orbits in order to decompose the displacement into its horizontal and vertical motion components. As a result of these data implementations, the outcoming PS targets are more easily detectable and comparable, going beyond the satellite parameter differences and enabling a more feasible and well-founded interpretation.

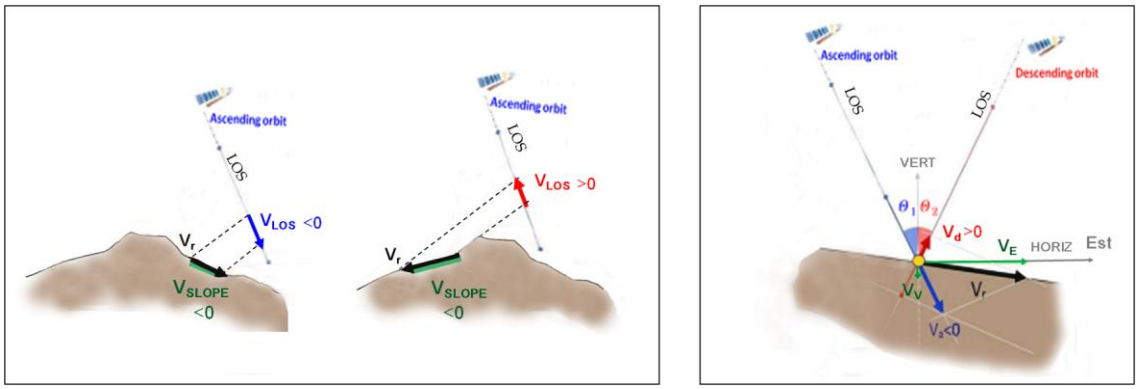

Fig. 37 - Operative procedures for homogenising PS data: LOS displacement projection along the steepest slope (left) and the combination of ascending and descending geometries for deriving vertical and horizontal East-West components of movement.

7.2.1 LOS displacement projection along the steepest slope

When we measure the displacement from the satellite, we can only detect the component of the movement that is parallel to the Line Of Sight (LOS) direction. Thus, PS displacement represents the one dimensional

projection, along the LOS, of the real displacement, which actually occurs in all three dimensions (Cascini et al., 2009).

As a result, a correction factor has to be applied to the LOS measurement , in order to determine the "real" velocity (not the one measured in the LOS direction but the one occurring in the landslide direction). Such correction factor must take into account topographic parameters (e.g. slope and orientation of landslide), as well as other satellite-dependant parameters (e.g. incidence angle and azimuth direction) (Fig. 38).

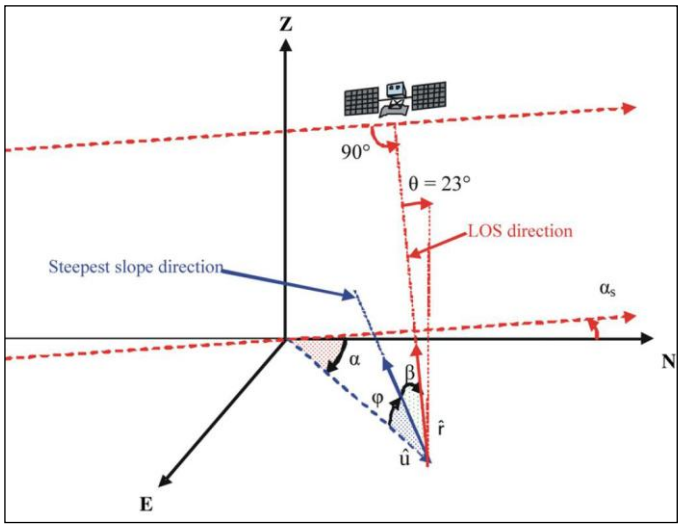

Fig. 38 - Satellite acquisition geometry for a point located on a given slope where : φ = Slope; α = Aspect; α_s = Angle between the azimuth and North direction (Azimuth-360°); θ = Incidence angle; β = Angle between the LOS and the steepest slope direction (From Cascini et al., 2010).

In order to overcome the differences given by ground aspect and satellite LOS, all the PS average yearly V_{LOS} (mm/yr) can be projected into the same direction of the steepest slope, obtaining V_{SLOPE} (mm/yr). The relation between the "real" velocity in the direction of the landslide direction (V_{SLOPE}), the measured velocity in the satellite LOS (V_{LOS}) and the correction factor (Corr3D) is given by the equation (8):

$$V_{SLOPE} = V_{LOS} * Corr3D \quad (8)$$

This LOS projection is designed to compare landslide velocities with different slope orientations, resolving the satellite acquisition orbit differences.

The most used methodology for LOS projection along the slope direction is the one proposed by Colesanti and Wasowski (2006) and Cascini et al. (2010) by means of equation (9), where for calculating V_{SLOPE} , V_{LOS} is divided into the fraction of motion measured by PS targets, represented by the correction factor called C coefficient, whose value depends on the slope and aspect map (S and A, respectively), and on the LOS directional cosines (nlos, hlos, elos) (Massonet and Feigl, 1998; Colesanti and Wasowsky, 2006).

$$\begin{aligned} &V_{SLOPE} = V_{LOS} / C \\ &C = \cos\beta \\ &where \\ &C = (\text{nlos} * \cos(S) * \sin(A - 90)) + (\text{elos} * (-1 * \cos(S) * \cos(A - 90)) + (\text{hlos} * \sin(S))) \end{aligned} \quad (9)$$

The coefficient C is the fraction of the 3D displacement that can be measured by the satellite and β the angle between the steepest slope and the LOS direction.

Bianchini et al. (2013c,d) **(Annex 12** and **Annex 13)** applied this projection and discussed that several limitations of this method must be taken into account: when β is almost 90°, C is close to 0 and V_{SLOPE} tends to infinity. Thus, an absolute maximum value of β =72° corresponding to cosβ =0.3 is fixed and, as a result, V_{SLOPE} cannot be higher than 3.33 times the V_{LOS} (Herrera et al., 2013). This threshold corresponds well to the condition number of 15 proposed also by Cascini et al. (2010) as the number for the inversion matrix solving the algebraic system used for the projection process.

Moreover, the V_{SLOPE} calculation is only valid when the landslide movement is parallel to the slope (Notti et al., in press). Since landslides are downslope movements usually characterized by a failure shear plane which is roughly parallel to the slope surface, we assume that the "real movement" occurs along the maximum slope direction; this could be almost true as the steepest gradient is the most probable direction of movement. By the way, the surface runoff of some mass movements could be not parallel to the slope, e.g. at the crown of a rotational landslide where also vertical motions can take place, or into a flow which usually undergoes internal derangement.

Valuable examples of the usefulness of this downslope projections can be found primarily in the annexes Bianchini et al. (2013c) **(Annex 12)**, Bianchini et al. (2013d) **(Annex 13)**, but also in Cigna et al. (2013) **(Annex 10)**, Notti et al. (in press) (**Annex 11**), Bianchini et al. (submitted) (**Annex 14**).

7.2.2 Horizontal East-West and Vertical estimation of the displacement

The same slope movement can be recorded by PS data with opposite sign and different module from ascending and descending orbits, making the interpretation of slope dynamics not immediately intelligible.

Under the assumption of the absence of N-S horizontal motion, the availability of two geometries (ascending and descending) allows the east-west (VEL_{EW}) and vertical (VEL_{VERT}) velocity components to be resolved (Manzo et al., 2006; Tamburini et al., 2012). The interpolation of ascending and descending velocities to provide the scomposition of the motion into its horizontal and vertical components has been already discussed by the scientific community. In particular, this elaboration can be accomplished by using either the raster of interpolated V_{LOS} values to create a map (raster-based approach) or using two single or more nearby PS with differing geometries (vector-based approach). In literature, the two traditional methods have been proposed and are usually used to combine ascending and descending datasets: the first one is the raster-based approach that interpolates the point-wise velocity values throughout a spatial interpolator of PS rates in each acquisition geometry (i.e. IDW, Inverse Distance Weighted) and a successive combination of the two derived maps (Manzo et al., 2006; Raspini et al., 2012). The second method used in literature is a fishnet-approach (vector-based) that resamples the PS points on the basis of a regular grid and obtain new points at the centre of each cell, characterized by a displacement velocity computed as the average of all the PS rates included within the cell, calculating separately ascending and descending mean velocity (Vel_a and Vel_d); these values are then combined mathematically, by means of equation (10), to determine the vertical and horizontal (East-West) components of the ground movement within the area of interest (MATTM, 2010).

$$VEL_{EW} = \frac{(([\,Vel_d\,]/hlos_d) - ([\,Vel_a\,]/hlos_a))}{(elos_d/hlos_d - elos_a/hlos_a)}$$

$$VEL_{VERT} = \frac{(([\,Vel_d\,]/elos_d) - ([\,Vel_a\,]/elos_a))}{(hlos_d/elos_d - hlos_a/elos_a)} \quad (10)$$

Being raster-based, the first approach risks to combine PS belonging to very different slope surfaces and, possibly, to different slope instability phenomena. Being fishnet-based, the second method couples many PS targets taking into account average values that may not be representative of the real displacement.

An innovative method to properly combine the radar LOS velocities achieved from the ascending and descending passes has been recently proposed by Notti et al. (in press) (**Annex 11**). This method overcome some problems of the previous procedures that risked to combine PS belonging to very different slope surfaces or to couple too many PS targets. This new procedure, explained in the Annex, exploits a buffers-intersection (vector-based) approach, which only couples PS pairs from the two different orbits (one PS ascending with one PS descending) on the basis of geometric relationships between neighbour points. The PS that come out from the combination of ascending and descending targets are called "Synthetic PS", on which the E-W and vertical displacement rates can be retrieved by applying equation 10.

7.3 Exploitation of "Out-points"

Point-wise ground motion information provided by PS data can have a purely geological or anthropogenic origin as well as a combination of both. As a result, from a geomorphological point of view, it is interesting to also give attention to all the PS candidates that, after processing and post-processing implementation, show significant ground motion, and it is straightforward to understand the triggering causes of the displacement.

Meisina et al. (2008) proposed a methodology to identify, besides landslides, the so-called "anomalous areas" consisting of clusters of minimum 3 PS with a maximum distance of 50 meters characterized by high displacement rates (> 2 mm/yr away or towards the satellite).

More recently, Bianchini et al. (2013c) **(Annex 12)** introduce the concept of "Out-points". Out-points are PS that are not included within any mapped landslide, but even moving, potentially referred to unmapped landslides or triggered by other kinds of geomorphological processes (Fig. 39).

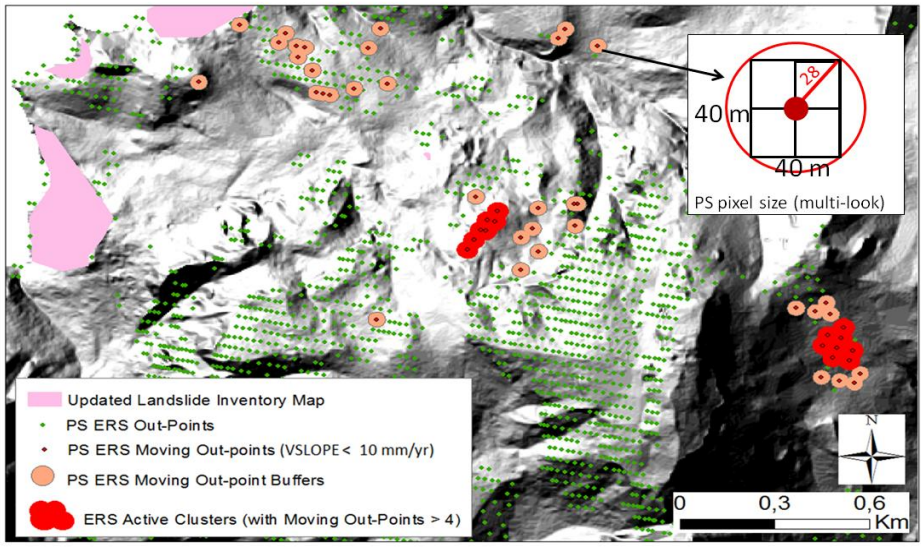

Fig. 39 - Procedure to derive Outpoints and consequently "Active clusters" to produce "Ground motion Activity map" (Modified from Bianchini et al., 2013c and from Deliverables of European DORIS project: http://www.doris-project.eu).

This aspect is important to address to, since these moving radar benchmarks can reveal other types of movements to be taken into account, i.e. some gravitational movements like erosion or downhill creep processes, characteristic of mountainous environments. A innovative methodology is proposed by Bianchini et al. (2013c) **(Annex 12)** to exploit Out-points for detecting "active PS clusters" over wide area, in order to highlight ground motion instability that is not recorded in landslide inventory, but anyhow measured by PSI

technique. Active clusters lead to the elaboration of the so-called Ground motion activity map at regional scale, in addition to the Landslide activity map (Bianchini et al., 2013c).

Out-Points represent a big percentage of each whole radar dataset (Bianchini et al., 2013c). This is a significant topic that is not usually taken into account in previous works. Bovenga et al. (2006) highlight that the locations of moving PS groups appear consistent with past or recent landslides or can even coincide with distressed buildings and structures. In general, in addition to landslide movements, there are several other more or less ground displacement phenomena such as local subsidence (whatever man-made or caused by natural processes such as compaction, thawing), settlement of engineering structures, sedimentary erosion, downhill creep, terrain shrink and swell.

Wasowski et al. (2002) pointed out that local ground surface displacement patterns and their variability may be related not only to landslide processes, but also to other more or less local movements (e.g. edifices settlement or volumetric changes of geological materials); *in situ* data and monitoring controls are usually needed to discriminate the exact cause of very slow ground surface active movements.

PSI technique must be considered an added value to the analyses of the areas affected by slope instability, since ground movement evidences obtained from radar data need to be compared with other kind of techniques and information. PSI analysis has to be used as complementary tool to traditional geomorphological techniques, ground-based monitoring techniques and *in situ* measurements, in order to achieve a reliable investigation.

A validation activity would be needed as much as possible to support the results provided by remote sensing data and to better understand the triggering factors of ground movements: field surveys would be carried out to confirm and improve information obtained by radar interpretation, e.g. in order to check geomorphological features induced by ground instability (Meisina et al., 2008; Righini et al., 2012) or to verify cracks on roads or buildings (Bianchini et al. (submitted): **Annex 14**; Bianchini et al. (2014): **Annex 15**; Ciampalini et al. (to be submitted): **Annex 16**).

Anyway, ground motion activity maps performed by means of PSI data turn out to be very useful since they can give a preliminary overview of the areas to put the attention to at regional scale, whatever referred to recorded landslides or to other natural phenomena. Further investigations, e.g. geophysical surveys or geotechnical monitoring, could be carried out to gather more subsurface data (Bovenga et al., 2006; Tamburini et al., 2012) and to analyze more in-depth slow-moving processes or gravitational movements.

7.4 Confidence degree evaluation

The confidence degree of landslide maps elaborated by means of PSI data can be evaluated throughout their comparison with external independent sources, such as damages inventories, *in situ* measurements, field checks etc..

Bianchini et al. (2013c) (**Annex 12**) proposed the confidence degree evaluation of "Landslide and Ground motion Activity Maps", where the "activity map" is intended as a spatial distribution of potentially active areas characterized by high ground motion rate. This evaluation aims at assessing if measured displacement represents landslides dynamics. It is important to highlight that the reliability on the PSI measurement itself is not evaluated, but whether this measurement is related to landslide activity or not. Three confidence degree levels are established - low, medium and high – depending upon ground truth data availability (Fig. 40).

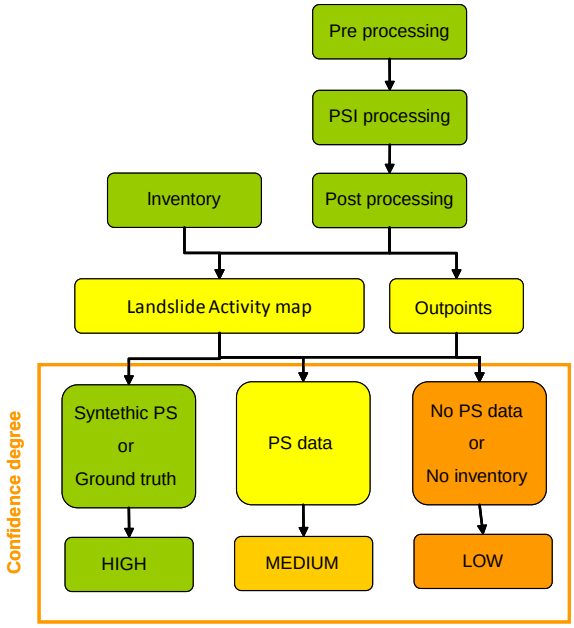

Fig. 40 - Confidence degree determination for landslide and ground motion activity maps.

A low confidence degree is assigned to landslide mapped areas (LIM – Landslide Inventory Mapping) where no sufficient PS data or no ground truth data provide evidence of the terrain displacement, and even to the Active PS clusters derived from moving Out-points since the triggering mechanism of the observed displacement is unknown (Tab. 15). A medium confidence degree is allocated to those landslide mapped areas where PS data have been detected from the PSI processing of SAR images, but no external independent data sources are available to confirm that the measured displacement corresponds to landslide dynamic. A high confidence degree can be assigned to landslides where sufficient PS data have been measured from the PSI processing and additional ground truth displacement data are available within the landslide areas (Tab. 15).

External independent sources consist of damage inventories, *in situ* measurements, field checks etc., which provide clear evidence of displacement, e.g. a landslide produced damages in the period when SAR displacement measurements are available.

<table>
<tr><td></td><td colspan="3">Geo-thematic data</td></tr>
<tr><td>Confidence degree</td><td>Low</td><td>Medium</td><td>High</td></tr>
<tr><td rowspan="2">Landslide and Ground motion activity map</td><td>No sufficent PS data</td><td rowspan="2">PS data and no Ground truth</td><td rowspan="2">PS data and Ground truth</td></tr>
<tr><td>No LIM (Outpoints)</td></tr>
</table>

Tab. 15 - Confidence degree determination for landslide and ground motion activity maps.

7.5 Impact and damage assessment

Landslides threat human lives, properties and structures, especially in urbanized and populated areas characterized by significant built-up fabric and cultural heritage, where the socio-economic losses and damages are stronger because of the higher value of the element at risk exposure.

Buildings are sensitive to movements due to ground deformation caused by natural processes such as landslides (or subsidence). On one hand, oldest and/or historical buildings with shallow and inadequate

foundations usually record ground motion phenomena throughout the development of structural cracks and fractures on their facades, until the complete fail. On the other hand, more recent and modern buildings, built in reinforced concrete better, resist to deformation, but, in case of deep landslides, they can be interested by tilting.

Detection and mapping of the spatial distribution and degree of building damages, with respect to their constructions characteristics, can help in understanding the mechanisms, magnitude and distribution of occurred landslides. Furthermore, the spatial and temporal evolution of a landslide can be observed by repeating the mapping of the damages in different time periods. Space-borne SAR interferometry can be used to map and monitor movements related to building deformations on landslide-prone and -affected areas. In particular, PSI analysis is widely employed to analyze slope instabilities thanks to the non-invasiveness and the availability of long temporal series of satellite radar data, acquired over the same area of interest at different times, retrieving millimeter precise displacement information. Additionally, the combined use of radar data with traditional geomorphological tools like field surveys and *in situ* campaigns give a useful effort to the mapping and monitoring of the impacts of landslide phenomena on buildings and manufactures of the affected sites. In particular, the use of X-band data significantly improves the level of detail of the analysis since many targets show up on facades and roofs, and even small structures can act as stable scatterers that can be separated due to the very high spatial resolution (Gernhardt et al., 2010; Notti et al., 2010; Roth et al., 2003).

Several works in literature deal with the use of SAR ground motion rates and time series for detecting and monitoring displacements in urbanized sites and cultural heritage areas (Herrera et al., 2010; Parcharidis et al., 2010; Cigna et al., 2011; Tapete et al., 2012; Tomàs et al., 2012).

Bianchini et al. (submitted) (**Annex 14**) and Bianchini et al. (2014) (**Annex 15**) performed a radar mapping and subsequent zoning of the unstable urban sectors of San Fratello village in South Italy, by over-layering and cross-comparing multi-temporal PSI data (acquired in C- and X-band) with the distribution of churches and sites of cultural interest and with *in situ* observations and crack-pattern survey on buildings.

Thanks to the combined use of SAR archival data and new images, it is possible to analyze the building deformations before and after a landslide event, in order to highlight the presence of precursory symptoms of displacement and the eventual residual risk related to deformation after the event. Ciampalini et al. (to be submitted) (**Annex 16**) present an analysis of the building deformation velocities obtained by the intersection of PSI data and buildings map, in order to understand the evolution of the displacements and cracks of the buildings of San Fratello village. In particular C-band data collected before the 2010 event have been used to evaluate the presence of precursory symptoms of instability, whereas the X-band data, collected after the event, have been considered to detect the residual risks in post-event phase. Finally, the post-event building deformation velocity map is compared with the damage assessment map (Cooper, 2008).

Annex 11: Notti D., Herrera G., BIANCHINI S., Meisina C., García-Davalillo J. C., Zucca F. (in press) A methodology for improving landslide PSI data analysis. Accepted in *International Journal of Remote Sensing.*

Annex 12: BIANCHINI S., Herrera G., Notti D., García-Moreno I., Mora O., Moretti S. (2013c) Landslide activity maps generation by means of Persistent Scatterer Interferometry. *Remote Sensing*, 5 (12), 6198-6222, doi: 10.3390/rs5126198.

Annex 13: BIANCHINI S., Herrera G., Mateos R. M., García-Moreno I., Mora O., Sanchez C., Sanabria M., López M., Merodo J. A., Hernández M., Mulas J. (2013d) Metodología para mejorar el análisis de datos satélite radar en el estudio de los movimientos de ladera: resultados del proyecto FP7 DORIS en la Serra de Tramuntana (Mallorca). In: *VIII Simposio Nacional sobre Taludes y Laderas Inestables,* Palma de Mallorca, Junio 2013, E.Alonso, J. Corominas y M. Hürlimann (Eds.), CIMNE, Barcelona, 2013.

<u>Annex 14:</u> BIANCHINI S., Ciampalini A., Raspini F., Bardi F., Di Traglia F., Moretti S., Casagli N. (submitted) Multi-temporal evaluation of landslide movements and impacts on buildings in San Fratello (Italy) by means of C- and X-band PSI data. Submitted to *PAGEOPH Special issue*.

<u>Annex 15:</u> BIANCHINI S. Tapete D., Ciampalini A., Del Ventisette C., Moretti S., Casagli N. (2014) Multi-temporal evaluation of landslide-induced movements and damage assessment in San Fratello (Italy) by means of C-and X- Band PSI data. In: *Mathematics of Planet Earth, Lecture Notes in Earth System Sciences*, Ed. Springer Berlin Heidelberg, pp. 263-266.

<u>Annex 16:</u> Ciampalini A., Bardi F., BIANCHINI S., Del Ventisette C., Moretti S., Casagli N. (to be submitted) Analysis of building deformation in landslide area using multisensor PSInSAR™ technique.

Chapter 8

Discussion

Within this PhD research, the potential applicability and exploitation of space-borne interferometric SAR data for hydrogeological landslide studies have been tested and critically analyzed.

Interferometric radar approach represents a powerful tool to detect movements on the Earth's surface. Thus, mapping and monitoring slope instability can greatly benefit from remote sensing and satellite data analysis, due to the high precision and great cost-benefits ratio.

Space-borne InSAR (Synthetic Aperture Radar interferometry) techniques can offer a useful support in detecting and characterizing slow-moving surface displacements: they provide rapid and easily updatable ground velocity measurements over large areas, along the satellite LOS, with great accuracy (up to 1 mm), high spatial resolution, cost-effectiveness, non-invasiveness, good temporal coverage (from 1992 up to present) and good sampling (monthly acquisitions).

In the last years, different InSAR techniques have been developed in many research studies to analyze different geological processes from regional to local scales, such as subsidence, landslides, tectonic and volcanic activity (Massonnet and Feigl, 1998; Singhroy et al., 1998; Hilley et al. 2004). The potential of remote sensing techniques is particularly relevant for wide mountainous areas, where conventional *in situ* surveys are not always economically and practically suitable for carrying out a systematic investigation of deformation phenomena, due to difficult accessibility and huge extension of such environments.

Differential InSAR (DInSAR), a technique that exploits the phase difference of two SAR images gathered at different times on the same area from slightly different positions, has been widely used since late '80s (Zebker et al., 1986; Gabriel et al., 1989) to detect surface deformation over large areas (Costantini et al., 2000). By the way, conventional DInSAR is limited by atmospheric effects, temporal and geometrical decorrelation.

Multi-temporal interferometric approaches, like PSI (Persistent Scatterer Interferometry), overcome these limitations, analyzing long temporal series of SAR data, and providing annual velocities and deformation time series on grids of stable reflective point-wise targets, called Persistent Scatterers or PS (Ferretti et al., 2001).

Advanced multi-temporal interferometric techniques, i.e. PSI, are being carried out in the last years for natural hazards and in particular for landslide processes, demonstrating their applicability to different environments and the flexibility to different landslide-induced movements. PSI analysis has been mainly used for mapping and monitoring slow-moving landslides ("extremely slow" and "very slow" phenomena, Cruden and Varnes, 1996) and for evaluating their state of activity and intensity (e.g. Farina et al., 2008; Righini et al., 2012; Frangioni et al., 2013: **Annex 4**; Bianchini et al., 2013a: **Annex 6**).

In particular, in this PhD work, PSI-based investigations have been successfully performed to spatially and temporally characterize slope instability and to map geomorphological processes such as slow-moving landslides. PSI data have allowed mapping and monitoring of ground displacements at both regional and local scales, dealing with different landslide typologies and dimensions.

However, InSAR techniques yield both advantages and constraints, as reported in several works (Singhroy, 2002; Rott, 2004; Crosetto et al., 2005; Metternicht et al., 2005).

The potential and effectiveness of space-borne InSAR techniques mainly rely on wide area coverage, cost-efficiency and a good cost/benefit ratio, data availability, accuracy, systematic acquisition and updating, density of measurements.

Satellite InSAR provide precise ground motion measures even on areas that are usually not economically and practically accessible. Moreover radar data can identify localized zones characterized by high movement rates (and so by an high potential hydrological hazard) over regional areas, consequently reducing efforts and time-

consuming *in situ* surveys, and permitting to *a priori* know the most critical areas to which attention must be focalized and further investigation carried out.

The very high resolution (0.1-1 mm/yr for LOS average velocity and 1-3 mm on single measures at each times acquisition) of SAR data increases the geomorphological information on slopes, generating more reliable landslide inventory maps and more accurate instability studies (Metternicht et al., 2005).

The availability of large datastacks of SAR data covering almost more than 20 years with monthly sampling allows reconstructing the extent and the magnitude of ground motion over target areas back to the early 90s, providing an unprecedented and concurrent historical and updated overview of the investigated phenomena.

In particular, both historical archives of SAR images (e.g., ERS1/2, ENVISAT and JERS data) and currently operational SAR missions (e.g. RADARSAT1/2, TerraSAR-X, COSMO-SkyMed) can be exploited to carry out the "back-monitoring" (Cigna et al., 2011) of past and recent ground displacements and to reconstruct the deformation history of the observed scene, with millimetre precision.

InSAR techniques show up some constraints and limitations, including satellite configuration in SAR image acquisition, the limitation in measuring "fast" deformation phenomena, the impact of the linear deformation model assumption made in many PSI approaches.

The most significant drawback of PSI data refers to the technical acquisition parameters of the satellites. Overall, all the presently available SAR data, from both historical archives and currently operational missions, do not allow the measurement of deformations faster than few tens of cm per year. This is because aliasing effects, due to the ambiguous nature of the 2π-wrapping of interferometric phases, limit to a quarter of the wavelength the maximum detectable displacement between two successive acquisitions and between two close neighbouring PS of the same dataset (Hanssen, 2005; Crosetto et al., 2010). Velocities compromising the PSI processing depend on the employed SAR wavelengths and on the satellite repeat cycle; these displacement rates are about from 15 cm/yr up to 20 cm/yr in C-band (for ERS/ENVISAT satellites and RADARSAT satellite, respectively), about 25 cm/yr for TerraSAR-X and 70 cm/yr for Cosmo-SkyMed system with 4 operating satellites in X band, 45 cm/yr for ALOS/JERS in L-band. Consequently, rapid surface movements characterized by higher motion rates cannot be correctly detected and interpreted.

Future missions like Sentinel by ESA will allow monitoring faster movements: the higher discernible velocity will be up to 42.6 cm/yr for Sentinel satellite, thank to its shorter revisiting time (14 days). Moreover, the launch of new satellite systems (Sentinel 1 and Radarsat Constellation Mission) will facilitate the research and analysis of land surface phenomena, ensuring the continuity of C-band SAR data and coupling wide coverage, high precision and short revisiting time.

An important limit of satellite InSAR is referred to the solely LOS measurement capability. Space-borne InSAR only measures displacement in slant range (e.g. the displacement in the direction of the radar illumination). The component of velocity vector in the flight direction (i.e. N-S direction since the satellite has a near polar orbit and a side-looking acquisition) cannot be measured (Rott, 2004). For instance, the LOS displacement projection along the local steepest slope can be performed to compare different PS data (from different sensors with different acquisition angles and from ascending and descending orbits) and consequently landslide velocities with different aspects. This is because when we measure the displacement from the satellite we can only detect the component of the motion that is parallel to the satellite LOS, but the real displacement can actually occurs in all three dimensions (Cascini et al., 2009). So, the measurements along the LOS can be projected along the maximum gradient (assumed to be the most probable direction of movement), with the aim to homogenize all the PS acquired by different satellite systems or in different acquisition geometries (Bianchini et al., 2013c: **Annex 12**; Bianchini et al., 2012d: **Annex 13**).

Another attempt is the combination of ascending and descending SAR data in order to retrieve the vertical and the approximately East-to-West horizontal components of deformation (as already mentioned, SAR satellites are basically blind to South-to-North horizontal deformation components due to their polar orbiting)

for each available multi-band datasets, but it is not always possible due to the requirement of both acquisition geometries on the same area, which is usually quite rare (Notti et al., in press: **Annex 11**).

Interferometry can be complicated by changes on vegetation canopy across time. Decorrelation caused by dense vegetation (e.g. forest) that prevents many stable coherent scatterers to be retrieved, is the main limiting factor for PSInSAR applications in natural environments. Thus, in urbanized zones and cities, PSI gets a reasonably good sampling, while in vegetated, rural and forested areas, benchmarks are very few and PSI tends to systematically fail. This is particularly true when using higher frequencies (e.g. C-band), while lower frequencies (e.g. L-band sensors) are characterized by less opacity in the atmosphere, a less attenuation in the vegetation canopy, and higher penetration in the soil.

In order to overcome this low target density, the concept of DS (Distributed Scatterers) has been introduced, as exploited in SqueeSAR algorithm (Ferretti et al., 2011).

The number of processed SAR images and the spatial resolution in azimuth and range of the satellite acquisition, also contribute to influence the targets density on the areas of interest. This is critical especially when focusing on specific critical area or dealing with a single phenomenon at local scale, which needs to be investigated at high detail.

Different satellites and SAR data are available nowadays, each one bearing specific characteristics mainly depending on the employed wavelength and technical acquisition parameters. The main features and opportunities can be summarized as follow:

- C-band satellites (i.e. ERS and ENVISAT missions) provide the availability of long temporal archives of rates and time series, covering wide areas at a low cost and providing data since the 1990s at medium resolution.
- X-band SAR systems can facilitate the research and application of terrain-related phenomena with high precision and short revisiting cycle compared with the medium resolution SAR systems in C-band. This high spatial resolution and the short repeat cycle (up to 4 days with COSMO-SkyMed) allow studying highly localized surface displacements. The use of a short wavelength such as X-band ($\lambda \approx 3.1$ cm) on one hand allows reaching a higher precision in the deformation rates, but on the other hand increases ambiguity phase problems, since the probability that deformations between two successive acquisitions could exceed the threshold of $\lambda/4$ (the limit of maximum detectable movement in InSAR analysis) is higher.
- L-band data reduce temporal decorrelation effects induced by the vegetation coverage, due to the major penetration capacity of the radar signal. Moreover, L-band SAR data have the intrinsic capability to detect faster ground movements without ambiguities: the use of a grater wavelength ($\lambda \approx 23$ cm for ALOS) allow reducing InSAR problems related to phase ambiguity. In fact, assuming a repeat pass interval (δt) coincident with the ALOS orbital repeat cycle (46 days), the maximum detectable displacement rate along the LOS (Line Of Sight) is $V_{max} = \lambda/4\delta t = 46.8$ cm/yr, compared to the threshold value of 14.6 cm/yr valid for the C-band ERS/ENVISAT missions, where the orbital repeat cycle is 35 days. This increases the probability that, between two successive acquisitions, if operating in L-band the displacements occurred in the investigated area do not exceed the threshold.

The different available radar datasets show different temporal coverage and this is an important facet to account for, when performing PSI analysis. Each PS dataset has a different temporal coverage, so when detecting and monitoring landslides e.g. for generating landslide inventory or landslide activity maps, these products are consequently referred only to a single specific temporal interval, coincident with the temporal coverage of the satellite acquisition; sometimes, when more than one dataset area available, they are not "continuous" in time and some gaps are present in the PS temporal distributions. Therefore, we obtained results for each available dataset necessarily pointing out the different temporal period they are referred to. A further analysis could include a comparison of historical, recent and current radar rates and e.g. the application of activity matrices (Bianchini et al., 2012a: **Annex 3**; Cigna et al., 2013: **Annex 7**) in order to

provide, when it is possible, the more accurate evaluation of the state of the activity (WP/WLI, 1993) of the detected phenomena.

Another limit that encompasses all the multi-frequency PSI data is the possibility to improve detection and monitoring of hydrogeological events not in real-time, but only mainly in the deferred time, and, partially, in the near-real time, e.g. allowing analyzing the evolution patterns of deformations across time and the temporal reconstruction of ground motions back in time, up to 1992 in case of availability of ERS 1/2 satellite imagery ("back-monitoring", as firstly defined by Cigna et al., 2011).

A key point of PSI analysis for landslide studies is the choice of the velocity stability thresholds, necessary to firstly distinguish moving from not moving PS and, consequently, moving areas from stable ones. The choice of velocity thresholds has always to be performed taking into account both the characteristics of investigated processes (e.g. geometry, expected velocity, typology) and the technical characteristics of available PSI measures (e.g. LOS direction, measurement precision, relativity of PSI measures with respect to the reference point etc.). There are no fixed rules to define stable velocity values and the choice is usually based on visual or statistical parameters of the PS population. In literature, the "standard" stability threshold of ±2 mm/yr is usually used in C-band, since the chosen velocity threshold must be the minimum value exceeding the precision of the technique, which is about few millimetres per year (e.g. Colesanti and Wasowski, 2006; Righini et al., 2012). By the way, this threshold is suitable usually when the PS velocity distribution is Gaussian (normal) with coincident media and median values and when PS data show almost no dispersion. Other works used, for projected LOS velocities along the slope, a threshold of ±5 mm/yr, obtained by a calibration procedure (Cigna et al., 2013) or a stable threshold that has to contain a certain percentage of PS data, e.g. 68% that corresponds to the percentile of standard deviation in a data population (Herrera et al., 2013), found at the same distance from 0 for all the available PS data, since the PS velocity values projected along the steepest slope show a negatively skewed distribution (Bianchini et al., 2013c).

Bianchini et al. (2013c) **(Annex 12)** use also 10 mm/yr because of dealing with potential damages occurrence at given ground displacement rates, as proposed by Mansour et al. (2012) from a literature review. This threshold establishes that moderate damages are produced by landslides to buildings and infrastructures when the displacement velocity is between -10 and -100 mm/yr, whereas major damages occur in the 100 to 1600 mm/yr velocity range.

It is worth to highlight that the velocity threshold values are typically site-specific since they are strictly dependent on the case studies at hand, and are empirically determined, bearing in mind that the chosen velocity threshold must be always higher than the errors and noises within the measurements.

Chapter 9

Conclusions

SAR data and interferometric techniques demonstrated to have a fundamental role to play for studying geohazard-related events at different risk prediction, prevention and emergency stages, such as detection, mapping, monitoring and hazard zonation. Nowadays, InSAR-based applications are widely accepted and consolidated in Europe thanks to the efforts spent by the scientific community and end-users (e.g. geological surveys, local authorities and Civil Protection Authorities) in the last decade (**Annex 1**).

This PhD research programme exploited advanced satellite interferometric techniques for spatial and temporal ground displacement detection and mapping, and for quantitatively and qualitatively analysis of landslide movements at regional and local scale.

The research was mainly based on the combined use of PSI (Persistent Scatterer Interferometry) data with geo-thematic and *in situ* information, and with further ground-truth data.

Some PSI-based procedures were elaborated to successfully update landslide inventory and to evaluate the state of activity of landslide phenomena. In particular PSI data were used for the identification of localized areas affected by high ground motion rates within wide regions and for the improvement of pre-existing landslide inventory maps, throughout the assessment of qualitative (e.g. state of activity) and quantitative (e.g. velocity movement) information of each identified phenomenon. In some cases, radar-interpretation of PSI data also allow mapping additional new phenomena not previously identified by means of conventional investigations (**Annexes 3, 4, 5, 6, 7**).

Ground-based InSAR technique was also employed for accurate monitoring of slope instability at local scale (**Annex 2**).

Time series of displacement, available for each PS, are ideally appropriate for defining the temporal behaviour of landslides, in order to monitor ground motion trends and to observe kinematic dynamics of the investigated phenomena. In-depth analysis of PS time series in selected sites demonstrated to be a significant tool for supporting the study of temporal evolution patterns of ground movements. SAR data from different wavelength bands and from different satellite systems were used, i.e. historical C-band SAR archives from ESA missions, L-band data (e.g. from ALOS PALSAR sensor), as well as new generation SAR satellites acquiring in X-band (TerraSAR-X and COSMO-SkyMed), to properly monitor ground deformations at local and large scale (**Annexes 8, 9, 10**).

A methodology for the implementation of PSI data for landslide studies was experimented and proposed, aiming at the evaluation of the geometrical visibility and PS detection suitability in a given area with respect to topographical site-specific features and to the satellite acquisition parameters. The proposed approach also includes the proposal of the so-called "Out-points" analysis and the homogenization procedures in order to make heterogeneous radar data more easily detectable and comparable, resolving the satellite parameter differences and enabling a more feasible and well-founded interpretation. Moreover, an innovative procedure for the so-called "confidence degree" evaluation was carried out, in order to attest the reliability of the measured displacement for representing landslide dynamics (**Annexes 11, 12, 13**).

Radar data exploitation in landslide-prone and -affected areas also deal with damage assessment. In particular, the combined use of radar data with traditional geomorphological tools like field surveys and *in situ* campaigns gave useful efforts to the mapping of the impacts of landslide phenomena on buildings and manufactures of the affected sites, and to the monitoring of displacements in urbanized and cultural heritage areas (**Annexes 14, 15, 16**).

All the case studies of the work, dealing with test sites affected by slope instability in Italy and in Spain, were studied and critically analyzed, attesting the reliability and effectiveness of SAR data exploitation to support geo-hazard investigations.

Thus, in conclusion, SAR data processed through interferometric approaches, especially PSI data, demonstrated their usefulness and suitability for landslide investigations within different activities such as mapping, monitoring and damage assessment, for different end-users in charge of risk management (i.e. local authorities, Civil Protection Department), in various environments and both at local and large scale.

References

Adam N., Rodriguez-Gonzalez F., Parizzi A., Liebhart W. (2011) Wide Area Persistent Scatterer Interferometry. *Proceedings of IGARSS 2011,* Vancouver, Canada.

Agnesi V., Angileri S., Arnone G., Calì M., Calvi F., Cama M., Cappadonia C., Conoscenti C., Costanzo D., Lombardo L., Rotigliano E. (2012) A multi-scale regional landslide susceptibility assessment approach: the SUFRA_Sicilia (SUscettibilità da FRAna in Sicilia) project. *Proceeding of 7th EUREGEO,* June 2012, Bologna, Italy.

Aleotti P., Chowdhury R. (1999) Landslide hazard assessment: summary review and new perspectives. *Bulletin of Engineering Geology and the Environment,* 58, pp. 21-44.

Antonello G., Casagli N., Farina P., Leva D., Nico G., Sieber A. J., Tarchi D. (2004) Ground-based SAR interferometry for monitoring mass movements. *Landslides,* 1, 21-28.

Arnaud A., Adam N., Hanssen R., Inglada J., Duro J., Closa J., Eineder M. (2003) ASAR ERS interferometric phase continuity. *Proceedings of IGARSS 2003,* Toulouse, France.

Bamler R., P. Hartl (1998) Synthetic aperture radar interferometry. *Inverse Problems*, 14 (4), R1-54.

Bardi F., Frodella W., Ciampalini A., Bianchini S., Del Ventisette C., Gigli G., Fanti R., Moretti S., Basile G., Casagli N. (to be submitted) Integration between ground based and satellite SAR data in landslide mapping: the case study of San Fratello (Sicily, Italy).

Berardino P., Costantini M., Franceschetti G., Iodice A., Pietranera L., Rizzo V. (2003) Use of differential SAR interferometry in monitoring and modelling large slope instability at Maratea (Basilicata, Italy). *Engineering Geology,* 68 (1–2), 31–51.

Berti M., Corsini A., Franceschini S., Iannacone J. P. (2013) Automated classification of Persistent Scatterers Interferometry time series. *Natural Hazards and Earth System Sciences,* 13, 1945-1958, doi:10.5194/nhess-13-1945-2013.

Bianchini S., Cigna F., Righini G., Proietti C., Casagli N. (2012a) Landslide HotSpot Mapping by means of Persistent Scatterer Interferometry. *Environmental Earth Sciences*, 67(4), 1155-1172.

Bianchini S., Cigna F., Del Ventisette C., Moretti S., Casagli N. (2012b) Detecting and monitoring landslide phenomena with TerraSAR-X persistent scatterers data: the Gimigliano case study in Calabria region (Italy). In: *IEEE International Geoscience and Remote Sensing Symposium. Remote Sensing for a Dynamic Earth - IGARSS2012,* Munich, Germany, 22-27 July 2012, pp. 982-985.

Bianchini S., Cigna F., Casagli N. (2013a) Improving landslide inventories with multi-temporal measures of ground displacements retrieved through Persistent Scatterer Interferometry. In: *Landslide Science and Practice,* Springer Berlin Heidelberg Ed., Proceedings of The Second World Landslide Forum - WLF2, Rome (Italy), October 3th-9th, 2011, pp. 119-125.

Bianchini S., Cigna F., Del Ventisette C., Moretti S., Casagli N. (2013b) Monitoring landslide-induced displacements with TerraSAR-X Persistent Scatterer Interferometry (PSI): Gimigliano case study in Calabria Region (Italy), *International Journal of Geosciences,* 4 (10).

Bianchini S., Herrera G., Notti D., Mateos R.M., Garcia I., Mora O., Moretti S. (2013c) Landslide activity maps generation by means of Persistent Scatterer Interferometry. *Remote Sensing*, 5 (12), 6198-6222.

Bianchini S., Herrera G., Mateos R.M, Garcia I., Mora O., Sànchez C., Garcìa-Davadillo J.C., Mulàs J., Sanabria M., Lòpez M., Merodo J. (2013d) Metodología para mejorar el análisis de datos satélite radar en el estudio de los movimientos de laderas: resultados del proyecto FP7 DORIS en la Serra de Tramuntana (Mallorca). In: *VIII Simposio de Taludes y Laderas Inestables*, E. Alonso, J. Corominas y M. Hürlimann Eds., Palma de Mallorca,11-14 Junio 2103. Vol. II, pp. 811-821.

Bianchini S., Ciampalini A., Raspini F., Bardi F., Di Traglia F., Moretti S., Casagli N. (submitted) Multi-temporal evaluation of landslide movements and impacts on buildings in San Fratello (Italy) by means of C- and X-band PSI data. Submitted to *PAGEOPH Special issue.*

Bianchini S. Tapete D., Ciampalini A., Di Traglia F., Del Ventisette C., Moretti S., Casagli N. (2014) Multi-temporal evaluation of landslide-induced movements and damage assessment in San Fratello (Italy) by means of C-and X- Band PSI data. In: *Mathematics of Planet Earth, Lecture Notes in Earth System Sciences,* Springer Berlin Heidelberg Ed., pp. 263-266.

Biescas E., Crosetto M., Agudo M., Monserrat O., Crippa B. (2007) Two radar interferometric approaches to monitor slow and fast land deformations. *Journal of Surveying Engineering*, 133, 66-71.

Blanco-Sanchez P., Mallorquì J.J., Duque S., Monells D. (2007) The coherent pixels technique (CPT): An advanced DInSAR technique for nonlinear deformation monitoring. *Pure Applied Geophysics,* 165 (6), 1167 -1193.

Bliss D.W., Forsythe K.W. (2003) Multiple-input multiple-output (MIMO) radar and imaging: Degrees of freedom and resolution. In: *Proceedings of 37th Asilomar Conference on Signals, Systems, and Computers,* Pacific Grove, CA, 1, pp. 54–59.

Blöchl A., Braun B. (2005) Economic assessment of landslide risks in the Schwabian Alb, Germany research framework and first results of homeowners and experts surveys. *Natural Hazards and Earth System Sciences*, 5, 389–396.

Bovenga F., Nutricato R., Refice A., Wasowski J. (2006) Application of multi-temporal differential interferometry to slope instability detection in urban/peri-urban areas. *Engineering Geology,* 88, 218-239.

Bovenga F., Wasowski J., Nitti D.O., Nutricato R., Chiaradia M.T. (2012) Using COSMO-SkyMed X-band and ENVISAT C-band SAR interferometry for landslides analysis. *Remote sensing of environment,* 119, 272-285.

Bovenga F., Nitti D.O., Fornaro G., Radicioni F., Stoppini A., Brigante R. (2013) Using C/X-band SAR interferometry and GNSS measurements for the Assisi landslide analysis. *International Journal of Remote Sensing,* 34, 4083–4104.

Bozzano F., Cipriani I., Mazzanti P., Prestininzi A. (2011) Displacement patterns of a landslide affected by human activities: insights from ground-based InSAR monitoring. *Natural Hazards,* 59, 3, 1377-1396, doi 10.1007/s11069-011-9840-6.

Brabb E.E. (1991) The world landslide problem. Episodes 14 (1), 52–61.

Brardinoni F., Slaymaker O., Hassan M.A. (2003) Landslide inventory in a rugged forested watershed: a comparison between air-photo and field survey data. *Geomorphology,* 54 (3–4), 179–196.

Canuti P., Focardi P. (1986) Slope stability and landslides investigation in Tuscany. *Memorie Società Geologica Italiana*, 31, 307-315.

Canuti P., Casagli, N. (1996) Considerazioni sulla valutazione del rischio di frana, Fenomeni franosi e centri abitati, Bologna, 27 maggio 1994, CNR-GNDCI-Regione Emilia-Romagna, Pubbl. n. 846, 58 pp.

Canuti P., Casagli N., Ermini L., Fanti R., Farina P. (2004) Landslide activity as a geoindicator in Italy: signifcance and new perspectives from remote sensing. *Environmental Geology,* 45(7), 907-919.

Carnec C., Massonnet D., King C. (1996) Two examples of the application of SAR interferometry to sites of small extent. *Geophysical Research Letters,* 23, 3579-3582.

Carrara A., Merenda L. (1976) Landslide inventory in northern Calabria, southern Italy. *Geological Society of America Bullettin,* 87, 1153–1162.

Carson M.A., Kirkby M.J. (1972) Hillslope form and process, 475 pp., Cambridge University Press, Cambridge.

Casagli N., Farina P., Leva D., Tarchi D. (2006) Application of ground based radar interferometry to monitor an active rockslide and implication for emergency management. In: *Landslide from Massive Rock Slope Failure,* Evans S.G. et al. (eds.), 157-173.

Casagli N., Colombo D., Ferretti A., Guerri L., Righini G. (2008) Case Study on Local Landslide Risk Management During Crisis by Means of Remote Sensing Data. *Proceedings of the First World Landslide Forum*, Tokyo, Japan, 125-128.

Casagli N., Cigna F., Del Conte S., Liguori V. (2009) Nuove tecnologie radar per il monitoraggio delle deformazioni superficiali del terreno: casi di studio in Sicilia. *Geologi di Sicilia, Anno XVII,* 3, 17-27.

Casagli N., Catani F., Del Ventisette C., Luzi G. (2010) Monitoring, prediction and early-warning using ground-based radar interferometry. *Landslides,* 7(3), 291-301.

Cascini L., Fornaro G., Peduto D. (2009) Analysis at medium scale of low-resolution DInSAR data in slow-moving landslide-affected areas. *Journal of Photogrammetry and Remote Sensing,* 64(6):598–611

Cascini L., Fornaro G., Peduto D. (2010) Advanced low- and full-resolution DInSAR map generation for slow-moving landslide analysis at different scales. *Engineering Geology,* 112:29–42.

Cascini L., Peduto D., Pisciotta G., L. Arena, Ferlisi S., Fornaro G. (2013) The combination of DInSAR and facility damage data for the updating of slow-moving landslide inventory maps at medium scale. *Natural Hazards and Earth System Sciences,* 13, 1527-1549.

Casu F., Manzo M., Lanari R. (2006) A quantitative assessment of the SBAS algorithm performance for surface deformation retrieval. *Remote Sensing of Environment,* 102(3–4), 195–210.

Catani F., Farina P., Moretti S., Nico G., Strozzi T. (2005) On the application of SAR interferometry to geomorphological studies: estimation of landform attributes and mass movements. *Geomorphology,* (66), 119–131.

Ciampalini A., Bardi F., Bianchini S., Del Ventisette C., Moretti S., Casagli N. (to be submitted) Analysis of building deformation in landslide area using multi-sensor PSInSAR™ technique.

Cigna F., Bianchini S., Righini G., Proietti C., Casagli N. (2010) Updating landslide inventory maps in mountain areas by means of Persistent Scatterer Interferometry (PSI) and photo-interpretation: Central Calabria (Italy) case study. In: *Bringing Science to Society*, Malet JP, Glade T, Casagli N (eds), Mountain Risks: Proceedings of the International Conference, CERG Editions, Florence, Italy, November 24-26, 2010, pp 3-9.

Cigna F., Del Ventisette C., Liguori V., Casagli N. (2011) Advanced radar-interpretation of InSAR time series for mapping and characterization of geological processes. *Natural Hazards and Earth System Sciences, 11,* 865-881, doi:10.5194/nhess-11-865.

Cigna F., Tapete D., Casagli N. (2012) Semi-automated extraction of Deviation Indexes (DI) from satellite Persistent Scatterers time series: tests on sedimentary volcanism and tectonically-induced motions. *Nonlinear Processes in Geophysics,* 19 (6), 643-655.

Cigna F., Bianchini S., Casagli N. (2013) How to assess landslide activity and intensity with Persistent Scatterer Interferometry (PSI): the PSI-based matrix approach. *Landslides,* 10 (3), 267–283, doi: 10.1007/s10346-012-0335-7.

Colesanti C., Ferretti A., Prati C., Rocca F. (2003a) Monitoring landslides and tectonic motion with the Permanent Scatterers technique. Engineering Geology 68(1–2), 3–14.

Colesanti C., Ferretti A., Novali F., Prati C., Rocca F. (2003b) SAR monitoring of progressive and seasonal ground deformation using the permanent scatterers technique. *IEEE Transactions on Geoscience and Remote Sensing*, 41 (7), 1685 – 701.

Colesanti C., Wasowski J. (2006) Investigating landslides with space-borne Synthetic Aperture Radar (SAR) interferometry. *Engineering Geology*, 88, 173–199.

Colombo A., Mallen L., Pispico R., Giannico C.; Bianchi M., Savi G. (2006) Mappatura regionale delle aree monitorabili mediante l'uso della tecnica PS. *Proceedings of 10th National Conference ASITA*, Bolzano, Italy, 14-17 November 2006.

Cooper R.G. (2007) Mass Movements in Great Britain, Geological Conservation Review Series, 33, Joint Nature Conservation Committee, Peterborough, 348 pp.

Cooper A.H. (2008) The classification, recording, databasing and use of information about building damage caused by subsidence and landslides. *Quarterly Journal of Engineering Geology and Hydrogeology*, 41 (3), 409-424, doi: 10.1144/1470-9236/07-223.

Costantini M., Iodice A., Magnapane L., Pietranera L. (2000) Monitoring terrain movements by means of sparse SAR differential interferometric measurements. In: *Proceedings of IGARSS 2000, 20th IEEE international Geoscience and Remote sensing symposium*, Honolulu, Hawaii, USA, July 24–28, p 3225–3227.

Crosetto M., Crippa B., Biescas E. (2005) State-of-the-art of land deformation monitoring using differential SAR interferometry. *ISPRS High- Resolution Earth Imaging for Geospatial Information,* Hannover (DE).

Crosetto M., Biescas E., Duro J., Closa J., Arnaud A. (2008a) Generation of advanced ERS and ENVISAT interferometric SAR products using the Stable Point Network technique. *Photogrammetric Engineering and Remote Sensing,* 74(4), 443–451.

Crosetto M., Monserrat O., Adam N., Parizzi A., Bremmer C., Dortland S., Hanssen R.F., van Leijen F.J. (2008b) Final report of the Validation of existing processing chains in Terrafirma stage 2, Terrafirma project, ESRIN/Contract no. 19366/05/I-E, available on-line at www.terrafirma.eu.com/Terrafirma_validation.htm.

Crosetto M., Monserrat O., Junger A., Crippa B. (2009) Persistent scatterer interferometry: potential and limits, *Proceedings of ISPRS Workshop on High- Resolution Earth Imaging for Geospatial Information*, Hannover, 2-5 June 2009.

Crosetto M., Monserrat O., Iglesias R., Crippa B. (2010) Persistent scatterer interferometry: potential, limits and initial C- and X-band comparison. *Photogrammetric Engineering and Remote Sensing*, 76, 9, pp. 1061–1069.

Crosetto M., Monserrat O., Cuevas M., Crippa B. (2011) Spaceborne Differential SAR Interferometry: Data Analysis Tools for Deformation Measurement. *Remote Sensing,* 3, pp. 305-318; doi:10.3390/rs3020305

Crozier M.J. (1984) Field assessment of slope instability. In: *Slope Instability*, Brunsden D and Prior DB (Eds.). London, John Wiley & Sons Ltd:103-42.

Crozier M.J. (1986) Landslides: Causes, Consequences and Environment. Croom Helm, England. 252 pp

Cruden D.M. (1991) A simple definition of a landslide. *Bulletin of Engineering Geology and the Environment*, 43(1), 27-29.

Cruden D.M., Varnes D.J. (1996) Landslide types and processes. In: Turner AK, Schuster RL (eds) *Landslides: investigation and Mitigation*, Sp. Rep. 247, Transportation Research Board, National research Council. National Academy Press, Washington DC, 36–75.n

Cumming I.G., Wong F.H. (2005) Digital processing of synthetic aperture radar data: Algorithms and implementation. Artech House, 660 p.

Dai F.C., Lee C.F., (2002) Landslide characteristics and slope instability modeling using GIS, Lantau Island, Hong Kong, *Geomorphology*, 42, 213-228.

De Zan F., Monti Guarnieri A. (2006) TOPSAR: Terrain Observation by Progressive Scans, *IEEE Transaction on Geoscience and Remote Sensing*, 44(9).

Del Ventisette C., Ciampalini A., Manunta M., Calò F., Paglia L., Ardizzone F., Mondini A., Reichenbach P., Mateos R.M., Bianchini S., Garcia I., Füsi B., Villő Deák Z., Rádi K., Graniczny M., Kowalski Z., Piatkowska A., Przylucka M., Retzo H., Strozzi T., Colombo D., Mora O., Sánchez F., Herrera G., Moretti S., Casagli N., Guzzetti F. (2013) Exploitation of Large Archives of ERS and ENVISAT C-Band SAR Data to Characterize Ground Deformations. *Remote Sensing,* 5, 3896-3917. doi:10.3390/rs5083896.

Dikau R., Brunsden D., Schrott L., Ibsen M.L. (Eds.) (1996) Landslide Recognition. Identification, Movements and Causes. John Wiley & Sons, Chichester, West Sussex, England. 251 pp.

Duque S., Mallorquí J.J., Blanco-Sanchez P., Monells D. (2007) Application of the coherent pixels technique (CPT) to urban monitoring. *Urban Remote Sensing Joint Event*, Vol.2, Paris, France.

Duro J., Closa J., Biescas E., Crosetto M., Arnaud A. (2005). High resolution differential interferometry using time series of ERS and ENVISAT SAR data. *Proceedings of the 6th. Geomatic week conference,* Barcelona, Spain.

Einstein H.H. (1988) Landslide risk assessment procedure. *Special Lecture, Proceedings of 5th International Symposium on Landslides*. Lausanne, Switzerland, Rotterdam, Balkema, 2, 1075–1090.

Escario M.V., George L.A., Cheney R.A., Yamamura K. (1997) Landslides: techniques for evaluating hazard . Report of PIARC Technical Committee on Earthworks, Drainage, Subgrade (C12), 12.04B. Paris: PIARC, World Road Association.

Farina P., Colombo D., Fumagalli A., Gontier E., Moretti S. (2003) Integration of Permanent Scatterers analysis and high resolution optical images within landslide risk analysis. In: FRINGE, Frascati, Italy, 1–8.

Farina P., Colombo D., Fumagalli A., Marks F., Moretti S. (2006) Permanent Scatterers for landslide investigations: outcomes from the ESA-SLAM project. *Engineering Geology*, 88, 200–217.

Farina P., Casagli N., Ferretti A. (2008) Radar-interpretation of InSAR measurements for landslide investigations in civil protection practices. In: *Proceedings of 1st North American Landslide Conference*, Vail, Colorado, 272–283.

Fell R., Corominas J., Bonnard C., Cascini L., Leroi E., Savage W.Z., Eng J-J-TCL (2008) Guidelines for landslide susceptibility, hazard and risk-zoning for land use planning. *Engineering Geology*, 102, 85–98.

Ferretti A., Prati C., Rocca F. (1999) Multibaseline InSAR DEM reconstruction: the wavelet approach. *IEEE Transaction on Geoscience and Remote Sensing*, 37 (2), 705– 715.

Ferretti A., Prati C., Rocca F. (2000) Nonlinear subsidence rate estimation using Permanent Scatterers in differential SAR interferometry. *IEEE Transactions on Geoscience and Remote Sensing,* 38 (5), 2202–2212.

Ferretti A., Prati C., Rocca F. (2001) Permanent Scatterers in SAR interferometry. *IEEE Transactions on Geoscience and Remote Sensing*, 39 (1), 8 –20.

Ferretti A., Prati C., Rocca F., Casagli N., Farina P., Young B. (2005) Permanent Scatterers technology: a powerful state of the art tool for historic and future monitoring of landslides and other terrain instability phenomena. *Proceedings of 2005 International Conference on Landslide Risk Management*, Vancouver, Canada.

Ferretti A., Monti-Guarnieri A., Prati C., Rocca F. (2007) InSAR principles: guidelines for SAR interferometry processing and interpolation. In: Fletcher K ed., *European Space Agency -publications-ESA*, TM-19, February 2007.

Ferretti A., Fumagalli A., Novali F., Prati C., Rocca F., Rucci A. (2011) A new algorithm for processing interferometric data-stacks: SqueeSAR™. *IEEE Transactions on Geoscience and Remote Sensing,* 99, 1-11.

Fornaro G., Franceschetti G., Lanari R. (1996) Interferometric SAR phase unwrapping using Green's formulation. *IEEE Transactions on Geoscience and Remote Sensing,* 34, 720-727.

Franceschetti G. (1999) Synthetic Aperture Radar Processing, pp. 9-17.

Frangioni S., Bianchini S., Moretti S. (2013) Landslide inventory updating by means of Persistent Scatterer Interferometry (PSI): the Setta basin (Italy) case study. Accepted in *Geomatics, Natural Hazards and Risk,* doi: 10.1080/19475705.2013.866985.

Fu L.L., Holt B. (1982) Seasat view oceans and sea ice with synthetic aperture radar. Tech. rept. Jet Propulsion Lab.

Gabriel A.K., Goldstein R. M., Zebker H.A. (1989) Mapping Small Elevation Changes Over Large Areas: Differential Radar Interferometry. *Journal of Geophysical Research,* 94, 9183–9191.

Galli M., Ardizzone F., Cardinali M., Guzzetti F., Reichenbach P. (2008) Comparing landslide inventory maps. *Geomorphology,* 94, 268–289. doi:10.1016/j.geomorph.2006.09.023

Glade T., Crozier M. (2005) The nature of landslide hazard impact. In: Landslide hazard and risk. Glade T., Anderson M. and Crozier M. (Eds), Wiley, Chichester, 43–74.

Gomes J. (2003) Landslide susceptibility and risk maps of Regua (Douro basin, NE Portugal), *Proceeding of the IAG and IGU-C12 Regional Conference "Geomorphic hazards; towards the prevention of disasters",* Mexico City, Mexico, 2003.

Graham L.C. (1974) Synthetic interferometric radar for topographic mapping. *Proceedings of the IEEE.* 62, 763–768.

Greif V., Vlcko J. (2012) Monitoring of post-failure landslide deformation by the PS-InSAR technique at Lubietova in Central Slovakia. *Environmental Earth Sciences*, 66, 1585–1595.

Guzzetti F. (2000) Landslide fatalities and evaluation of landslide risk in Italy. *Engineering Geology,* 58, 89–107.

Guzzetti F. (2006) Ph.D. Thesis, landslide hazard and risk assessment. Mathematisch-Naturwissenschaftlichen Fakultät der Rheinischen Friedrich-Wilhelms-Universität, University of Bonn, Bonn, Germany, 389 pp.

Guzzetti F., Carrara A., Cardinali M., Reichenbach P. (1999) Landslide hazard evaluation: an aid to a sustainable development. *Geomorphology,* 31, 181-216.

Guzzetti F., Stark C.P., Salvati P. (2005) Evaluation of Flood and Landslide Risk to the Population of Italy. doi: 10.1007/s00267-003-0257-1.

Guzzetti F., Mondini A.C., Cardinali M., Fiorucci M., Santangelo M., Chang K.T. (2012) Landslide inventory maps: new tools for an old problem. *Earth Science Reviews*, 112, 1–25.

Hanssen R.F. (2001) Radar Interferometry. Data Interpretation and Error Analysis. Kluwer Academic Publishers, Dordrecht, The Netherlands.

Hanssen R.F. (2005) Satellite radar interferometry for deformation monitoring: a priori assessment of feasibility and accuracy. *Int. J. Appl. Earth Obs.,* 6, 253–260.

Helmer M., Hilhorst D. (2006) Natural Disasters and Climate Change, Disasters, 30(1), 1–4.

Herrera G., Fernández-Merodo J.A., Mulas J., Pastor M., Luzi G., Monserrat O. (2009a) A landslide forecasting model using ground based SAR data: The Portalet case study. *Engineering Geology*, 105, 220–230.

Herrera G., Fernandez J.A., Tomas R., Cooksley G., Mulas J. (2009b) Advanced interpretation of subsidence in Murcia (SE Spain) using A-DInSAR data - modelling and validation. *Natural Hazards Earth System Science,* 9, 647-661.

Herrera G., Tomás R., Monells D., Centolanza G., Mallorqui J.J., Vicente F., Navarro V.D., Lopez-Sanchez J. M., Cano M., Mulas J., Sanabria M. (2010) Analysis of subsidence using TerraSAR-X data: Murcia case study. *Engineering Geology*, 116, 284-295.

Notti D., García-Davalillo J.C., Mora O., Cooksley G., Sánchez M., Arnaud A., Crosetto M. (2011) Analysis with C- and X-band satellite SAR data of the Portalet landslide area. *Landslides*, 8, 195-206.

Herrera G., Gutiérrez F., García-Davalillo J.C., Guerrero J., Galve J.P., Fernández-Morodo J.A., Cooksley G. (2013) Multi-sensor advanced DInSAR monitoring of very slow landslides: the Tena valley case study (central Spanish Pyrenees). *Remote Sensing of Environment,* 128, 31-43.

Hilley G.E., Bürgmann R., Ferretti A., Novali F., Rocca F. (2004) Dynamics of Slow-Moving Landslides from Permanent Scatterer Analysis. Science, 304, 1952-1955.

Hollenstein K. (2005) Reconsidering the risk assessment concept: Standardizing the impact description as a building block for vulnerability assessment. *Nat. Hazards Earth Syst. Sci.,* 5, 301–307.

Holzner J., Bamler R. (2002) Burst-mode and ScanSAR interferometry. *IEEE Transaction on Geoscience and Remote Sensing*, 40(9), 1917–1934.

Hong Y., Adler R., Huffman G. (2007) Use of Satellite Remote Sensing Data in the Mapping of Global Landslide Susceptibility*, Natural Hazards,* 43, 245–256.

Hooper A. (2006) Persistent scatterer radar interferometry for crustal deformation studies and modeling of volcanic deformation. Ph.D. thesis, Stanford University

Hooper A., Zebker H.A., Segall P., Kampes B. (2004) A new method for measuring deformation on volcanoes and other natural terrains using InSAR persistent scatterers. *Geophysical Research Letters,* 31.

Hooper A., Segall P., Zebker H.A. (2007) Persistent scatterer interferometric synthetic aperture radar for crustal deformation analysis, with application to Volcán Alcedo, Galápagos. *Journal of Geophysical Research,* 112.

Hungr O. (1995) Model for the runout analysis of rapid flow slides, debris flows, and avalanches. Canadian Geotechnical Journal, 32, 610-623.

Hungr O. (1997) Some methods of landslide intensity mapping. In: *Landslide risk assessment.* Cruden D, Fell R (eds), Proceedings of the International Workshop on Landslide Risk Assessment, Honolulu, USA, February 19–21, 1997. Balkema, Rotterdam, pp 215–226

Hungr O., Evans S.G., Bovis M.J., Hutchinson J.N. (2001) A review of the classification of landslides of the flow type. *Environmental and Engineering Geoscience*, 7(3), 221–228.

Hutchinson J.N. (1988) General report: morphological and geotechnical parameters of landslide in relation to geology and hydrogeology. In: *Landslides,* Vol. I, C. Bonnard ed., 5th Int. Symp. On Landslides, Balkema, Rotterdam, pp. 3-35.

IGOS GEOHAZARDS (2004) Geohazards theme report: for the monitoring of our environment from space and from earth. European Space Agency Publication, p. 55.

ISPRA (2008) Landslides in Italy. Special report 2008, Vol 83, ISPRA.

IUGS/WGL-International Union of Geological Sciences Working Group on Landslides (1995) A suggested method for describing the rate of movement of a landslide. *IAEG Bull.* 52, 75–78 Hamburg, pp. 1993–1939.

JRC (2003) Lessons Learnt from landslide disasters in Europe, EUR 20558 EN, 91 pp.

Kampes B.M. (2006) Radar interferometry: persistent scatterer technique. Springer ed., Netherlands.

Kampes B. M., Adam N. (2006) The STUN Algorithm for Persistent Scatterer Interferometry. In: Fringe 2005 Workshop, Proceedings of the Conference held 28 November - 2 December, 2005 in Frascati, Italy, H. Lacoste and L. Ouwehand (eds), ESA SP-610. European Space Agency, 2006. Published on CDROM., p.16.1.

Kirschbaum D.B., Adler R., Hong Y., Lernerlam A. (2009) Evaluation of a preliminary satellite-based landslide hazard algorithm using global landslide inventories. *Natural Hazards and Earth System Science,* 9, 673-686.

Klees R., Massonnet D. (1999) Deformation measurements using SAR interferometry: Potential and limitations. Geologie en Mijnbouw, 77, 161–176.

Lanari R., Mora O., Manunta M., Mallorquì J.J., Berardino P., Sansosti E. (2004) A Small Baseline Approach for Investigating Deformation on Full resolution Differential SAR Interferograms. *IEEE Transaction on Geoscience and Remote Sensing.*

Leva D., Nico G., Tarchi D., Fortuny-Guasch J., Sieber J. (2003) Temporal analysis of a landslide by means of a ground-based SAR interferometer. *IEEE Transactions on Geoscience and Remote Sensing*, 41(4), 745– 752.

Lillesand T. M., Kiefer R.W. (1987) Remote Sensing and Image Interpretation. Wiley, New York, NY., 1987. 10

Lu P., Casagli N., Catani F. (2010) PSI-HSR: a new approach of representing Persistent Scatterer Interferometry (PSI) point targets using hue and saturation scale. *International Journal Of Remote Sensing,* 31, 2189-2196.

Lu P., Stumpf A., Kerle N., Casagli N. (2011) Object-oriented change detection for landslide rapid mapping. *IEEE Geosci Remote*, 8, 701–705.

Lu P., Casagli N., Catani F., Tofani V. (2012) Persistent Scatterers Interferometry Hotspot and Cluster Analysis (PSI-HCA) for detection of extremely slow-moving landslides. . *International Journal Of Remote Sensing,* 33, 466–489.

Lu P., Catani F., Tofani V., Casagli N. (2013) Quantitative hazard and risk assessment for slow-moving landslides from Persistent Scatterer Interferometry. *Landslides,* Doi 10.1007/s10346-013-0432-2.

Luzi G., Pieraccini M., Mecatti D., Noferini L., Macaluso G., Galgaro A., Atzeni C. (2006). Advances in ground-based microwave interferometry for landslide survey: a case study. *International Journal of Remote Sensing,* 27(12), 2331-2350.

Mansour M.F., Morgenstern N.R., Derek Martin C. (2011) Expected damage from displacement of slow-moving slides. *Landslides*, 8, 117-131.

Mantovani F., Soeters R., van Westen C. (1996) Remote sensing techniques for landslide studies and hazard zonation in Europe. *Geomorphology*, 15, 213– 225.

Manzo M., Ricciardi G.P., Casu F., Ventura G., Zeni G., Borgstrom S., Berardino P., Del Gaudio C., Lanari R. (2006) Surface deformation analysis in the Is-chia Island (Italy) based on spaceborne radar interferometry. *Journal of Volcanology and Geothermal Research*, 151, 399-416.

Massonnet D., Feigl K.L. (1998) Radar interferometry and its application to changes in the Earth's surface. *Reviews of Geophysics,* 36.

MATTM, A.A.V.V. (2010). Piano Straordinario di Telerilevamento Ambientale (PST-A), Lotto 2. Linee guida per l'analisi di dati interferometrici satellitari in aree soggette a dissesti idrogeologici.

Meisina C., Zucca F., Conconi F., Verri F., Fossati D., Ceriani M., Allievi J. (2007) Use of Permanent Scatterers technique for large-scale mass movement investigation. *Quaternary International*, 171–172, pp.90-107.

Meisina C., Zucca F., Notti D., Colombo A., Cucchi G., Giannico C., Bianchi M. (2008), Geological Interpretation of PSInSAR Data at Regional Scale. *Sensors,* 8(11), 7469-7492.

Meta A., Mittermayer J., Prats P., Scheiber R., Steinbrecher U. (2010) TOPS imaging with TerraSAR-X: Mode design and performance analysis. *IEEE Transaction on Geoscience and Remote Sensing*, 40(2), 759–769.

Metternicht G., Hurni L., Gogu R. (2005) Remote sensing of landslides: an analysis of the potential contribution to geo-spatial systems for hazard assessment in mountain environments. *Remote Sensing of Environment,* 98, 284-303.

Mondini A.C., Guzzetti F., Reichenbach P., Rossi M., Cardinali M., Ardizzone F. (2011) Semiautomatic recognition and mapping of rainfall induced shallow landslides using satellite optical images. *Remote Sensing of Environment*, 115, 1743–1757.

Monti Guarnieri A., Prati C. (1996) ScanSAR focusing and interferometry. *IEEE Transaction on Geoscience and Remote Sensing,* 34(4), 1029–1038.

Monti Guarnieri A., Rocca F. (1999) Combination of low- and highresolution SAR images for differential interferometry. *IEEE Transaction on Geoscience Remote Sensing,* 37, 2035–2049.

Mora O., Mallorquì J.J., Broquetas A. (2003) Linear and nonlinear terrain deformation maps from a reduced set of interferometric SAR images. *IEEE Transactions on Geoscience and Remote Sensing*, 41, 2243-2253.

Moreira A., Mittermayer J., Scheiber R. (1996) Extended chirp scaling algorithm for air- and spaceborne SAR data processing in stripmap and ScanSAR imaging modes. *IEEE Transaction on Geoscience Remote Sensing*, 34(5), 1123–1136.

Nadim F., Kjekstad O., Peduzzi P., Herold C., Jaedicke C. (2006) Global landslide and avalanche hotspots. *Landslides,* 3(2), 159-173.

Noferini L., Pieraccini M., Mecatti D., Luzi G., Atzeni C., Tamburini A., Broccolato M. (2005) Permanent scatterers analysis for atmospheric correction in ground-based SAR interferometry. *IEEE Trans. Geosci. Remote Sens.,* 43(7), 1459–1471.

Notti D., Davalillo J.C., Herrera G., Mora O. (2010) Assessment of the performance of X-band satellite radar data for landslide mapping and monitoring: Upper Tena Valley case study. *Natural Hazards Earth System Science,* 10, 1865-1875.

Notti D., Meisina C., Zucca F., Crosetto M., Montserrat O. (2011) Factors that have an influence on time series. *Proceedings of the Fringe 2011 Workshop,* Frascati, Italy,19–23 September 2011.

Notti D., Herrera G., Bianchini S., Meisina C., García-Davalillo J.C., Zucca F. (in press) A methodology for improving landslide PSI data analysis. Accepted in *International Journal of Remote Sensing.*

Notti D., Meisina C., Zucca F., Colombo A. (2014) Non Linear PS Time Series: Analysis and Post-Processing for Landslides Studies. In: *Mathematics of Planet Earth*, Springer Berlin Heidelberg Ed., pp. 245-248.

Pagliara P., Basile P.G., Corazza A., Cara P., Duro A., Manfré B., Onori R. , Proietti C., Sansone V. (2014)Integration of Earth Observation and groundbased HRdata in the civil protection emergency cycle: the c ase of the DORIS Project. In: *Mathematics of Planet Earth*, Springer Berlin Heidelberg Ed., pp. 263-266.

Papathoma-Köhle M., Neuh¨auser B., Ratzinger K., Wenzel H., Dominey-Howes D. (2007) Elements at risk as a framework for assessing the vulnerability of communities to landslides. *Nat. Hazards Earth Syst. Sci.,* 7, 765–779.

Parcharidis I., Foumelis M., Pavlopoulos K., Kourkouli P. (2010) Ground deformation monitoring in cultural heritage areas by time series SAR interferometry: the case of ancient Olympia site (Western Greece). In: *European Space Agency - publications-ESA* SP, 677; 90, Fringe Conference, ESA , Noordwijk.

Peltzer G., Rosen P. (1995) Surface displacement of the 17 May 1993 Eureka Valley earhtquake observed by SAR interferometry. *Science,* 268, 1333-1336.

Perissin D., Prati C., Engdahl M.E., Desnos Y.L. (2006) Validating the SAR wavenumber shift principle with the ERS-Envisat PS coherent combination. *IEEE Transactions on Geoscience and Remote Sensing,* 44 (9).

Piacentini D., Troiani F., Soldati M., Notarnicola C., Savelli D., Schneiderbauer S., Strada C. (2012) Statistical analysis for assessing shallow-landslide susceptibility in South Tyrol (south-eastern Alps, Italy). *Geomorphology,* 151/152, 196–206.

Plank S., Singer J., Minet C., Thruro K. (2012) Pre-survey suitability evaluation of the differential synthetic aperture radar interferometry method for landslide monitoring. *International Journal of Remote Sensing*, 33(20), 6623-6637.

Prati C., Rocca F., Ferretti A. (2004) Radar Interferometry using spaceborne data: Potentials and operational capabilities. In: J. R. Centre (Ed.), Workshop on risk mitigation of slope instability. Ispra, Italy' JRCInstitute for the Protection and Security of the Citizen.

Raspini F., Cigna F., Moretti S. (2012) Multi-temporal mapping of land subsidence at basin scale exploiting Persistent Scatterer Interferometry: case study of Gioia Tauro plain (Italy). *Journal of Maps*, 8 (4), 514-524.

Raspini F., Moretti S., Casagli N. (2013) Landslide mapping using SqueeSAR data: Giampilieri (Italy) case study. In: *Landslide Science and Practice,* Springer Berlin Heidelberg eds, pp. 147-154.

Raucoules D., Bourgine B., De Michele M., Le Cozanet G., Closset L., Bremmer C., Veldkamp H., Tragheim D., Bateson L., Crosetto M., Agudo M., Engdahl M. (2009) Validation and Intercomparison of Persistent Scatterers Interferometry: PSIC4 project results. *J. Appl. Geophys.,* 68 (3), 335–347.

Rengers N., Soeters R., van Westen C.J. (1992) Remote sensing and GIS applied to mountain hazard mapping. *Episodes,* 15(1), 36-45.

Richman D. (1971) Three dimensional azimuth-correcting mapping radar, Tech. rep., USA: United Technologies Corporation.

Righini G., Pancioli V., Casagli N. (2012) Updating landslide inventory maps using Persistent Scatterer Interferometry(PSI), *International Journal of Remote Sensing,* 33 (7), pp. 2068-2096.

Rosen P.A., Hensley S., Joughin I.R., Li F.K., Madsen S.N., Rodriguez E., Goldstein R.M. (2000) Synthetic aperture radar interferometry. *Proceeding of IEEE,* 88 (3).

Rott H. (2004) Requirements and applications of satellite techniques for monitoring slope instability in Alpine areas. Workshop on risk mitigation of slope instability. Ispra, Italy' JRC-Institute for the Protection and Security of the Citizen.

Rudolf H., Tarchi D. (1999) LISA: The Linear SAR Instrument. Technical Report, Note I.99.126, European Commission, JRS, July 1999.

Salvati P., Bianchi C., Rossi M., Guzzetti F.(2010) Societal landslide and flood risk in Italy. *Natural Hazards and Earth System Sciences,* 10, 465–483.

Sammartino P.F., Baker C.J., Griffiths H.D. (2010) Range-angle dependent waveform. *Proceedings of the IEEE Radar Conference*, pp. 511–515.

Sang-Ho Yun (2008) Volcano Deformation Modeling Using Radar Interferometrry. VDM Verlag Ed., 152 pp.

Scavia C., Castelli M. (2003) The IMIRILAND project- Impact of Large Landslides in the Mountain Environment: identification and Mitigation of Risk, in: Seismic and Landslide Risk in the European Union, edited by: Yeroyianni, M., Workshop Proceedings, 12–13 November 2002, 82–91.

Schuster R.L., Fleming R.W. (1986) Economic losses and fatalities due to landslides. *Bulletin of American Association of Engineering Geology,* 23, 11–28

Selby M.J. (1993) Hillslope: Material and processes. Oxford University Press, Oxford (UK).

Shanker P., Casu F., Zebker H. A., Lanari R. (2011) Comparison of Persistent Scatterers and Small Baseline Time-Series InSAR Results: A Case Study of the San Francisco Bay Area. *IEEE Geoscience and Remote Sensing Letters,* 8 (4), July 2011.

Singhroy V. (2002) Landslide hazards: CEOS, The use of earth observing satellites for hazard support: Assessments and scenarios. Final report of the CEOS Disaster Management Support Group, NOAA, p. 98.

Singhroy V., Mattar K., Gray A. (1998) Landslide characterization in Canada using interferometric SAR and combined SAR and TM images. *Adv. Space Res*, 21(3), 465-476.

Singhroy V., Molch K. (2004) Characterizing and monitoring rockslides from SAR techniques. Advances in Space Research, 33 (3), 290-295.

Skolnik M. L. (2001) Introduction to RADAR systems. 3 edn. 1221 Avenue of the Americas, New York, NY 10020: Tata McGraw-Hill.

Soeters R., van Westen C.J. (1996) Slope instability recognition, analysis and zonation. In Turner A.K. & Schuster R.L. (eds), *Landslides: Investigation and Mitigation*: Sp. Rep. 247, 129-177, Transportation Research Board, National research Council, Washington DC: National Academy Press.

Soumekh M. (1999) Synthetic Aperture Radar Signal Processing with MATLAB Algorithms, Ed. Wiley-Interscience, 616 pp.

Sousa J.J., Hooper A.J., Hanssen R.F., Bastos L.C., Ruiz A.M. (2011) Persistent Scatterer InSAR: a comparison of methodologies based on a model of temporal deformation vs. spatial correlation selection criteria. *Remote Sensing of Environment*, 115, 2652–2663.

Squarzoni C., Delacourt C., Allemand P. (2003) Nine years of spatial and temporal evolution of the La Valette landslide observed by SAR Interferometry. *Enginering Geology*, 68.

Strozzi T., Farina P., Corsini A., Ambrosi C., Thüring M., Zilger J., Wiesmann A., Wegmüller U., Werner C. (2005) Survey and monitoring of landslide displacements by means of L-band satellite SAR interferometry. *Landslides,* 193-201.

Strozzi, T., Wegmuller, U., Keusen, H.R., Graf, K., Wiesmann, A. (2006) Analysis of the terrain displacement along a funicular by SAR interferometry. *IEEE Geoscience and Remote Sensing Letters*, 3-1, pp. 15-18.

Strozzi T., Ambrosi C., Raetzo H. (2013) Interpretation of Aerial Photographs and Satellite SAR Interferometry for the Inventory of Landslides. *Remote Sensing,* 5(5), 2554-2570; doi:10.3390/rs5052554.

Tamburini A., Del Conte S., Lopardo L., Malaguti C., Larine G., Broccolato M., Martelli D.C., Vescovi P. (2012) Advance InSAR Techniques for landslide assessment at regional and local scale. *Proceeding of 7th EUREGEO*, June 2012, Bologna, Italy.

Tapete D., Fanti R., Cecchi R., Petrangeli P., Casagli N. (2012) Satellite radar interferometry for monitoring and early-stage warning of structural instability in archaeological sites. *Journal of Geophysics and Engineering 9*, S10-S25. doi: 10.1088/1742-2132/9/4/S10.

Tarchi D., Ohlmer E., Sieber A.J. (1997) Monitoring of structural changes by radar interferometry. *Res. Nondestruct. Eval.*, 9, pp. 213– 225.

Tarchi D., Casagli N., Fanti R., Leva D., Luzi G., Pasuto A., Pieraccini M., Silvano S. (2003) Landslide monitoring by using ground-based SAR interferometry: an example of application to the Tessina landslide in Italy. *Engineering Geology,* 68, 1–2.

Tarchi, D., Oliveri, F., Sammartino, P.F. (2012) MIMO Radar and Ground-Based SAR Imaging Systems: Equivalent Approaches for Remote Sensing. *IEEE Commun. Mag.*, DOI 10.1109/TGRS.2012.2199120.

Tofani V., Raspini F., Catani F., Casagli N. (2013) Persistent Scatterer Interferometry (PSI) technique for landslide characterization and monitoring. *Remote Sensing*, 5, 1045–1065.

Tomás R., Márquez Y., Lopez-Sanchez J. M., Delgado J., Blanco P., Mallorquí J.J., Martínez M., Herrera G., Mulas J. (2005) Mapping ground subsidence induced by aquifer overexploitation using advanced Differential SAR Interferometry: Vega Media of the Segura River (SE Spain) case study. *Remote Sensing of Environment,* 98(2–3), 269–283.

Trigila A., Iadanza C. (2008) Progetto IFFI: Inventario dei Fenomeni Franosi d'Italia (Indicatore A11.09). In: APAT, Annuario dei dati ambientali – Edizione 2008.

USGS (2001) Socioeconomic and Environmental Impact of Landslides, U.S. Geological Survey Open-File report 01-0276, 39 pp.

Varnes D. J. (1978) Slope movement types and processes. In: R. L. Schuster and R. J. Krizek, eds, *Landslides: Analysis and Control,* pp. 11-33. Transportation Research Board, 1, 81.

Varnes D.J. (1984) Landslide hazard zonation: a review of principles and practice. In: Commission on landslides of the IAEG, UNESCO, Natural Hazards, Vol. 3.

Wasowski J., Refice A., Bovenga F., Nutricato R., Gostelow P. (2002) On the Applicability of SAR Interferometry Techniques to the Detection of Slope Deformations, *Proceedings of 9th IAEG Congress,* Durban, CD-ROM.

Wasowski J., Bovenga F., Florio N., Gigante G. (2008) PSInSAR for the investigating of unstable slopes and landslides. *Proceedings of the 1st World Landslide Forum*, Tokyo, Japan, 653–655.

Wegmuller U., Werner C., Strozzi T., Wiesmann A. (2004) Monitoring mining induced surface deformations. Proceedings of IGARSS 2004, Anchorage (USA).

Werner C., Wegmüller U., Strozzi T., Wiesmann A. (2000) Gamma SAR and interferometric processing software. *Proceedings of ERS-ENVISAT Symposium,* Gothenburg, Sweden.

Werner C., Wegmuller U., Strozzi T., Wiesmann A. (2003) Interferometric Point Target Analysis for deformation mapping. *Proceedings of IGARSS 2003,* Toulouse (Francia).

Werner C., Strozzi T., Wesmann A., Wegmuller U. (2008) Gamma's portable radar interferometer. *13th FIG Symposium on Deformation Measurements and analysis, LNEC*, Lisbon May 12-16 2008.

Wieczorek G.F. (1984) Preparing a detailed landslide-inventory map for hazard evaluation and reduction. *IAEG Bull* 21(3), 337–342.

WP/WLI-Working Party on World Landslide Inventory (1993) Multilingual Glossary for Landslides. The Canadian Geotechnical Society, BiTech Publisher, Richmond BC.

WP/WLI-International Geotechnical societies' UNESCO - Working Party on World Landslide Inventory (1990) A suggested method for reporting a landslide. Inter. Assoc. *Engineering Geology Bull*., 41, 5-12.

Zebker H.A., Goldstein R.M. (1986) Topographic Mapping From Interferometric Synthetic Aperture Radar Observations. *Journal of Geophysical Research*, (91), 4993–4999.

Zebker H.A., Werner C.L., Rosen P.A., Hensley S. (1994) Accuracy of topographic maps derived from ERS-1 interferometric radar. *IEEE Trans. Geosci. and Remote Sensing*, 32(4), 823-836.

Zhao C.Y., Lu Z., Zhang Q., De la Fuente J. (2012) Large-area landslide detection and monitoring with ALOS/PALSAR imagery data over Northern California and Southern Oregon, USA. *Remote Sensing of Environment,* 124, 348–359.

Žibret G., Komac M., Jemec M. (2012) PSInSAR displacements related to soil creep and rainfall intensities in the Alpine foreland of western Slovenia. *Geomorphology,* 175–176, 107-114.

Chapter 10

Annexes

Annex 1: Ph. Bally Ed. (2012) "Scientific and Technical Memorandum of the International Forum on Satellite EO and Geohazards", 21-23 May 2012, Santorini Greece. doi:10.5270/esa-geo-hzrd-2012, 59-80.

Annex 2: Bardi F., Frodella W., Ciampalini A., Bianchini S., Del Ventisette C., Gigli G., Fanti R., Moretti S., Basile G., Casagli N (to be submitted) "Integration between ground based and satellite SAR data in landslide mapping: the case study of San Fratello (Sicily, Italy)".

Annex 3: Bianchini S., Cigna F., Righini G., Proietti C., Casagli N. (2012a) "Landslide HotSpot Mapping by means of Persistent Scatterer Interferometry". *Environmental Earth Sciences*, 67(4), 1155-1172.

Annex 4: Frangioni S., Bianchini S., Moretti S. (2013) "Landslide inventory updating by means of Persistent Scatterer Interferometry (PSI): the Setta basin (Italy) case study". Accepted in *Geomatics, Natural Hazards and Risk.* doi: 10.1080/19475705.2013.866985.

Annex 5: Cigna F. Bianchini S., Righini G., Proietti C., Casagli N. (2010) "Updating landslide inventory maps in mountain areas by means of Persistent Scatterer Interferometry (PSI) and photo-interpretation: Central Calabria (Italy) case study". In: Malet JP, Glade T, Casagli N (eds) *Mountain Risks: Bringing Science to Society,* CERG Ed., Florence, Italy, pp. 3-9.

Annex 6: Bianchini S., Cigna F., Casagli N. (2013a) "Improving landslide inventories with multi-temporal measures of ground displacements retrieved through Persistent Scatterer Interferometry". In: *Landslide Science and Practice. Proceedings of The Second World Landslide Forum - WLF2*, Rome (Italy), October 3th-9th, 2011, Springer eds, pp. 119-125.

Annex 7: Cigna F., Bianchini S., Casagli N. (2013) "How to assess landslide activity and intensity with Persistent Scatterer Interferometry (PSI): the PSI-based matrix approach". *Landslides,* 10 (3), 267-283, doi: 10.1007/s10346-012-0335-7.

Annex 8: Del Ventisette C., Ciampalini A., Manunta M., Calò F., Paglia L., Ardizzone F., Mondini A., Reichenbach P., Mateos R.M., Bianchini S., Garcia I., Füsi B., Villő Deák Z., Rádi K., Graniczny M., Kowalski Z., Piatkowska A., Przylucka M., Retzo H., Strozzi T., Colombo D., Mora O., Sánchez F., Herrera G., Moretti S., Casagli N., Guzzetti F. (2013) "Exploitation of Large Archives of ERS and ENVISAT C-Band SAR Data to Characterize Ground Deformations". *Remote Sensing,* 5 (10), 3896-3917.

Annex 9: Bianchini S., Cigna F., Del Ventisette C., Moretti S., Casagli N. (2013b) "Monitoring landslide-induced displacements with TerraSAR-X Persistent Scatterer Interferometry (PSI): Gimigliano case study in Calabria Region (Italy)". *International Journal of Geosciences,* 4 (10).

Annex 10: Bianchini S., Cigna F., Del Ventisette C., Moretti S., Casagli N. (2012b) "Detecting and monitoring landslide phenomena with TerraSAR-X persistent scatterers data: the Gimigliano case study in Calabria region (Italy)". In: *IEEE International Geoscience and Remote Sensing Symposium. IGARSS2012*, Munich, Germany, 22-27 July 2012, 982 – 985.

Annex 11: Notti D., Herrera G., Bianchini S., Meisina C., García-Davalillo J. C., Zucca F. (in press) "A methodology for improving landslide PSI data analysis". Accepted in *International Journal of Remote Sensing.*

Annex 12: Bianchini S., Herrera G., Notti D., Garcìa-Moreno I., Mora O., Moretti S. (2013c) "Landslide activity maps generation by means of Persistent Scatterer Interferometry". *Remote Sensing*, 5 (12), 6198-6222, doi:10.3390/rs5126198.

Annex 13: Bianchini S., Herrera G., Mateos R. M., García-moreno I., Mora O., Sanchez C., Sanabria M., López M., Merodo J. A., Hernández M., Mulas J. (2013d) "Metodología para mejorar el análisis de datos satélite radar en el estudio de los movimientos de ladera: resultados del proyecto FP7 DORIS en la Serra de Tramuntana (Mallorca)". In: *VIII Simposio Nacional sobre Taludes y Laderas Inestables,* Palma de Mallorca, Junio 2013, E.Alonso, J. Corominas y M. Hürlimann (Eds.), CIMNE, Barcelona, 2013.

Annex 14: Bianchini S., Ciampalini A., Raspini F., Bardi F., Di Traglia F., Moretti S., Casagli N. (submitted) "Multi-temporal evaluation of landslide movements and impacts on buildings in San Fratello (Italy) by means of C- and X-band PSI data". Submitted to *PAGEOPH Special issue.*

Annex 15: Bianchini S. Tapete D., Ciampalini A., Di Traglia F., Del Ventisette C., Moretti S., Casagli N. (2014) "Multi-temporal evaluation of landslide-induced movements and damage assessment in San Fratello (Italy) by means of C-and X-Band PSI data". In: *Mathematics of Planet Earth, Lecture Notes in Earth System Sciences,* Springer Ed., pp. 263-266.

Annex 16: Ciampalini A., Bardi F., Bianchini S., Del Ventisette C., Moretti S., Casagli N. (to be submitted) "Analysis of building deformation in landslide area using multisensor PSInSAR^{TM} technique".